

## The cosmos thermodynamics axis manifests decoherence that integrates into a multi-level space-metrics for coherence for brain function

Dr. Alfred Bennun  
Full Professor Emeritus of Biochemistry  
Rutgers University

### Abstract

The Doppler shift could be applied to directional neuronal connectivity involving change in frequency  $\nu \pm \Delta\nu$  of wave that is moving relative to the wave source, acting over neuronal circuit distancing. The 1s orbital of the hydrogen atom allows the electron spin-flip up and down to emit radio emission at 18cm from hydroxyl radical and 21cm atomic hydrogen, which combined form water. This strongest spectral line of the hydrogen, present in the Dark Ages and by radio astronomy detected from primordial galaxies, is emitted by the water of all tissues, medically applied for brain studies, by magnetic resonance imaging (MRI). Hence, a Doppler Effect imaging of the distancing dynamics allows neuronal connectivity by their emission spectrum frequencies. Hence, the assay of nano scales coherence or distancing thermodynamics, equivalent to the plasticity strength of neuronal movement for electric connectivity. Therefore its interpreting measure an equivalent of *crostalk* between neurons and its elucidation became an analog to a translation of this unknown process. The transmembrane enzymes generate the enthalpy, coupled to the metabolism of glucose and water cluster. The products CO<sub>2</sub> and water as vapor are exhaled at the mouth as entropy. This integrative model allows a joint perspective of multiple layers of the reality, conditioned by scale dimension. Thus, the metrics of the quantum mechanics realm could show the locals frames for superposition of space and simultaneity. The brain thermodynamics relationship between inputs of glucose and the enthalpy process of metabolic energy (heat), coupled homeostatically at 36.6°C to water cluster H-bond breakdown, which in the cerebrospinal fluid (CSF) flow in microtubules could circulate in a liquid state as dimers (H<sub>2</sub>O~OH<sub>2</sub>) to dissipate entropy as vapor in the oral cavity. The multi-layers at neuron scale manifest spin in antenna role to signal connectivity for axon, dendrites, microtubules and tunneling. Myelinated space is a thermodynamic closed system, which eventually tends to equilibrium between enthalpy and entropy in which free energy cannot produce work. At a myelinated axon the Nodes of Ranvier “jumps” from node to node operate the unmyelinated stretches as a nano open space-time system. Quantic thermodynamic allows a repetitive sequence at the nano level of close to open, close to open, close ... Hence, a maximal value of enthalpy is conserved and entropy became dissipated outside the system, maintaining the action potential level in steady state. Hence, the ions channels could refill the Na<sup>+</sup>/K<sup>+</sup> concentrations for an enthalpy increase of potential hilling up for the recovery of higher enthalpy with dissipative entropy out of the system. Thus, a kinetic of multiplicative association by synchronizing photon emission allows a common signaling for multi-neuronal functional coherence. This reinforcement is required for operating a near null noise, to avoid chaotic asynchrony. The effect involves nano scale of space and time because is mediated by photons moving in a liquid phase:  $2.25 \times 10^9 \text{m/s}$  (0.75 *c*). Hence, allowing *crostalk* between neurons at a very high velocity, integrating the operative time of systems synchronizing the activity of G-protein-linked receptors in the insulin/glutamatergic and catecholaminergic pathways. The nano space maintains a high rate of molecular collisions, maximizing affinity at saturation values by low concentration of hormones, etc. The structural changes of the transmembrane enzymes coupled to the metabolism of glucose and coupled water cluster H-bond breakdown could reach a high enthalpy to low entropy into the system. Thus, separated structures in nano space could integrate more efficiently their function, maximizing connectivity between neurons and microtubules, for an operative open system inflow of substrate and outflow of products. Hence, the effect of insulin at the tyrosine kinase level would be simultaneously affecting all over the neuronal cytoskeleton of microtubules system and the cell cycle. Thus, overcome the catalytic inanimate thermodynamics for converging from a microscopic reversibility principle to a life itself, adapting at the membrane level a kinetic vectorial order overcoming reversibility. At the cell physiological level NA-AC and insulin receptor tyrosine kinase (IRTK) auto-phosphorylation regulate responsiveness to hormones of ionic concentrations vs chelating metabolites. Thus, a decreased Mg<sup>2+</sup> produces deactivated AC by releasing free ATP<sup>+</sup> and activate IRTK. Thus, allows an integration of the hormonal response of both enzymes by ionic controls. This effect could supersede the metabolic feedback control by energy charge. Accordingly, maximum hormonal response of both enzymes, to high Mg<sup>2+</sup> and low free ATP<sup>+</sup>, allows a correlation with the known effects of low caloric intake increasing the level of free ions could elevate the average life expectancy.

## Introduction

*The structural changes of the transmembrane enzymes coupled to the metabolism of glucose and water cluster*

Mg<sup>2+</sup> coordinated by negative R groups in oxyHb hydrophilic state, characterizes by mutually exclusion of hydrophobic state of the deoxyHb. The release of O<sub>2</sub> jointly with kosmotropic Mg<sup>2+</sup>, which by competition for the hydration shells of Na<sup>+</sup>/K<sup>+</sup>, maintains the action potential across membrane. The 6×10<sup>4</sup> neurons of the locus coeruleus with noradrenaline-adenylate-cyclase (NA-AC) long axons, reaching all regional neuronal circuits located to function as conectomas for the input from the five sensory perceptions areas that the human mind would integrate into its totalizing everyday reality.

The sensorial neurons have dendrites connecting to axons of the hypothalamic-NA-AC with axons across the blood-brain barrier (BBB) through the vomeronasal organ that activate the hypothalamic-pituitary-adrenal axis to modulate secretions into the capillary arterioles irrigating the oral cavity for hormonal feedback emotional response of the nurturing infant.

The brain NA-AC response is protected from a feedback by the body adrenaline because BBB is not permeable to adrenaline. Thus, the selective exclusion of the adrenaline controlled AC allows the brain could exhaust nutritional reserves without turning-off. Thus, have unimpeded access to glucose, which during starvation could only partially replace by acetoacetate and acetone generated from fats, which in this period cross the BBB to enter in cerebrospinal fluid (CSF).

The excess of Mg<sup>2+</sup> over Mg-ATP activates NA-AC in an obligatory step to configure a hydrophilic active site for the water attack by water cluster (H<sub>2</sub>O)<sub>n=3,4</sub> of the binding MgATP active site, releasing PPi and AMP. The H-bond breakdown configures by mutual exclusion a hydrophobic domain, in response to calmodulin release of Ca<sup>2+</sup>. The opening of the hydrophobic active site allows the release H-bond depleted water without significant decreasing the concentration of water cluster. Hence, the hydrophobic condition decreases the highly prize to be pay for endergonic thermodynamics cycling the phosphoryl group of AMP into cAMP.

Mg<sup>2+</sup> releases cAMP from the enzyme enclosed structure and hydration shell after 10<sup>-15</sup>s the quantum timing of the process maximizes entropy release for efficiently open system thermodynamics. The process involves H-bonds depolarized water to circulate as hydrophobic dimers (H<sub>2</sub>O~OH<sub>2</sub>). The dimers transit a route created from hydrophilic plasma, depleted from hormones, into the hydrophobic CSF. Using contrastive divergence, a statistical machine learning technique, had been calculated a maximum entropy-based correlated mutation measures (CMMs) to obtain a new probabilistic model for β-contact prediction, of both residue- and strand-level contacts for microtubules circulation. The applied math approach may allow to differentiate microtubules conducting structure: parallel for enthalpy vs an inverse sense antiparallel release of entropy exhaled as vapor into the oral cavity.

The quantum space-time at the spin of electron of H operating as the distension-contraction by analogy of an antenna wavelength emission, signaling photons as a sum of angular moments, at the instant of vector re-configuration of the electric and magnetic fields.

The transitory wavelength of the photon pair superposition can be characterized by two exclusive states: constructive (distension of the E field) or destructive (contraction of the E field). Quantum entanglement acts as a dissipative coherence-decoherence oscillatory potential, with momentum conservation. The reason for the Doppler Effect is that when the source of the waves is moving towards the observer, each successive wave crest is emitted from a position closer to the observer than the crest of the previous wave and when the expansion of space increase the waves show a redshift.

In quantum entanglement each photon is close enough to apply the uncertainty principle as a whole. This contraction of space-time imposes that the electric fields are arranged orthogonally, with the lower configuration of the energy and an increase in the density and mutually add their energetic fluidity. Thermodynamically the entangled system is subject to statistical parameters that force it to decoherent by the flow from a higher to a lower density.

The relationship between moment ( $p$ ) and total angular momentum ( $L$ ) allows an alternative expression. Thus,  $\Delta p = \frac{\Delta L}{r}$  and  $\Delta x = \Delta \phi r$ , where  $\phi$  is the angle in radians and  $x$  is a measure of the curvature or circumference of a circle, and therefore,  $\Delta L \Delta \phi \geq \frac{h}{4\pi}$ . The latter shows the uncertainty between angular momentum ( $L$ ) vs angular position ( $\phi$ ).

The total angular momentum of the system of two entangled photons would be composed mainly by the sum of their spins  $L = s_1 + s_2 = 2s$ . Therefore  $\Delta(s_1 + s_2) \Delta \phi \geq \frac{h}{4\pi} \Rightarrow \Delta(2s_1) \frac{\Delta \phi}{2} \geq \frac{h}{4\pi}$ . On the other hand, in a coherent photon system  $\Delta(s_1) \Delta \phi \geq \frac{h}{4\pi}$ . This allows us to conclude that  $\Delta x = \frac{\Delta \phi}{2} r$ , and therefore explains the space-time contraction of entangled photons.

The value of the total angular momentum of the system of two entangled photons would be less than that of a coherent photon. Therefore, due to the uncertainty principle, the dimension of the entanglement is less than the coherence.

In the interference of two photons, the superposition allows locating the position, but due to the uncertainty principle, the moment of the system cannot be known. This may have implications for the quantum entanglement of two photons. The state of the entangled pair is precisely known but the individual quantum state of each one cannot be known simultaneously. Therefore, it produces a zone of probability and superposition for the electric field to operate, which gives it a dynamic or plasticity of energetic configuration.

In the electromagnetic wave, the coherence time ( $\tau$ : *tau*) is the time it takes to be considered coherent, which means that its phase ( $T$  period) is predictable. Is calculated by dividing the coherence length (is the propagation distance over which a coherent wave maintains a specified degree of coherence.) by the phase velocity of light (is the rate at which the wave propagates in some medium), approach:  $\tau = \frac{1}{\Delta \nu} \approx \frac{\lambda^2}{c \Delta \lambda}$ .

Where  $\lambda$  is the central wavelength of the source,  $\Delta \lambda$  is the spectral width of the source in frequency units:  $\Delta \nu$ .

A single mode fiber laser has a linewidth of a few kHz, corresponding to a coherence time of a few hundred microseconds. Hydrogen masers have linewidth around 1 Hz, corresponding to a coherence time of one second. Their coherence length corresponds to the distance from the Earth to the Moon.

The coherence length ( $L_c$ ) is defined as the distance the wave travels in time ( $\tau_c$ ). At a delay of  $\tau = 0$  the degree of coherence is perfect, whereas it drops significantly as the delay phases:  $\tau = \tau_c$ .

In terms of the hypothesis of De Broglie all mass  $m$ , has associate a wavelength ( $\lambda$ ), by the equation  $mv = \frac{2\pi\hbar}{\lambda}$   $\vee$   $mv = \frac{h}{\lambda}$ . Consequently this relationship introduce in the expression of Schrodinger's box.

Temporal coherence is the measure of the average correlation between the value of a wave and its delayed by  $\tau$ , between two instants, and shows how monochromatic a source is. Thus, it characterizes how well a wave can interfere with itself at a different time.

For long distance transmission, the coherence time can be reduced by scattering, spreading and diffraction.

Tunnel ionization is a process in which electrons in an atom (or a molecule) pass through the potential barrier and escape from the atom (or molecule). When the atom is in an electrostatic external field, the suppression of Coulomb potential barrier or to lower one and the electron has an increased, non-zero probability of tunneling through the potential barrier, an approximation to match the ground state hydrogen wavefunction.

In the case of an alternating electric field, the direction of the electric field reverses after the half period of the field.

The size of the diameter of the microscopic tunnels of the axons of the neuron does not allow the water cluster to circulate, but accommodates the smaller dimers.

The frequent and continuum transmission current against an oscillation resistance will induce a microwave voltage across the axon. The electrical current allows super magnetic junction and spin-torque up and down, nano-oscillator of the mean of the bell-shaped frequency induced in the electric response of a sensory neuron. These ones

simultaneously activate all the same enzymes of a neuronal circuit to reach the coherence required for multiplicity of a firing potential at a unidirectional sense because very few neurons may not respond the signal will show null noise. Thus, coherence coordinates and integrates neuronal pathway at the hypothalamic neurons with AC axonal response Hypothalamus (CRH/Corticotropin releasing hormone) → Anterior Pituitary (ACTH/Adrenocorticotrophic hormone) → Adrenal Cortex (CORT/cortisol). The cortisol crosses the blood-brain barrier (BBB) for negative feedback, which is exercised over the anterior pituitary and hypothalamus. The meninges are not permeable to adrenaline flow into CSF exhaustion of mobilized reserves [1] flow into the brain without negative feedback over NA-AC. However, stress releases the permeable cortisol, with deleterious effect in brain structure and function.

### Receptors

Insulin is synthesized as an inactive precursor molecule, a 110 amino acid-long “preproinsulin”. This one is translated directly into the rough endoplasmic reticulum (RER), where its signal peptide is removed by signal peptidase to form “proinsulin”, which folds its opposite ends of the protein, the “A-chain” and the “B-chain”, are fused together with three disulfide bonds. Folded proinsulin then transits through the Golgi apparatus and is packaged into specialized secretory vesicles. In the granule, proinsulin is cleaved by proprotein convertase 1/3 and proprotein convertase 2, removing the middle part of the “C-peptide”. Finally, carboxypeptidase E removes two pairs of amino acids from the protein's ends, resulting in active insulin – the insulin A- and B- chains, now connected with two disulfide bonds.

Insulin-like growth factor 1 (IGF-1) (or somatomedin C) is a hormone similar in molecular structure to insulin with a function on childhood growth, and only anabolic effects in adults.

IGF-1 is a protein that in humans is encoded by the IGF1 gene. IGF-1 consists of 70 amino acids in a single chain with three intramolecular disulfide bridges. IGF-1 has a molecular weight of 7,649 Daltons. In dogs, an ancient mutation in IGF1 is the primary cause of the toy phenotype.

IGF-1 is produced primarily by the liver. Production is stimulated by growth hormone. Most of IGF-1 is bound to one of 6 binding proteins (IGF-BP). IGFBP-1 is regulated by insulin. IGF-1 is produced throughout life; the highest rates of IGF-1 production occur during the pubertal growth spurt. The lowest levels occur in infancy and old age.

A synthetic analog of IGF-1, mecasermin, is used in children for the treatment of growth failure.

Paired do at a rate of  $1.6E16$  pairs per ms, greater than adenylate cyclase (AC) operational turnover. The water paired structure could oscillate between two states, one entangled by two oxygen atoms and the other, by two entangled hydrogen atoms in the pair. Their flow through micro-tubules by tunnel magneto resistance in which spin wave resonance is excited the spin polarization auto-oscillate at the lowest energy spin wave modes acting as a radio waves antenna.

The model for intact human brain neurons in the physiological choroid plexus generates from plasma the cerebrospinal fluid (CSF), as an instable liquid state of the dimers by hierarchical of the initial effect function as a forming rate of  $1.6E16$  pairs per ms dissipative through astrocytes (glial cells) path of entropy.

In the human brain the quantum physiology of the electrogenic action potential along myelin-sheath axons gaps requires recovery of voltage. Hence, at the uninsulated “Nodes of Ranvier” (exposed to the extracellular space, mass and energy) are short unmyelinated segments of a myelinated axon, which are found periodically, interspersed between segments of the myelin sheath. Therefore, at the point of the node of Ranvier, the axon is reduced in diameter.

These nodes are areas where action potentials can be generated. In saltatory conduction, electrical currents produced at each node of Ranvier are conducted with little attenuation to the next node in line, where they remain strong enough to generate another action potential.

Thus, in a myelinated axon, action potentials effectively “jump” from node to node, bypassing the myelinated stretches in between, resulting in a propagation speed much faster at microtubules than even the fastest unmyelinated axon can sustain.

Hence, operate as nano open systems, structuring the *capacitance* through the nodes' ions channels, refilling the  $\text{Na}^+/\text{K}^+$  concentrations that will respond to the *inductor* ion (*nascent*  $\text{Mg}^{2+}$ ). The thermodynamics functional analysis is neuronal maintenance of the optimal enthalpy level occurs by an anatomic structure for an oscillatory microscopic opening at the internal space-time system, enclosed by myelin, conform a nano-mechanism of life structured quantum mechanics.

Hence, the mass and energy input allowed by the "Nodes of Ranvier" structure, allowing the enthalpy increase by water clusters, and other H-bonds integrated structures when are coupled for their breakdown. The generated single molecules of water organize by their polarity in dimers configuration:  $2\text{H}_2\text{O} \rightarrow \text{H}_2\text{O} \sim \text{OH}_2$ , circulating within microtubules. This dissipative pathway allows the randomness of entropy to be incorporated into the kinetics resonance of dimer structures. This favors a microscopic one dissipative sense entanglement by magnetic tunneling unions. The dimers could manifest at the H atom level the up and down-spin of electrons turning around the oxygen-oxygen orbitals superposition. Thus, function as antenna oscillators with emission signaling frequency connecting neuronal network. Thus, the input for enthalpy incorporation generates a dissipative flow of differentiable frequencies signaling other neurons in a quantum space-time level for near simultaneous integration from a basal to the excited state.

At the physiological neurons the *inductor* signals a need for enthalpy gain, even if creates a delay on the flow from one node to the next, along the axon. The relationship between inflow and outflow of enthalpy vs entropy preserve the information of the sinusoidal curves registering frequency.

The dimers function for spin emission as natural nano hydrogen atoms electrons spin up and down polarization as resonance oscillator that flow inside the microtubules, to act as a transmitter-receptor antenna of radio waves.

The brain function has led to the design of nano-circuits by a quantum technology that uses the term *memristor* - a word contraction for memory and resistor.

Glial cells could transmit harmonics by synaptic signaling consistency through widely

separated regions by a firing synchronization, decreasing the random interference tendency to generate noise.

For inter-trial phase, clusters of strong firing associations were found in the temporal and frontal lobes, especially in the bilateral auditory and pre-motor cortices. Higher phase-locking values corresponded to higher cortical thickness in the frontal, temporal, occipital and parietal lobes [2]. The pyramidal neurons in the cortex [3], by mapping from a probabilistic spiking nature may relate into neuronal circuit their function for emotional learning and cognition.

### **The molecular folding of AC at the $\text{Mg}^{2+}$ coordinative hydrophilic phase configures enthalpy and with $\text{Ca}^{2+}$ input a hydrophobic phase for enthalpy axis into microtubules entropy dissipation**

Incubation with noradrenaline (NA) of isolated membranes of rat's brain corpus striatum, cortex and hypothalamus showed that ionic  $\text{Mg}^{2+}$  is required for the neurotransmitter activatory response of adenylate cyclase (AC).

Adrenaline stimulates AC-III in human liver to mobilize the energy stored in fat [4] in the "fight-or-flight" response. The effect of adrenaline is via a G protein signaling cascade which transmits chemical signals from outside the cell across the membrane to the inside of the cell (cytoplasm).

The AC protein is organized with 6 transmembrane segments, then the C1 cytoplasmic domain, then another 6 membrane segments, and then a second cytoplasmic domain C2. This is preceded by a short, variable amino terminus. There are two large homologous cytoplasmic domains (C1 is larger, with 360 to 390 amino acids and C2 with 255 to 330 amino acids) similar to each other.

Amino acid sequences show that AC contains two regions: M1 and M2. The C1a and C2a subdomains are homologous and form an intramolecular 'dimer' that forms the active site. The smaller C1b and C2b regions appear to be involved in regulation of catalytic activity.

An intramolecular dimer proline allows bending for the common sliding of C1 and C2 to organize reactive domains: a hydrophilic  $\text{Mg}^{2+}$  coordinating site in exergonic function and a

hydrophobic state coordinated  $\text{Ca}^{2+}$  in endergonic function [5]. The important parts for function are the N-terminus and the C1 and C2 subdomains/regions are homologous asymmetric H-bonded polypeptide segments, which form an intramolecular 'dimer' for an integrated active site function into two stages.

AC is glycosylated and show several potential sites for phosphorylation. The enzyme shows  $\text{Ca}^{2+}$ -dependent dead-end inhibition and by adenosine analogues P-site inhibition. The breakdown of the kinetic intermediates at the R groups within the shared active sites structures of AC results in the first stage product  $\text{P}_1$ : AMP and pyrophosphate ( $\text{PP}_i$ ) and the H-bond breakdown. The C1 and C2 regions slides themselves to dynamically reconstruct in the same polypeptide chains a sequence of differential H-bond linkage of enthalpy inputs by coupling water cluster H-bonds breakdown favoring the vectorial axis of exergonic transitions between enthalpy and entropy.

Thus, responds in a second stage to  $\text{Ca}^{2+}$  released by the  $\text{Ca}^{2+}/\text{CaM}$  influx, allowing the  $\text{S}_2$  substrates, the endergonic cycling of AMP and coupled water cluster into the products  $\text{P}_2$ : cAMP and release of free water. The molecule of water lacking de polarity of H-bonds reconfigure into dimers ( $\text{H}_2\text{O}\sim\text{OH}_2$ ).

Animal membrane-bound ACs belongs to class IIIa.  $\text{Mg}^{2+}$  in excess is obligatory required for substrate Mg-ATP binding at the active site. A first phase produces AMP, and a second phase cAMP (cyclic adenosine monophosphate or 3'-5'-cyclic adenosine monophosphate) acts as a second messenger for other proteins and the cyclic nucleotide-gated ion channels.

The cAMP formation depends on G-protein coupled receptors (GPCRs). PKA activated by cAMP that activates the small GTP-binding protein Rap1 and the cyclic nucleotide-gated channels (CNGCs). The respond to cAMP signaling functions include control of metabolism, gene transcription and ion channel activity, the activity modulating the cross-talk between signaling pathways, evident in the case of  $\text{Ca}^{2+}$  signaling in

both neuronal and muscle cells. The off-reactions are responsible for removing cAMP by either hydrolysis or by efflux from the cell.

An  $\text{Mg}^{2+}$ -dependent response to the activatory effects of adrenaline, and subsequent inhibition by calcium, suggest capability for a turnover, associated with cyclic changes in membrane potential and participation in a short-term memory pathway. Calcium entrance in the cell inhibits the enzyme. The increment of cAMP activates kinase A and their protein phosphorylating activity, allowing a long-term memory pathway.

The physiological integration between psyche and soma was analyzed for the purpose to obtain a consistent molecular framework. Signaling by sensor neurons activates the fight-or-flight response at the hypothalamic pituitary adrenal axis and pancreas, increasing the adrenaline output, which at the adrenal stimulates secretion of glucagon and inhibits the release of insulin, distorting the pulsatile rhythm of glucose metabolism. This flattens the normal circadian modulation of glucose levels, to allow the rate of ATP generation and consumption to exceed the modulatory limits of Energy Charge, and oppose the ATP-requiring regeneration of glycogen and fat reserves. An "*in common*" signaling results from depletion of chelating metabolites by the tendencies of ionic equilibrium to increase free  $\text{Mg}^{2+}$  vs the decrease of inhibitors  $\text{CaATP}$ ,  $\text{ATP}^+$  and  $\text{Ca}^{2+}$ . Hence, integrates a network of tissues "*in common*"  $\text{Mg}^{2+}$ -dependent AC responsiveness to NA in brain and adrenaline on the tissue network hormonal responding to support brain function [6].

Hence, consolidating neuronal circuits, related to emotional learning and memory affirmation. The activatory effect relates to an enzyme-NA complex, which may participate in the physiology of the fight-or-flight response because by prolonged incubation results in inactivatory effect on NA-AC in the particulate preparation of the transmembrane enzyme complex. Hence, is concordant with physiological observations that the etiology of stress on the adrenergic system relates to chronic pathologies like depression.

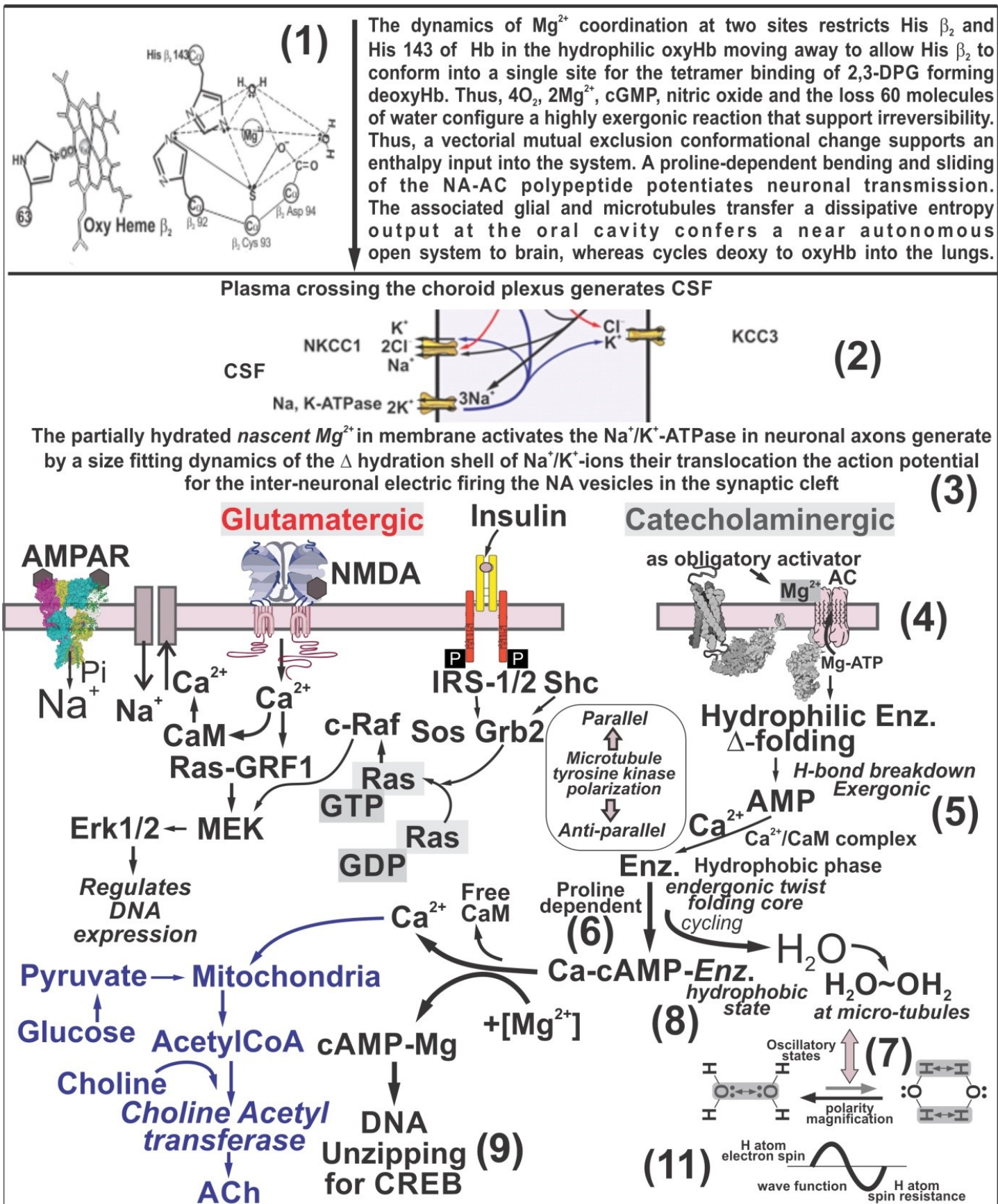


Figure 1: Integrated catecholaminergic (adrenergic pathway, dopaminergic, etc.). Glutamatergic synaptic transmission by AMPAR-type, the N-methyl-D-aspartate (NMDA) ion channel ionotropic glutamate receptors. Cholinergic pathway is involved in the synthesis, storage secretion, receptor interaction and acetylcholine lysis.

Insulin receptor tyrosine kinase (IRTK) and epidermal growth factor (EGF) receptor are activated by extracellular ligand insulin and EGF. The MAPK/ERK (Ras-Raf-MEK-ERK) pathway signals from surface of the cell for DNA transcription. The thermodynamics structure and function interrelation of these systems contributes to the integration into a shared microtubules system. The  $\epsilon$  spin of H atoms emits at the 21cm wavelength from coordinative antennas, allowing that the multi-neuronal weak signals, integrates to organize their firing time of action potentials involved in crosstalk that avoid electromagnetic molecular noises.

The figure 1 shows 11 steps involved in the thermodynamics structure and function of transmembrane AC type 7. The enzyme is expressed in all tissues, predominantly in multiple brain processes as synaptic plasticity, learning and memory. The neuronal phospholipid hydrophobic membrane shows its outside receptors involved in a primordial development of life evolution. In neurons is located next to  $\text{Ca}^{2+}/\text{CaM}$  ion channels influx for faster reaction.

The polypeptide structure of AC shows proline dependence for bending at segments of the two asymmetric domains integrated for sliding in between reactive regions which became separated by H-bonds breakdown dynamics. The latter is also coupled to the function dynamics of DNA, proteins and water clusters.

A particle membrane purified AC enzyme with RARE BiBi - two substrates (S) two products (P) – kinetics sequence. The hydrophilic state by  $[\text{Mg}^{2+}]$   $S_1$  in excess of  $S_1'$  MgATP by the mass action of 55.5M water. Water cluster:  $(\text{H}_2\text{O})_{n=3.4}$  – the sub-index “n” number of H-bonds – averaging 55.5:3.4=16.3M to calculate saturation kinetic but an still not allowing procedures capable to differentiate between the saturation state of the two states of water.

Multiple-equilibrium equations were solved to investigate the individual and separate effects of  $\text{Mg}^{2+}$ ,  $\text{Mn}^{2+}$ ,  $\text{Ca}^{2+}$ ,  $\text{ATP}^+$ , and their complexes on the kinetics of brain AC. The effects of divalent metals and/or  $\text{ATP}^+$  in excess of their participation in complex formation were determined. Hence, allowing measuring of apparent affinity kinetic constants values:  $K_m(\text{MgATP}) = 1.0 \text{ mM}$ ,  $K_i(\text{ATP}^+$

) = 0.27 mM,  $K_m(\text{MnATP}) = 0.07 \text{ mM}$ , and  $K_i(\text{CaATP}) = 0.015 \text{ mM}$ . MgATP, MnATP,  $\text{ATP}^+$ , and CaATP were shown to compete for the active site of the enzyme. Hence, it is proposed that endogenous metabolites with a strong ligand activity for divalent metals, such as citrate and some amino acids become integrated into a metabolite feedback control of the enzyme through the release of  $\text{ATP}^+$  from MgATP.  $\text{Ca}^{2+}$  fluxes may participate in the endogenous regulation of adenylate cyclase by modifying the level of CaATP.

Experimental studies were done in rat's brain slices of cerebral cortex, hypothalamus, and corpus striatum to obtain particulate membrane preparations [7] [8] [9] at constant 1 mM-ATP the  $\text{Mg}^{2+}$  saturation curves show that addition of 0.1 mM-NA increases the apparent  $V_{max}$  for  $\text{Mg}^{2+}$  by 300% in corpus striatum particles, and by 280% in cortex particles. At 10mM- $\text{MgCl}_2$ , the addition of 0.1 mM-NA increased by 800% the AC activity of corpus striatum particles [10]. NA activated AC-Mediated Hypothalamic-Pituitary-Adrenal Axis. Analysis indicates a native molecular mass of over 200 kDa.

The process shows the vectorial *mutual exclusion* between R groups participating in the conversion of a catalytic core from hydrophilic to hydrophobic domain, which could not proceed for a simultaneous to change of direction from hydrophobic to hydrophilic state of the active site configuration that would be a death end inhibition. The G protein-linked receptor changing is dissociation state as inhibitory  $G_i$ , releasing the  $G_z$  alpha from  $\beta\gamma$ .

Hence, is necessary the additional third step in which the core active site of the enzyme requires to be release from the endergonic trapping into the hydrophobic stage. Hence, the influx of  $\text{Mg}^{2+}$  in excess of the substrate Mg-ATP is required to displace the  $\text{Ca}^{2+}$  from the enzyme  $\text{Ca}^{2+}$  complex, which adds a third stage for a return of the active site to a catalytic state. This involves coupling to the H-bond breakdown to initiate the obligatory formation of an Mg-AC complex, a highly exergonic step before could react with the substrate Mg-ATP.

The process could be thermodynamic characterized by a vector of hydrophilic to hydrophobic sense, in which a single polypeptide

could not show reversibility because a mutual exclusion operate for the two domains of the active site core cannot exist at the same time. In a first stage the amino acids residues (R groups) coordinating the ions conform an active core for  $Mg^{2+}$ .

The presence of a proline at the AC polypeptide chain allows bending and sliding to replace the first stage R groups for other ones binding  $Ca^{2+}$ . Additionally, interaction with the protein kinase C (PKC) by phosphorylation of the hydroxyl groups of threonine amino acid residues (R groups) could differentiate and facilitate to differentiated structural pathways for the sliding steps involving in the folding sequence.

Coupling H-bond breakdown allows non-reversible events. But substitution at other sites or for turnover depends on the mass action saturation by the remnant pools of water cluster.

A hydrophilic  $Mg^{2+}$  stage preceding and hydrophobic  $Ca^{2+}$  stage follows an exergonic to endergonic sense, which could not proceed simultaneously at the same time by opposite  $Ca^{2+}$  to  $Mg^{2+}$  functions separating events within a single pathway as organizing the protein structure of AC to obtain kinetic energy out of the functional transition during of ion response at the hydrophilic to hydrophobic stages.

Parallel senses allow turnover to overpass the microscopic reversibility principle, kinetically AC is a system synchronized for the flow of energy within the polypeptide from a vectorial hydrophilic to a hydrophobic sense by the coupled of non-reversible H-bond breakdown.

NA-AC as a thermodynamics system of the enzyme itself became folded and unfolded to confer dynamics structuring/restructuring to produce transitional event by reorganizing the active site into a directional kinetics without reversibility. Thus, operates within a compartmentalized membrane in a thermodynamic of open system by access to substrate and coupled by the dissipative entropy of H-bond breakdown, circulating within the microtubules pathway.

The microtubules constructed by tubulin molecules magnetized for tunneling function of preserving the dimers structure by the *quantum* interaction of the electrons at the up and down-spin torque function as magnetic oscillators. The

quantum function of receptor/emission antennas of radio microwaves could be to synchronize the electric potential. Hence, the fraction of the total photon emitted into the brain is transfer through axon/microtubule. Thus,  $\lambda$  patterns allow photon entanglement of quantum nano-time at axon/microtubule operating in neuronal circuits coordinate transmembrane signal responses, integrating their firing time to organize crosstalk avoiding electromagnetic neuronal noises.

Medical studies by Electroencephalography records an electrogram of the electrical activity on the scalp, to represent the macroscopic activity of the surface layer of the brain underneath and nuclear magnetic resonance imaging of atomic nuclei, which are able to absorb radio frequency energy when placed in an external magnetic field, evolving spin polarization.

### **Glutamatergic system NMDA and AMPAR**

Inotropic glutamate receptors integral membrane proteins are ligand-gated ion channels that are activated by the neurotransmitter ligands glutamate, D-serine and glycine, composed of four large subunits (>900 residues) that form a central ion channel pore a similar architecture for all known glutamate receptor subunits, including the AMPA, kainate, NMDA controlling synaptic plasticity learning and memory, etc. However, the binding of the ligands is typically not sufficient to open the channel as it may be blocked by  $Mg^{2+}$  ions, which are only removed when the neuron is sufficiently depolarized. Thus, the channel acts as a “coincidence detector” and only once both of these conditions are met, the channel opens and it allows positively charged ions (cations) to flow through the cell membrane.

Glutamatergic system is the major excitatory transmission of the mammalian brain: amino acid (glutamate/aspartate) in the body or brain includes receptor agonists, reuptake inhibitors. Thus, is mediated primarily through the AMPA-type glutamate receptor (AMPA). The cerebral cortex cortical areas (corticostriatal projections) distribution pattern in the striatum causes the basal ganglia circuits to be functionally segregated.

The regulation of this receptor underlies many forms of synaptic plasticity. In particular,

phosphorylation of GluR1, an AMPAR subunit, by PKA at serine 845 (S845) increases peak open channel probability and is permissive for both the synaptic expression of the receptor and NMDA-receptor (NMDAR)-dependent long-term potentiation (LTP).

The associative cortical areas from the frontal, parietal, and temporal lobes send projections to the caudate nucleus and the precommissural putamen; and the limbic cortices, the amygdala, and the hippocampus terminate preferentially in the ventral striatum. The dendritic spines of MSNs and the  $\gamma$ -aminobutyric acid (GABA)/parvalbumin interneurons target projections. Almost 40% of all neurons are classified as glutamatergic. The glutamatergic astrocyte-neuron is inseparable element of synapses interactions in the brain.

The NMDAR receptor regulates of synaptic plasticity. The mechanism of  $\alpha_1$ ,  $\alpha_2$ , and  $\beta$ AR regulating enhances NMDAR currents through cAMP-PKA pathways, whereas  $\alpha_2$ AR reduces NMDAR activity by inhibiting the same pathway or presynaptic glutamate secretion.  $\alpha_1$ AR, which is a protein-coupled receptor, decreases NMDAR activity through PLC-IP3 signals.

Phosphorylation of GluR1, an AMPAR subunit, by PKA at serine 845 (S845) operates for optimal open channel probability and is permissive for synaptic receptor expression and NMDA-receptor (NMDAR)-dependent long-term potentiation (LTP).

In the central nervous system, acetylcholine (ACh) in interneurons cell clusters, a few important long-axon cholinergic pathways exist as a projection in the basal forebrain to the forebrain neocortex, associated to limbic structures.

Regulation of gene expression is a major component of insulin action, which is classically thought to occur via phosphorylation, relocalization and/or processing of transcriptional regulators downstream of the insulin receptor (IR) signaling cascade. IR mechanism may translocate to the nucleus and forms transcriptional complexes with RNA polymerase II, host cell factor-1 and transcription factors to regulate gene expression, adding a new complementary pathway for insulin actions.

Insulin is the central regulator of metabolism, controlling the balance between fuel utilization and

storage and regulates gene expression in a tissue- and cell-specific manner. Thus, maintains glucose levels during cycles of feeding and fasting.

### **MAPK/ERK (Ras-Raf-MEK-ERK) pathway**

Insulin receptor (IR) activates MAPK pathway by activation of Shc-Grb2-Sos complex. MAPK pathway induces cell proliferation. This initiates a broad network of protein phosphorylation, including phosphorylation of IRS-1 leading to activation of the phosphatidylinositol 3-kinase (PI3K)/AKT pathway with activation of the RAS/MAP kinase pathway that mediates effects on growth and proliferation.

Insulin bidirectionally alters nucleus accumbens (NAc) medium spiny neurons (MSNs). Glutamatergic transmission: interactions between IR activation, enkephalins and endorphins, and glutamate release.

Human fMRI studies show that insulin influences brain activity in regions that mediate reward and motivation. Cortical and hippocampal neurons suggest that insulin influences excitatory transmission via presynaptic and postsynaptic mechanisms. Dysregulation accompanying obesity is linked to cognitive decline, depression, anxiety, and altered motivation that rely on NAc excitatory transmission [11]. The MAPK/ERK (Ras-Raf-MEK-ERK) pathway signals from a receptor on the surface of the cell to the DNA in the nucleus of the cell. The pathway includes many proteins, such as mitogen-activated protein kinases (MAPKs).

The signal that starts the MAPK/ERK (extracellular signal-regulated kinases) pathway phosphorylating “on” or “off” for activatory switching of neighboring protein. This allows a Ras protein (a small GTPase) to swap a GDP molecule for a GTP molecule, flipping the “on/off switch” of the pathway. The Ras protein can then activate MAP3K, which activates MAP2K, which activates MAPK.

The forkhead family box O (FOXO) transcription factor, evolution conserved pathway, upon insulin stimulation are phosphorylated by AKT, bind to 14-3-3 proteins and are thus excluded from the nucleus, limiting their ability to regulate gene expression. Insulin promotes phosphorylation of FOXK transcription factors and phosphorylation

and processing of sterol regulatory element binding protein 1c (SREBP-1c). By the combinations of post-translational modifications FOXO's serve as a 'molecular code' to sense external stimuli into activating specific regions of the genome.

### **Catecholaminergic or adrenergic system**

Catecholaminergic or adrenergic system: the catecholamine neurotransmitters include dopamine, adrenaline (AD), and noradrenaline (NA).

Another neurotransmitter of the catecholaminergic system is produced in synaptic vesicles when dopamine is converted to NA by dopamine  $\beta$ -hydroxylase. Noradrenergic cells in the central nervous system are most concentrated in the locus coeruleus of the brain stem. NA is used in the sympathetic autonomic nervous system, where its release by postganglionic neurons is mediated by stress. In the adrenal medulla, AD functional in the body is derived from NA via phenylethanolamine N-methyl-transferase. AD is released into the blood as a stress hormone functions as a neurotransmitter.

Degeneration of adrenergic neurons in the locus coeruleus expressing C1 adrenergic receptors causes the adrenergic system to compensate for the loss by increasing production of epinephrine in the cerebrospinal fluid (CSF).

Parkinson's disease (PD) often results in failure of the sympathetic nervous system, making patients vulnerable to falls.

Aging increases sympathetic activity and reduces norepinephrine uptake due to changes in the morphology of adrenergic receptors. Furthermore, stress causes activation of  $\beta_1$ -adrenergic receptors that mediate endothelial cell injury, leading to atherosclerosis. Such chronic events in which stress responses are enhanced make age a risk factor for cardiovascular conditions such as hypertension, ventricular arrhythmias, and heart failure.

Dopaminergic pathways in the human brain are involved in both physiological and behavioral processes including movement, cognition, executive functions, reward, motivation, and neuroendocrine control. Each pathway is a set of projection neurons, consisting of individual dopaminergic neurons or dopamine neurons.

The four major dopaminergic pathways are the mesocortical pathway, the nigrostriatal pathway, the tuberoinfundibular pathway and the mesolimbic pathway. Other dopaminergic pathways include the hypothalamospinal tract and the incerto-hypothalamic pathway.

The dopamine neurons of the dopaminergic pathways synthesize and release the neurotransmitter dopamine. Enzymes tyrosine hydroxylase and dopa decarboxylase are required for dopamine synthesis. Dopamine is stored in the cytoplasm and vesicles in axon terminals. Dopamine release from vesicles is triggered by action potential propagation-induced membrane depolarization. The axons of dopamine neurons extend the entire length of their designated pathway.

### **Mother and nurturing children**

The atrophy of the mammalian olfactory bulb lead humans into motor and re-adaptive brain needs. Thus, saliva transitional hormonal communication of infants, allows the brain itself to improve velocity by myelination of axons. After three years infants show a functional amygdala and hippocampus, but still have under developed parts of the frontal brain.

7-transmembrane (7TM)-hormonal receptors binding by noradrenaline (NA) activate adenylate cyclase (AC). The dendrites at the oral-cavity of NA-AC-Hypothalamic (OC-NA-AC-HT) axis have axons across the blood-brain-barrier (BBB). Its function is to modulate the hypothalamic-pituitary-adrenal (HTPA) axis and its secretions into the capillary arterioles irrigating the oral cavity.

The blood-cerebrospinal fluid barrier (BCSFB) is a fluid-brain barrier that is composed of a pair of membranes that separate blood from cerebrospinal fluid (CSF) at the capillary level and CSF from brain tissue.

The choroid plexus produce and secrete most of the CSF of the central nervous system are ependymal cells surrounding a core of capillaries and loose connective tissue, operating as an open system coupled to in-flow  $Mg^{2+}$  follow by  $Ca^{2+}$  reversible flow from calmodulin (CaM).

The thermodynamics relationship between structure and function requires an astrocytes network for circulation after of H-bond breakdown

at the transition of hydrated R-groups in proteins in mutual exclusion with the dehydrated ones in oxyHb to deoxyHb, and plasma to CSF.

The cAMP response element binding (CREB) protein via stimulatory or inhibitory receptors (R<sub>s</sub> and R<sub>i</sub>) on G protein phosphorylation could stimulate signaling rewards during stages of neuronal plasticity, allowing mechanisms for connectome development.

The CREB characterizes implementation of transcription by an Mg-cAMP to opening the double stranded DNA, at specific regions for a switch on-off for RNA synthesis. Insulinotropic cortisol-release-hormone (CRH) inactivated due to a reduced ATP and cAMP, and loss of intracellular Ca<sup>2+</sup> oscillations. Emotional learning allows to bypass genetic constraints of the non-mature brain to obtain a self-cognition, which adapts the individuals for family and social links at the unconscious level. The genetic vs environmental experiential learning is the paths along the nurturing context of emotional intelligence development not directly correlated to a genetic framework. The learning from a hormonal nurturing communication between infant and mother became a stage for the learning experience of acquiring correlations between sounds, movement of face muscle for expressions that allow imitative/mirror neurons to slowly replace the hormonal mother communication by the family behavior language.

Genes account for between approximately 50% and 70% of the variation in cognition at the population level. A connectome is a comprehensive map of neural connections in the brain, and may be thought of as its “wiring diagram”. An organism's nervous system is made up of neurons which communicate through synapses. A connectome is constructed by tracing the neuron in a nervous system and mapping where neurons are connected through synapses.

During childhood, cognitive abilities dramatically improve to make humans capable of multiple differential activities: academic, social, professional, etc.

Intelligence coefficient (IQ) differences between individuals have been shown to have a large hereditary component. However, it does not mean at groups-level that exist evidence for a genetic component differentiating racial groups.

The results suggest a synchrony between gender-related differences in the brain network and behavior. Since during nurturing mother's behavior differentiate by conditioning the child to conform to a sex differentiation that naturally develops in men by a prefrontal to visual cortex and in woman by transversal connectomes.

Stronger structural connectivity in motor, sensory, and executive functions matched higher spatial and motor skills in men. In men, there is increased neural connectivity within one hemisphere of the brain. Thus, suggesting that men's brains are structured to facilitate connectivity and coordination between perception and action.

In women, there are stronger neural connections between both cerebral hemispheres, which would facilitate communication between the analytical mind and intuition. In women, the subnets associated with social cognition, attention and memory showed greater connectivity, which was consistent with higher cognitive-social and memory skills in women than in men.

No differences have been found in the size of the corpus callosum or in the white matter, which allows the two sides of the brain to communicate with each other.

Studies of human patterns resulting from interaction of mother-infant separation, as related with decreased glucocorticoid receptor gene methylation of post-traumatic from early life stress. Thus, the family a frustration of non-accepted immigrants became manifested at child level by conditioning autism.

The microtubules (MTs) on the hormonal mother-infant [12] allow communication in an immature brain experiential learning. The synchronization in the spin-torque nano-oscillator as antennal signals of microwave frequencies participates in the emotional associations overcoming genetic dominance by all ready develops neuronal circuits. This period could effectively allow humans differentiation an evolution [13].

## Cell cycle

The development of the vertebrate central nervous system is reliant on a complex cascade of biological processes that include mitotic division,

relocation of migrating neurons, and the extension of dendritic and axonal processes. Each of these cellular events requires the diverse functional repertoire of the microtubule cytoskeleton for the

generation of forces, assembly of macromolecular complexes and transport of molecules and organelles.

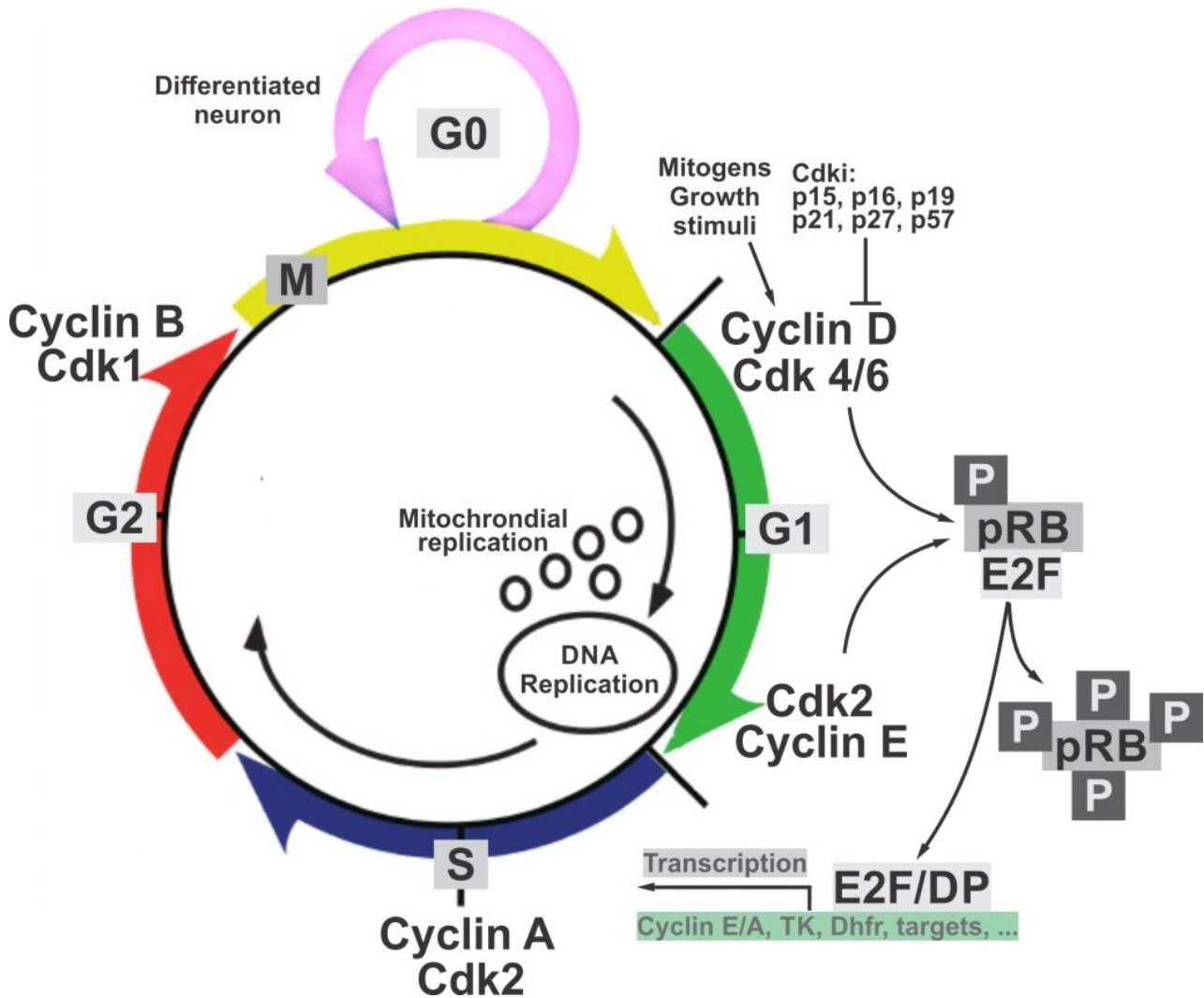


**Figure 2: The cell cycle consists of two main phases: interphase (G1, S, G2) and mitosis.** During interphase, the cell grows and replicates its DNA. In the mitosis phase, the cell undergoes nuclear division. The function of mitogen triggers signal transduction of mitogen-activated protein kinase (MAPK) for mitosis. The G1 is controlled by mitogens the cycle progression leads to a restriction point without mitogens, like mitogen-activated kinase. A cancer cells lose their dependence on mitogens. The hypothalamic-pituitary-gonadal (HPG) axis refers to the hypothalamus, pituitary gland, and gonadal glands as if these individual endocrine glands were a single entity, controls as the reproductive and immune systems and development and regulation as the reproductive and immune systems and aging in animals. The hypothalamus secretes the gonadotropin-releasing hormone (GnRH) from its expressing neurons. The anterior pituitary gland produces luteinizing hormone (LH) and follicle-stimulating hormone (FSH), and the gonads produce estrogen and testosterone. Gonadal sex steroids act in negative- and positive-feedback loops to regulate reproductive circuitry in the brain, including kisspeptin neurons, thereby modulating overall HPG axis status [14]. Checkpoints at the cell cycle indicate that neurons could not proceed further.

The mechanistic target of rapamycin complex (mTORC) is a nutrient/energy/redox sensor, controlling protein synthesis. mTORC1 is modulate by rapamycin, insulin, growth factors, phosphatidic

acid, certain amino acids and their derivatives (l-leucine and  $\beta$ -hydroxy  $\beta$ -methylbutyric acid), protein synthesis, mechanical stimuli, and oxidative stress. Manifest the deregulation of signaling in the

progression of cancer, diabetes and the aging process [15] [16] [17].

The hypothalamic-pituitary-gonadal (HPG) hormone axis deregulated leads to an aberrant in menopause and andropause promotes cell cycle reentry (dyosis) and eventual neuron dysfunction and death. The cell cycle signaling pathways in DNA replication, mitochondrial DNA replication, tau phosphorylation and altered A $\beta$  PP processing. This dysregulation leads to altered metal ion metabolism and oxidative stress. Hormonal signals stimulate the interphase of cell division the completion of metaphase is inhibited. The series of kinases from RAF to MEK to MAPK is a cascade, with feedback regulation and signal amplification.

*Kinase cascade:* Activated Ras then activates the protein kinase activity of a RAF kinase. The RAF kinase phosphorylates and activates a MAPK/ERK Kinase (MEK1 or MEK2). The MEK phosphorylates and activates a mitogen-activated protein kinase (MAPK). RAF and MAPK/ERK are both serine/threonine-specific protein kinases. MEK is a serine/tyrosine/threonine kinase.

In a technical sense, RAF, MEK, and MAPK are all mitogen-activated kinases, as is MNK. MAPKs, “extracellular signal-regulated kinases” (ERKs) and “microtubule associated protein kinases” (MAPKs).

*Regulation of translation and transcription:* Three of the many proteins that are phosphorylated by MAPK. One effect of MAPK activation is to alter the translation of mRNA to proteins. MAPK phosphorylates the 40S ribosomal protein S6 kinase (RSK). This activates RSK, which, in turn, phosphorylates ribosomal protein S6.

MAPK regulates the activities of several transcription factors. MAPK can phosphorylate C-myc. MAPK phosphorylates and activates MNK, which, in turn, phosphorylates CREB. MAPK regulates the transcription of the C-Fos gene. By altering the levels and activities of transcription factors, MAPK leads to altered transcription of genes that are important for the cell cycle.

*Role of mitogen signaling in cell cycle progression:* The presence of mitogens and growth factors trigger the activation of canonical receptor tyrosine kinases such as EGFR leading to their dimerization and subsequent activation of the small GTPase Ras. This then leads to a series of phosphorylation

events downstream in the MAPK cascade (Raf-MEK-ERK), resulting in the phosphorylation and activation of ERK. The phosphorylation of ERK results in an activation of its kinase activity and leads to phosphorylation of its many downstream targets involved in regulation of cell proliferation. In most cells, some form of sustained ERK activity is required for cells to activate genes that induce cell cycle entry and suppress negative regulators of the cell cycle.

*Downstream feedback control and generation of a bistable G1/S switch:* the restriction point (R-point) has been linked to various activities involved in the regulation of G1–S transition of the mammalian cell cycle. Growth and mitogen signals are transmitted downstream of the ERK pathway are incorporated into multiple positive feedback loops to generate a bistable switch at the level of E2F activation. This occurs due to three main interactions during late G1 phase. The first is a result of mitogen stimulation through the ERK leading to the expression of the transcription factor Myc, which is a direct activator of E2F. The second pathway is a result of ERK activation leading to the accumulation of active complexes of Cyclin D and Cdk4/6 which destabilize Rb via phosphorylation and further serve to activate E2F and promote expression of its targets.

Additional positive feedback loop by E2F on itself, as its own expression leads to production of the active complex of Cyclin E and CDK2, which further serves to lock in a cell's decision to enter S-phase. Most cells respond in a switch-like manner in entering S-phase. This mitogen stimulated, bistable E2F switch exhibits hysteresis, as cells are inhibited from returning to G1 even after mitogen withdrawal post E2F activation.

*ERK pathway signal processing:* The epidermal growth factor receptor extracellular-regulated kinase/mitogen-activated protein kinase (EGFR-ERK/MAPK) pathway stimulated by EGF is critical for cellular proliferation, but the temporal separation between signal and response obscures the signal-response relationship in previous research.

*Integration of mitogen and stress signals in proliferation:* Daughter cells starting with no significant signaling proteins after division, mitogen/ERK induced Cyclin D1 mRNA and

DNA damage induced p53 protein, both long lived factors in cells, can be stably inherited from mother cells after cell division. Chemical perturbations using inhibitors of ERK signaling or inducers p53 signaling in mother cells suggest daughter cells with high levels of p53 protein and low levels of Cyclin D1 transcripts were shown to primarily enter G0 whereas cells with high Cyclin D1 and low levels of p53 are most likely to reenter the cell cycle.

Receptor tyrosine kinases (RTKs) are the high-affinity cell surface receptors for many polypeptide growth factors, cytokines, and hormones. Of the 90 unique tyrosine kinase genes identified in the human genome, 58 encode receptor tyrosine kinase proteins. Mutations in receptor tyrosine kinases lead to activation of a series of signaling cascades which have numerous effects on protein expression. Receptor tyrosine kinases are part of the larger family of protein tyrosine kinases, encompassing the receptor tyrosine kinase proteins which contain a transmembrane domain, as well as the non-receptor tyrosine kinases which do not possess transmembrane domains.

To propagate its genome from one cell to the next each progenitor must successfully duplicate and segregate its complement of chromosomes. This requires the formation of a bipolar mitotic spindle in prometaphase, followed by the generation of force to separate sister chromatids. Aided by kinetochores microtubules are charged with the task of searching and capturing chromosomes. The cytokinesis plays an active role along the metaphase.

Upon induction of the anaphase a promotion of complex microtubules rapidly translocate the attached chromosomes to either end of the cell cortex (interkinetic nuclear migration) [18].

### **Crosstalk between insulin/glutamatergic and catecholaminergic systems**

Insulin receptor tyrosine kinase (IRTK) was studied by multiple equilibrium equations to solve the separate an individual effect of ionic divalent metals, free nucleotides and their chelated species. Basal IRTK is activated by divalent metal cations when present in excess of that required for substrate formation, indicating the presence of a divalent cation-dependent regulatory site on the kinase. The activatory order for basal activity was

$Mn^{2+}$  greater than  $Co^{2+}$  greater than  $Mg^{2+}$  and  $Ca^{2+} = 0$ .

Thus, the activities of IRTK and adenylate cyclase (AC) are subject to modulation not only by fluctuations in the concentration of intracellular ATP and the relative concentrations of phosphorylated metabolic intermediates.

In liver IRTK interacts in a mutually inclusive manner with AC for free divalent metal and metal-ATP substrate.  $CaCl_2$  saturation curves in the presence of constant  $MnCl_2$  and increasing  $MgCl_2$  showed that the affinity of IRTK for  $Ca^{2+}$  decreases and the affinity for  $CaATP$  increased with increasing  $Mg^{2+}$ . Thus, suggests that IRTK contains three sites for interaction with divalent metal cations: a  $MeATP$  (active) site, a regulatory site, and a metal-dependent site acting to couple the receptor with the kinase [19].

Insulin regulates glucose homeostasis, maintaining energy requirements for different neuronal functions, and is involved in neurite outgrowth. Phosphorylation of serine and threonine residues on the  $\beta$ -subunit of the receptor by either phorbol esters or catecholamines results in a decrease in IRTK activity. The presence of a membrane-bound protein phosphotyrosine phosphatase may play a role in the regulation of IRTK activity.

Insulin release is stimulated by beta-2 receptor stimulation and inhibited by alpha-1 receptor stimulation. Cortisol, glucagon and growth hormone antagonize the actions of insulin during times of stress. Insulin inhibits fatty acid release by hormone sensitive lipase in adipose tissue and more recently has been characterized the specific effect in brain.

The divalent metal cations ( $Mn^{2+}$ ,  $Mg^{2+}$  and  $Ca^{2+}$ ) involve activation and regulation of IRTK activity [20]. The phosphorylated metabolic intermediates produced during glycolysis and gluconeogenesis regulates IRTK and AC activity.

Thiocyanate ( $SCN^-$ ) in addition to being a potent inhibitor of gastric acid secretion is capable of cytoprotection against acid ethanol-induced mucosal injury in vivo and to relate this cytoprotection to the secretion of  $HCO$  and  $K^+$  into the gastric lumen in vitro [21].

IRTK, upon activation by insulin, increases the flux of glucose through the glycolytic pathway and

AC in the body, upon activation by glucagon, will stimulate gluconeogenesis.

Both of these pathways result in an increase in phosphorylated chelating metabolites and are thus subject to an integrative regulatory mechanism since both IRTK and AC share common positive modulators. If the rate of utilization of these metabolites decreases, their resulting accumulation may function as a signal to decrease the activities of IRTK and/or AC via a decrease in the concentration of activating divalent metals.

The kinetic and thermodynamic interrelationships of peptide substrate (Val5-angiotensin 11), metal-ATP, and divalent metal cations with rat liver IRTK were investigated [22]. Results of the initial rate studies with varying peptide and MnATP substrates indicates that the kinetic mechanism for IRTK is of the sequential type and therefore rules out a ping pong Bi Bi pathway. Hence, peptide substrate and metal-ATP bind to the kinase prior to the release of products. MnADP was a linear competitive inhibitor of MnATP and a noncompetitive inhibitor of peptide substrate. A synthetic tyrosine-containing pentapeptide, Glu-Glu-Phe-Tyr-Phe (EEFYF), was a linear competitive inhibitor of peptide substrate and a noncompetitive inhibitor of MnATP. Accordingly, the data show that phosphorylation of peptide substrate occurs via a rapid random equilibrium Bi Bi mechanism in which the kinase has the potential to react initially with either of the two substrates. In contrast, divalent metal cations and metal-ATP were found to interact with the kinase in a mutually inclusive manner, with metal binding to the kinase prior to MnATP. It was found that divalent metals increase the affinity of the kinase for metal-ATP but do not affect the affinity of IRTK for metal-ADP product. Hence, divalent metals, during the reaction of association of enzyme with one of its substrates to form the binary complex, increase the relative concentration of E-ATP complex versus E-peptide complex, thus introducing a thermodynamic-dependent ordering for the interaction of substrates with the enzyme.

Downstream effects of hippocampal post-synaptic insulin signaling have been described to include inhibition of  $Ca^{2+}$  oscillations, mediated by ERK activation and  $K^+$  influx; depolarization because of enhanced exocytosis of NMDAR; long-

term depression as a result of exocytosis of GluA1- and endocytosis of GluA2-containing AMPAR ( $\alpha$ -amino-3-hydroxy-5-methylisoxazole-4-propionate receptor); reduced excitability because of enhanced exocytosis of GABAAR; and increased spine formation or survival, mediated by PI3K activation.

Anaplastic lymphoma kinase (ALK) receptor tyrosine kinase: This gene encodes a receptor tyrosine kinase, which belongs to the insulin receptor superfamily [23]. This protein comprises an extracellular domain, a hydrophobic stretch corresponding to a single pass transmembrane region, and an intracellular kinase domain. The organization of the microtubule system incorporates motor movement for thermodynamic cargo, incorporating enthalpy contribution and the exclusion of entropy.

Diacylglycerol (DAG), cAMP, cyclic guanosine monophosphate (cGMP) and arachidonic acid acting from the cytoplasmic side opens second messenger-operated channels (SMOCs) in the plasma membrane. Cell-surface receptors inositol 1,4,5-trisphosphate (InsP3), which then diffuses into the cell to activate the InsP3 receptor to release  $Ca^{2+}$  from the ER.

In cardiac tissues, there are three pharmacologically distinct subtypes of  $\beta$ ARs.  $\beta_1$  and  $\beta_2$ AR stimulate AC activity via Gs protein to produce cAMP, which binds to and activates PKA. This leads to phosphorylation of a number of targets including phospholamban (PLB) a pentamer substrate for the cAMP-dependent PKA in cardiac muscle. In the unphosphorylated state PLB is an inhibitor of cardiac

The activated GLP-1 receptor facilitates insulin secretion by inciting AC, which accelerates the transformation of ATP to cAMP. The downstream molecules of cAMP, the cAMP-dependent protein kinase A (PKA) and Epac (exchange protein activated by cyclic-AMP) 2, stimulate inositol 1,4,5-trisphosphate (IP3) receptor on the ER and lead to the release of  $Ca^{2+}$  from ER, thus intensifying insulin secretion. GPR40 and GLP-1 suppressed by statins reopen  $K^+$ -ATP channels and decrease intracellular  $Ca^{2+}$ , further hindering insulin secretion [24].

The muscle sarcoplasmic reticulum  $Ca^{2+}$ -ATPase (SERCA2) transports  $Ca^{2+}$  from cytosol into the sarcoplasmic reticulum. Troponin-I (TnI),

and L-type  $\text{Ca}^{2+}$  channel, all being responsible for cardiac contractile function [25].

Bidirectional action of insulin alters brain activity in the nucleus accumbens (NAc)

glutamatergic transmission and insulin receptor glutamate release, affecting brain activity that mediate reward and motivation [26].

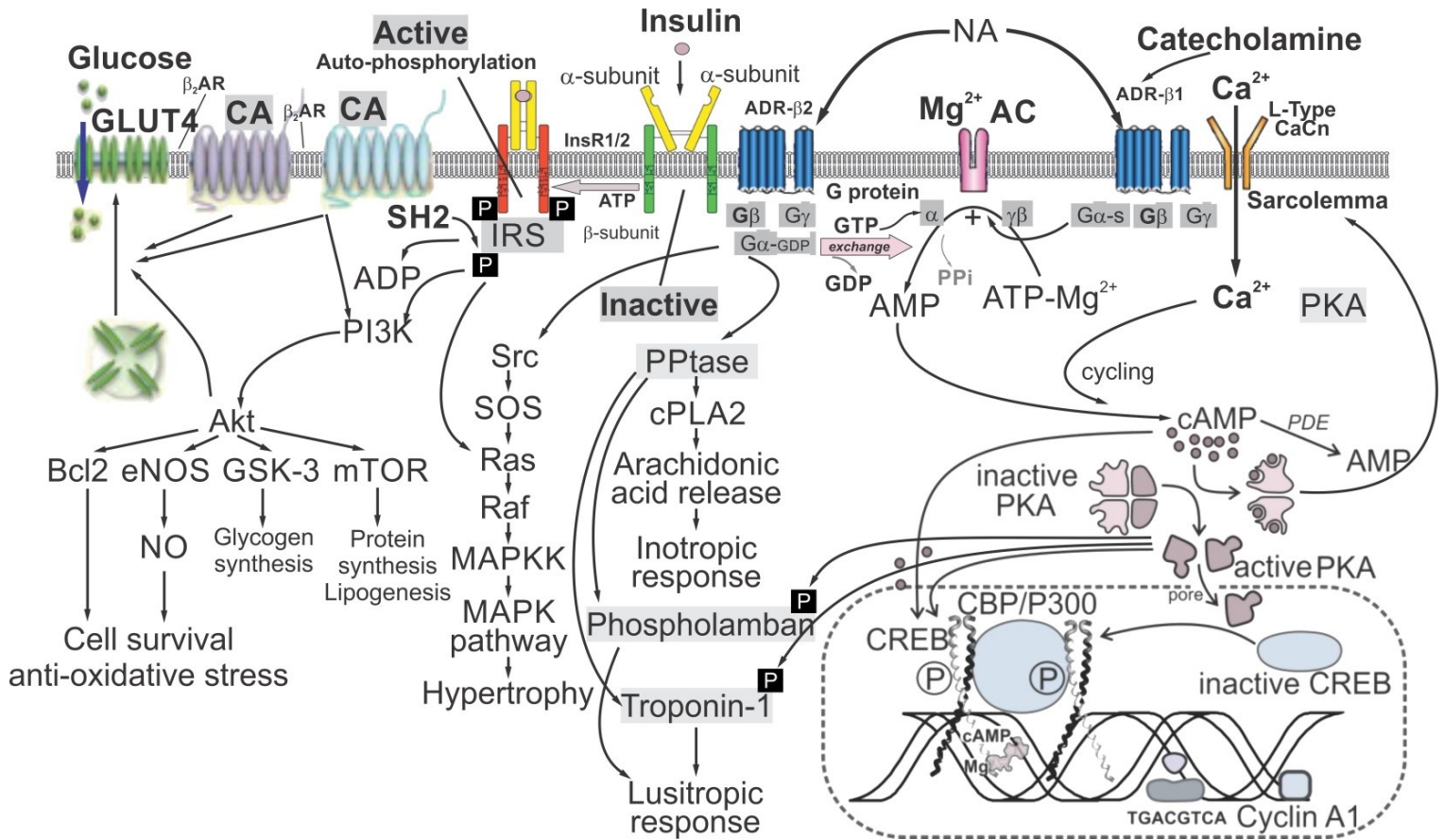


**Figure 3: Insulin receptor substrate 1 and 2. Adrenergic receptor activation and inhibitor.** Agonists: *salbutamol*; Antagonists: *labetalol*. Abbreviations:  $\beta$ AR,  $\beta$ -adrenergic receptor; Bcl-2, B cell lymphoma 2; CA, catecholamine; eNOS, endothelial nitric oxidase; ERK1/2, extracellular-regulated kinase 1/2;  $G_i$ , inhibitory regulatory G-protein; GRK2, G-protein receptor kinase 2;  $G_s$ , stimulatory G-protein; GSK, glycogen synthase kinase; MAPK, mitogen-activated protein kinase; mTOR, mammalian target of rapamycin; NO, nitric oxide; PI3K, phosphatidylinositol 3-kinase; PKA, protein kinase A; Ras, rat sarcoma; ROS, reactive oxygen species; SNA, sympathetic nervous activity. CaMKII, calmodulin-dependent kinase.

Crosstalk between tyrosine kinase and G-protein-linked receptors operative for the insulin/glutamatergic and catecholaminergic systems act for phosphorylation of adrenergic receptors in response to insulin.

The mature insulin receptor composed of two extracellular  $\alpha$ -subunits and two intracellular  $\beta$ -subunits. Contiguous modules of the two  $\alpha$  subunits are indicated by black or white labels and dashed tracings. The holoreceptor is stabilized extracellularly by disulfide bonds between cysteine residues (S-S) in the  $\alpha$ - and  $\beta$ -subunits, as well as by noncovalent interactions.

Two regions within the  $\alpha$ -subunit contribute to insulin binding S1 of insulin. The  $\beta$ -subunit contains the tyrosine kinase catalytic domain with an ATP-binding site (Lys1030) and several tyrosine phosphorylation sites.

### The mTOR signaling increase at aging is opposed by rapamycin restoration of life span

The Ras homolog enriched in brain (RHEB) kinase activity involves binding to mammalian target of rapamycin (mTOR) distally from the kinase active site, relieving the auto-inhibition RAPTOR-

TOS motif complexes reveal a second substrate-recruitment mechanism, and of a truncated mTOR-PRAS40 complex [27].

Arginine, an amino acid essential during mammalian embryogenesis and early development, acting independently of its metabolism, allow maximal activation of mTORC1 by growth factors via a mechanism that does not involve regulation of

mTORC1 localization to lysosomes. Arginine specifically suppresses lysosomal localization of the TSC complex (TSC-RHEB) and interaction with its target small GTPase protein, RHEB. Arginine cooperates with growth factor signaling promotes dissociation of TSC2 from lysosomes and activation of mTORC1 [28].

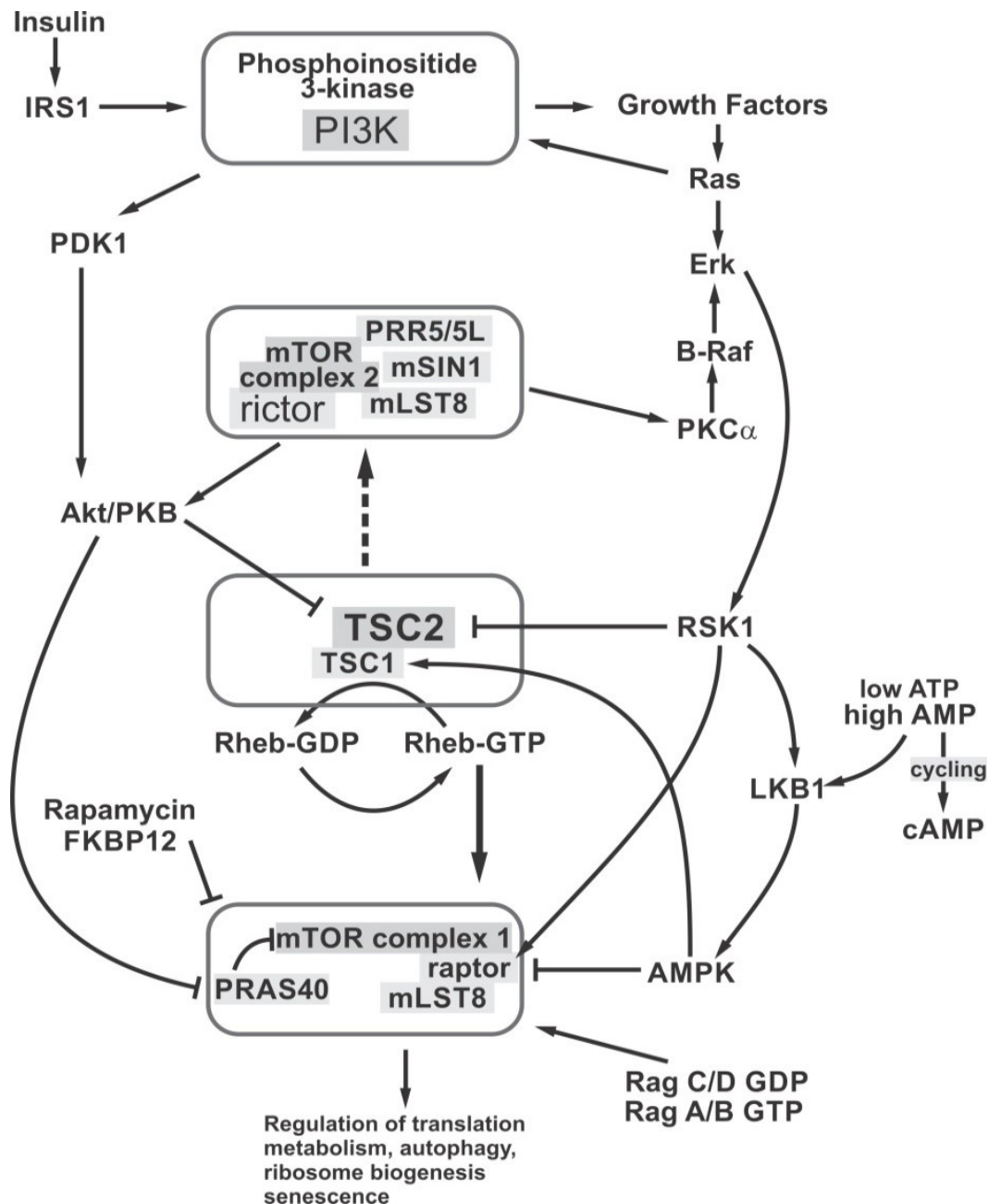


**Figure 4: mTOR signaling pathway.** The mTOR is the catalytic subunit of two structurally distinct complexes: mTORC1 and mTORC2. The two complexes localize to different subcellular compartments, thus affecting their activation and function. Upon activation by Rheb G-protein, mTORC1 localizes to the Ragulator-Rag complex (is a regulator of lysosomal signalling and trafficking in eukaryotic cells) on the lysosome surface where it then becomes active in the presence of sufficient amino acids.

It is hypothesized that some dietary regimes, like caloric restriction and methionine restriction, cause an extension of lifespan by decreasing mTOR activity. The mTOR signaling an antagonistic pleiotropy, and while high mTOR signaling is good during early life, it is maintained at an inappropriately high level in old age. Calorie restriction and methionine restriction may act in part by limiting levels of essential amino acids including leucine and methionine, which are potent activators of mTOR. The administration of leucine into the rat brain has been shown to decrease food intake and body weight via activation of the mTOR pathway in the hypothalamus [29].

Aging implicates reactive oxygen species damaging to mitochondrial proteins and decrease ATP production. Hence, via ATP sensitive AMPK, the mTOR pathway is inhibited and ATP-consuming protein synthesis is downregulated by mTORC1 initiating a phosphorylation cascade, activating the ribosome. Disruption of mTORC1 inhibits mitochondrial respiration. These positive feedbacks on the aging process are counteracted by protective mechanisms: Decreased mTOR via autophagy removes of dysfunctional cellular components. A metabolic organization at the cell physiological level of NA-AC and insulin receptor tyrosine kinase (IRTK) responsiveness to hormones could be modulated by the concentration of chelating metabolites because the stress activator role of adrenergic receptors could be inhibited and the response to insulin, activated by kinases-dependent protein phosphorylation and captures of cations, including  $Mg^{2+}$ . Thus, a decreased  $Mg^{2+}$  produces deactivated AC by releasing free  $ATP^{4-}$  and activate the IRTK. Thus, allows an integration of the hormonal response of both enzymes by ionic controls. This effect could supersede the metabolic feedback control by energy charge. Accordingly, maximum hormonal response of both enzymes, to high  $Mg^{2+}$  and low free  $ATP^{4-}$ , allows a correlation with the known effects of low caloric intake increasing the level of free ions could elevate the average life expectancy [30].

The mTOR is an important initiator of the senescence-associated secretory phenotype (SASP). Interleukin 1 alpha (IL1A) is highly dependent upon mTOR activity.

Insulin may affect  $\beta$  adrenergic receptor ( $\beta$ AR) signaling in the heart to modulate cardiac function in. Activation of  $\beta$ AR regulates cardiac glucose uptake and promotes insulin resistance (IR) in heart failure (HF). The interaction between insulin receptor (InsR) stimulation crosstalks with cardiac  $\beta$ AR, via InsR substrate (IRS)-dependent and G-protein receptor kinase 2 (GRK2)-mediated phosphorylation of  $\beta$ 2AR. Phosphodiesterase-4D eliminates and RNA interference-mediated overwhelming enhances memory and increase hippocampal neurogenesis via increased cAMP signaling.

AMPK is expressed in a number of tissues, including the liver, brain, and skeletal muscle.

The  $\alpha$ -subunit contains the kinase domain, which transfers a phosphate from ATP to the target protein. The  $\beta$ -subunits and  $\gamma$ -subunits are considered as regulatory components. All three subunits are required for expression of full activity of the AMPK enzyme complex, is allosterically regulated by the cellular AMP (adenosine 5-monophosphate)/ATP ratio and by upstream kinases.

Full activation of AMPK requires phosphorylation of its activation loop at Thr172 (Threonine-172) of its catalytic  $\alpha$ -subunit, by upstream kinases collectively known as AMPKKs (AMPK (AMP-Activated Protein Kinase) Kinases).

AMP stimulates the phosphorylation, both by binding to AMPK and making it a better substrate, and by activating the upstream AMPKKs. AMP binding to AMPK inhibits dephosphorylation by protein phosphatases. AMPK activation switches on anabolic pathways and other processes that consume ATP, while switching on catabolic pathways that generate ATP.

### Insulin receptor tyrosine kinase

The separate effects of the equilibrium species  $Mg^{2+}$ ,  $MgATP$  substrate, and  $ATP^{4-}$  on the reaction catalyzed by insulin receptor tyrosine kinase (IRTK) were examined. The separated kinetic constants show that the  $K_{0.5}$  value for  $Mg^{2+}$  decreased from 23 to 0.43 mM and the Hill coefficient for  $Mg^{2+}$  ( $hMg^{2+}$ ) decreased from 1.43 to 0.668 when the concentration of  $ATPT$  ( $MgATP + ATP^{4-}$ ) was increased from 50 to 1000 microM. The apparent

$K_i$  for  $ATP^+$  increased from 0.20 to 136  $\mu M$  and the Hill coefficient for  $ATP^+$  ( $hATP^+$ ) decreased from 1.41 to 0.82 as the concentration of total ATP increased. These findings suggest that the  $[ATP^+]/[Mg^{2+}]$  ratio modulates the shift from positive to negative cooperativity. It was shown that the apparent affinity of the kinase for MgATP increased as the concentration of free  $Mg^{2+}$  increased and that the apparent affinity of the kinase for free  $Mg^{2+}$  increased as the concentration of MgATP substrate increased.

$Mg^{2+}$  and MgATP interact with the kinase in a mutually inclusive manner which leads to an increase in the ratio of the enzyme (E) rate-limiting species,  $[Mg-E-MgATP]/[E-MgATP]$ . Free  $ATP^+$  not only acts as a competitive inhibitor of the substrate but decreases the relative concentration of Mg-E-MgATP. Hence, indicates that the effect of  $Mg^{2+}$  will be to form an enzyme complex (Mg-E) which will have a higher affinity for MgATP substrate and a lower affinity for  $ATP^+$  than E alone. The equilibrium concentrations of Mg-E, E and ATP-E on the activation of IRTK account for modulation of the cooperativity and the metal-dependent increase in turnover.

When phosphorylated by protein kinase A (PKA) disinhibition of the dead end inhibitor  $Ca^{2+}$ -ATPase leads to faster  $Ca^{2+}$  uptake into the sarcoplasmic reticulum to the myocardial relaxation elicited by beta-agonists.

Activation of  $\beta$ -adrenergic receptor ( $\beta$ AR) by catecholamines induces the production of cAMP through the Gs-adenylyl cyclase (AC) cascade, which promotes PKA activity for cellular responses in cardiomyocytes. In heart failure (HF),  $\beta$ 1AR undergoes endocytosis, whereas  $\beta$ 2AR is relocated from the t-tubular to the crest membrane.

Insulin promotes glucose uptake in cardiomyocytes through activation of an InsR-mediated phosphatidylinositol 3-kinase (PI3K)-Akt pathway, which mobilizes glucose transporter 4 (GLUT4) vesicles to the cell surface for glucose uptake. Stimulation of  $\beta$ AR in the heart induces an additive effect on insulin-induced glucose uptake, an effect that is mediated by phosphorylation of Akt at Thr308 through the protein kinase A (PKA)/ $Ca^{2+}$ -dependent pathway. At the cellular level, stimulation with either insulin or catecholamines antagonizes the ability of the other to activate glucose transport

and to modulate cardiomyocyte survival. Thus, was shown a counter-regulation between insulin and  $\beta$ AR signaling in the heart.

The cAMP-dependent PKA ability to phosphorylate appears in the human hearts cGMP dependent protein kinase G (PKG) [31].

The insulin-sensitive cells (adipocytes, myocytes, hepatocytes, etc.) show a transmembrane IRKT located in the plasma membrane. It mediates on specific cellular responses (glucose transport, glycogen synthesis, lipid synthesis, protein synthesis, etc.).

Insulin like growth factor-1 (IGF-1) is ubiquitously expressed growth factor that has profound effects on the growth and differentiation of many cell types and tissues, including cells of the central nerve system (CNS). IGF-1 is produced by a wide variety of cells and is found in many biological fluids including cerebrospinal fluid (CSF). IGF-1 acts during CNS development and repair function with neuroprotective effects at striatal neurons.

Each protomer of the insulin receptor (IR) contains a transmembrane  $\beta$  chain and an extracellular  $\alpha$  chain. In contrast with other cell types and the neuronal IRs lack exon 11. The intracellular domain contains both (self-) activating (tyrosine) and inhibitory (serine and threonine) phosphorylation sites in neurons. Synaptic terminal: the binding of insulin to a receptor increases the release of noradrenaline (NA) and dopamine and inhibits the uptake of noradrenaline; signaling of insulin through the IR increases dopaminergic firing frequency and decreases dopamine degradation.

Turnover, with release of  $Mg^{2+}$  from the regulatory site of the enzyme AC as a nascent  $Mg^{2+}$  acquires a stronger intrinsic charge.

### **Chelated metabolites modulate the concentration of free $Mg^{2+}$ vs $Ca^{2+}/CaM$**

Glucose intake and the capacity of its chelated metabolites to decrease the level of free obligatory magnesium ions in excess of substrate concentration decrease the activity of cerebral noradrenaline-adenylate-cyclase (NA-AC).

$ATP^+$  in excess deactivates the neuronal NA-AC and activates transmembrane enzymes like insulin receptor tyrosine kinase (IRTK) and other

enzyme that requires Mg-ATP to activation by auto-phosphorylation.

The normal levels of glucose in the cerebrospinal fluid (CSF) are greater than 50

mg/1dL to 80 mg/dL, or 2.8 mmol/L to 4.4 mmol/L, diurnal vs nocturnal levels of chelating metabolites capturing free  $Mg^{2+}$ .

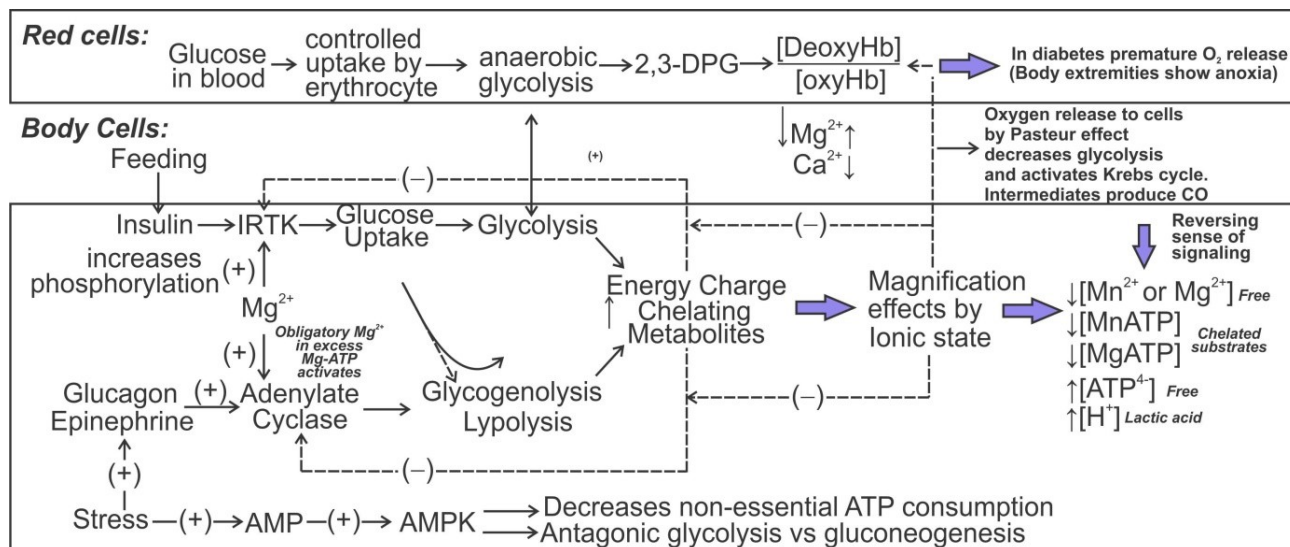


**Figure 5: Network integration of hormonal responsiveness of transmembrane AC and IRTK to metabolic-ionic feedback.**  $O_2$  uptake by the Pasteur Effect decreases glycolysis and activates the Krebs cycle. A decrease in chelating metabolism favors the release of nascent  $Mg^{2+}$  to activate the  $Na^+/K^+$ -pump. AC and IRTK-responsiveness enhancement by receptor kinases like liver IRTK, which by binding of insulin could phosphorylate downstream proteins inducing changes in cell responsiveness.

The network was idealized by an “in common” feedback control of hormone activity, by the metabolite modulated availability of free  $Mg^{2+}$  or  $Mn^{2+}$  and relative concentration  $[Mg^{2+}]/[Mn^{2+}]$  of the activators, versus the inhibitors  $[Ca^{2+}]$ ,  $[ATP^4]$  and  $[CaATP]$ , which acts as a dead-end inhibitor of NA-AC [32].

1-adrenaline, ACTH and glucagon activate the adenylate cyclase of rat adipocytes by decreasing its  $S_{0.5}(Mg^{2+})$  (concentration yielding 0.5  $V_{max}$ ) from its basal value of 11.5 to 1.2, 0.3 and 1.8 mM and by increasing its  $K_i(ATP^4)$  from 0.03 basal to 0.25; 0.62 and 0.16 mM respectively. The kinetic properties of the enzyme are regulated by its state of saturation with  $ATP^4$  or  $Mg^{2+}$ ; its saturation with  $ATP^4$  and citrate- suppressed its basal and hormone-dependent activities. The hormone-dependent decrease in the one half affinity for  $Mg^{2+}$   $K_m(Mg^{2+})$  and increase in  $V_{max}$  of the enzyme occur when shifting from suboptimal low concentrations of hormone and  $Mg^{2+}$  to optimal conditions, high concentration of hormone and low concentration of  $Mg^{2+}$ . The increase in the state of

saturation of the enzyme by  $Mg^{2+}$  decreases the hormone-dependent effects on  $V_{max}$  and results in identical values of affinity concentration  $K_m(0.14mM)$  for its basal and 1-adrenaline dependent activities.  $CaCl_2$  saturation curves at 5mM ATP with either 5, 10 or 20 mM  $MgCl_2$  show that the substitution of 5mM  $MgCl_2$  by 10 mM and 20 mM  $MgCl_2$  increased the  $K_i(Ca^{2+})$  of the enzyme from 0.19 to 0.49 and 0.94 mM but decreased its  $K_i(CaATP)$  from 0.42 to 0.19 and 0.14 mM respectively. Only when the concentration of  $MgCl_2$  exceeded that of  $ATP^4$  did 1-adrenaline and ACTH activate the enzyme by increasing its  $K_i(Ca^{2+})$ , only ACTH increased its inhibitory  $K_i(CaATP)$ . An increase in energy charge would decrease the intracellular concentrations of  $Mg^{2+}$  and  $Ca^{2+}$  because  $ATP^4$  has stronger binding constants for  $Mg^{2+}$  and  $Ca^{2+}$  than  $ADP^3-$  and  $AMP^2-$ . Hence, the reported properties of the enzyme suggests that changes in energy charge may allow for metabolic feedback control of the hormonal responsiveness of the  $Mg^{2+}$ ,  $Ca^{2+}$ ,  $ATP^4$  sensitive AC.

*The Metabolic Regulatory Role of Hormones:* The pathways for lipogenesis and lipolysis could not function simultaneously. Insulin deficiency and high levels of counter regulatory hormones adrenaline, glucagon, and cortisol combine to increase the activity of hormone-sensitive lipase to increase the release of free fatty acids, and decrease the activity of acetyl-coenzyme A (CoA) carboxylase [33].

The hormone is involved in fat, protein and carbohydrate metabolism, development, and the bone reabsorption decrease in bone formation and suppresses the immune system.

The released amino acids support liver gluconeogenesis and its output of glucose to maintain in the awoken individual the metabolic activity of brain.

Protein kinase-A (PKA) activation involves phosphorylation of other enzymes, such as phosphorylase-b inactive to its active form phosphorylase-a. Dephosphorylation of the latter reverts to the form “b”.

Liver has glucose-6-phosphatase (G-6-Pase), delivering of glucose by liver into blood. Peroxisome proliferator-activated receptor-coactivator-1 (PGC-1) decreases the glucose entry into the glycolytic cascade.

Thirteen kinds of mammalian phospholipase-C (PLC) are classified into six isotypes ( $\beta$ ,  $\gamma$ ,  $\delta$ ,  $\epsilon$ ,  $\zeta$ ,  $\eta$ ) and according to structure phosphorylate other molecules, leading to altered cellular activity.

PLC cleave the phospholipid phosphatidylinositol 4,5-bisphosphate (PIP<sub>2</sub>) into diacylglycerol (DAG) and inositol 1,4,5-triphosphate (IP<sub>3</sub>). IP<sub>3</sub> functions by raising cytosolic [Ca<sup>2+</sup>], which bind to its receptors like calcium channels in the smooth endoplasmic reticulum (ER). The Ca<sup>2+</sup> concentration at the cytosol increases inducing a cascade of intracellular changes. Ca<sup>2+</sup> and diacylglycerol (DAG) are intracellular second messengers which activate protein kinase C.

Physiologically, the early morning increase in cortisol release increases muscle proteolysis, releasing into blood an amino acids equivalent to about 1% per day of the total muscle weight.

Subsequently a release of testosterone reincorporates the amino acids in blood into muscle. The heart responsiveness to cortisol allows the release of amino acids from its muscular

structure, which could be a factor linking the time of maximal dead rate to a peaking on cortisol levels.

In central nervous system structures the glucocorticoid receptor has interactions with noradrenaline and serotonin. At the neural level has been implicated in short and long-term adaptation to stressors, including some mood dysregulation and dysfunctions like depression.

## Cholinergic

Cholinergic and glutamatergic neural activities are implicated in taste aversion learning. Choline acetyltransferase (CAT), acetylcholine (ACh) is synthesized by a single step reaction catalyzed by the biosynthetic enzyme choline acetyltransferase. As is the case for all nerve terminal proteins, CAT is produced in the cholinergic cell body and transported down the axon to the nerve endings. Both CAT and ACh may be found throughout the neuron, but their highest concentration is in axon terminals. The presence of CAT is the “marker” that a neuron is cholinergic, only cholinergic neurons contain CAT.

The rate-limiting steps in ACh synthesis are the availability of choline and acetyl-CoA. During increased neuronal activity the availability of acetyl-CoA from the mitochondria is upregulated as is the uptake of choline into the nerve ending from the synaptic cleft. Ca<sup>2+</sup> appears to be involved in both of these regulatory mechanisms. As will be described later, the inactivation of ACh is converted by metabolism to choline and acetic acid. Consequently much of the choline used for ACh synthesis comes from the recycling of choline from metabolized ACh. Another source is the breakdown of the phospholipid, phosphatidylcholine. One of the strategies to increase ACh neurotransmission is the administration of choline in the diet. However, this has not been effective, probably because the administration of choline does not increase the availability of choline in the central nerve system (CNS).

Most of the cellular ATP is present as an MgATP complex, which is the substrate for many enzymes including ATPases, adenylyl cyclase (AC) and insulin receptor tyrosine kinase (IRTK). Mg<sup>2+</sup> regulates many enzymes and transporters, and the release of Ca<sup>2+</sup> from the sarcoplasmic reticulum

(SR), modifying the activity of many ion channels in the plasma membrane.

The transcription factor DREAM (calsenilin/KChIP3), an EF-hand calcium-binding protein that represses transcription of prodynorphin and c-fos genes, when binding  $Mg^{2+}$  alters transcription. Free  $Mg^{2+}$  is buffered at about 1mM cytosolic  $Mg^{2+}$ , leading to claims that this ion does not play a direct signaling regulatory role.

Cytosolic free  $Mg^{2+}$  is regulated by plasma membrane and organelle transport, and by intracellular binding, is maintained far from electrochemical equilibrium.

$\beta$ -adrenergic agonists stimulate a large  $Mg^{2+}$  efflux from perfused heart and isolated myocytes. Noradrenaline (NA)-induced  $Mg^{2+}$  efflux from the cell is blocked by removing extracellular  $Ca^{2+}$ .

The involved mechanism may depend of the alteration of  $Mg^{2+}$  buffering and the release of  $Mg^{2+}$  into the cytosol, which cannot exceed the maximum rate of efflux across the plasma membrane.

$\beta$ -adrenergic agonists increase the NA responsiveness of AC and the formed cyclic adenosine monophosphate (cAMP) induce from mitochondria the efflux of  $Mg^{2+}$ , which is blocked by an inhibitor of the adenine nucleotide translocator (ANT).

It has been suggested that oxygenation increase the affinity for  $Mg^{2+}$  of Hb, allowing this protein to function as an  $Mg^{2+}$  carrier in the transition of oxyHb to deoxyHb. Cellular uptake of  $O_2$  could deliver  $Mg^{2+}$  for cellular metabolic activation, at the synaptic cleft  $Mg^{2+}$  initiate responsiveness to presynaptic NA activation of postsynaptic AC.

### **Parallel and anti-parallel**

The sympathetic nervous system (SANS or SYNS) is one of the three divisions of the autonomic nervous system, the others being the parasympathetic nervous system and the enteric nervous system. The enteric nervous system is sometimes considered part of the autonomic nervous system, and sometimes considered an independent system.

The autonomic nervous system functions to regulate the body's unconscious actions. The sympathetic nervous system's primary process is to stimulate the body's fight-or-flight response [34]. It

is, however, constantly active at a basic level to maintain homeostasis. The sympathetic nervous system is described as being antagonistic to the parasympathetic nervous system which stimulates the body to "feed and breed" and to (then) "rest-and-digest".

Initially, in a glutamatergic synapse, the neurotransmitter glutamate is released from the neurons and is taken up into the synaptic cleft. Glutamate residing in the synapse must be rapidly removed in one of three ways:

Postsynaptic neurons remove little glutamate from the synapse. There is active reuptake into presynaptic neurons, but this mechanism appears to be less important than astrocytic transport.

Astrocytes capillaries enveloping the endothelial cells allow a  $Ca^{2+}$ -contracting and  $Mg^{2+}$ -distending the tightness, between pericytes to modulate access across the blood-brain-barrier (BBB).

BBB occupies the largest surface area delimiting Blood-CNS (central nerve system) interface other barriers: the blood-retinal, blood-nerve, blood-labyrinth, and endothelial of brain with the choroid plexus to form the blood-cerebrospinal fluid (CSF).

Astrocytes could dispose of transported glutamate in two ways. They could export it to blood capillaries, which abut the astrocyte foot processes. However, this strategy would result in a net loss of carbon and nitrogen from the system. An alternate approach would be to convert glutamate into another compound, preferably a non-neuroactive species. The advantage of this approach is that neuronal glutamate could be restored without the risk of trafficking the transmitter through extracellular fluid, where glutamate would cause neuronal depolarization. Astrocytes readily convert glutamate to glutamine via the glutamine synthetase pathway and released into the extracellular space. The glutamine is taken into the presynaptic terminals and metabolized into glutamate by the phosphate-activated glutaminase (a mitochondrial enzyme). The glutamate that is synthesized in the presynaptic terminal is packaged into vesicles. The vesicular glutamate transporter (VGLUT) is responsible for the uptake of the excitatory amino acid. Once the vesicle is released, glutamate is removed from the synaptic cleft by

excitatory amino-acid transporters (EAATs). This allows synaptic terminals and glial cells to work together to maintain a proper supply of glutamate, which can be produced by transamination of 2-oxoglutarate, an intermediate in the citric acid cycle. Active synapses require presynaptically localized glutamine-glutamate cycle is a metabolic pathway to maintain excitatory neurotransmission from neurons which is then taken up into astrocytes (non-neuronal glial cells). In a return, astrocytes release glutamine to be taken up into neurons for use as a precursor to the synthesis of either glutamate or GABA.

The neuronal-capillary-astrocyte network for  $Mg^{2+}$ -activated adrenergic vs  $Ca^{2+}$ -activated glutamatergic modulation by the coupling to metabolism and the rate of the tricarboxylic acid (TCA) cycle.

The glycolysis and the pentose phosphate pathway, glycogen synthesis and degradation, gluconeogenesis, the TCA cycle, ketogenesis, ureogenesis, and the Glu-Gln/GABA cycle in brain, among others. This provides an *in vivo* evaluation of cerebral metabolic compartmentalization.

The  $\gamma$ -aminobutyric acid (GABA) ionotropic receptors ligand-gated channels  $Cl^-$  ion conducting through its pore, results in hyperpolarization of the neuron. The inhibitory effect at the neuronal central system decreases transmission of successful action potential at pH sensitive. Subunits could be activated and some inhibited by extracellular protons. The reversal potential of the GABA(A)-mediated inhibitory postsynaptic potentials (IPSP) in normal solution is  $-70$  mV.

GABA(B) receptors are metabotropic transmembrane receptors for GABA coupled to G-protein and linked to  $K^+$  channels are found in the central as well as in the autonomic division of the peripheral nervous system.  $[K^+]$  hyperpolarize the cell at the end of an action potential. The reversal potential GABA(B)-mediated IPSP (inhibitory postsynaptic potential) is  $100$  mV, more hyperpolarized than the GABA(A) IPSP. Acid-sensing ion channels (ASICs) near in the post-synaptic membrane are proteins that could respond rapidly to acid transients, affecting extracellular acidosis. This inhibits N-methyl-D-aspartate (NMDA) receptors and  $\alpha$ -amino-3-hydroxy-5-

methyl-4-isoxazolepropionic acid (AMPA) receptors.

The NMDA receptor is one of three types of ionotropic glutamate receptors, the other two being AMPA and kainate receptors. Depending on its subunit composition, its ligands are glutamate and glycine (or D-serine). However, the binding of the ligands is typically not sufficient to open the channel as it may be blocked by  $Mg^{2+}$  ions which are only removed when the neuron is sufficiently depolarized. AMPA ionotropic transmembrane receptor an ion channel for glutamate mediates fast synaptic transmission on the CNS.

The NMDA receptor is ionotropic, meaning it is a protein which allows the passage of ions through the cell membrane. The NMDA receptor is so named because the agonist molecule NMDA binds selectively to it, and not to other glutamate receptors.

NMDA receptors promote repolarization in pancreatic beta cells and thereby reduce glucose-stimulated insulin secretion patterns result from well-synchronized beta cell behavior mediated by calcium waves, signaling the receptor inhibition on beta cells functional connectivity.

The reaction catalyzed by insulin receptor tyrosine kinase was examined.  $Mg^{2+}$  and  $MgATP$  interact with the kinase in a mutually inclusive manner, which leads to an increase in the ratio of the enzyme (E) rate-limiting species,  $[Mg-E-MgATP]/[E-MgATP]$ .  $MgATP$  increases the affinity of the kinase for  $Mg^{2+}$ , thereby leading to saturation of the enzyme by lower concentrations of  $Mg^{2+}$  [35] [36] [37]. Thus, decrease saturation of the kinase with  $ATP^{4-}$  competitive inhibitor, not only at the active site but at a kinetically distinct regulatory site [38] [39] [40].

### **Integrated function of adenylate cyclase and insulin receptor tyrosine kinase (IRTK) Relationship between glutamatergic and catecholaminergic neurons**

Stress activates distinct neuronal circuits in the brain and induces multiple changes on the cellular level, including alterations in neuronal molecular structures of R groups of enzymes thermally responding to a nano space-time under quantum dynamics by a coordinative divalent metal ( $Mg^{2+}$ ,

Ca<sup>2+</sup>, etc.) R group chelation, could function as an enzyme metal complex became vectorial organize for active site dynamics transition. Thus, overcome the catalytic inanimate thermodynamics for converging from a quantum microscopic reversibility principle to a life itself adapting for a differential state in which can separate the

organization order of the space-time for the dimensionality of enzyme system.

The non-receptor tyrosine kinase c-Abl (ABL1) is a strategic signal transducer of intra and extracellular signals, and it shuttles between the cytoplasm and the nucleus [41].

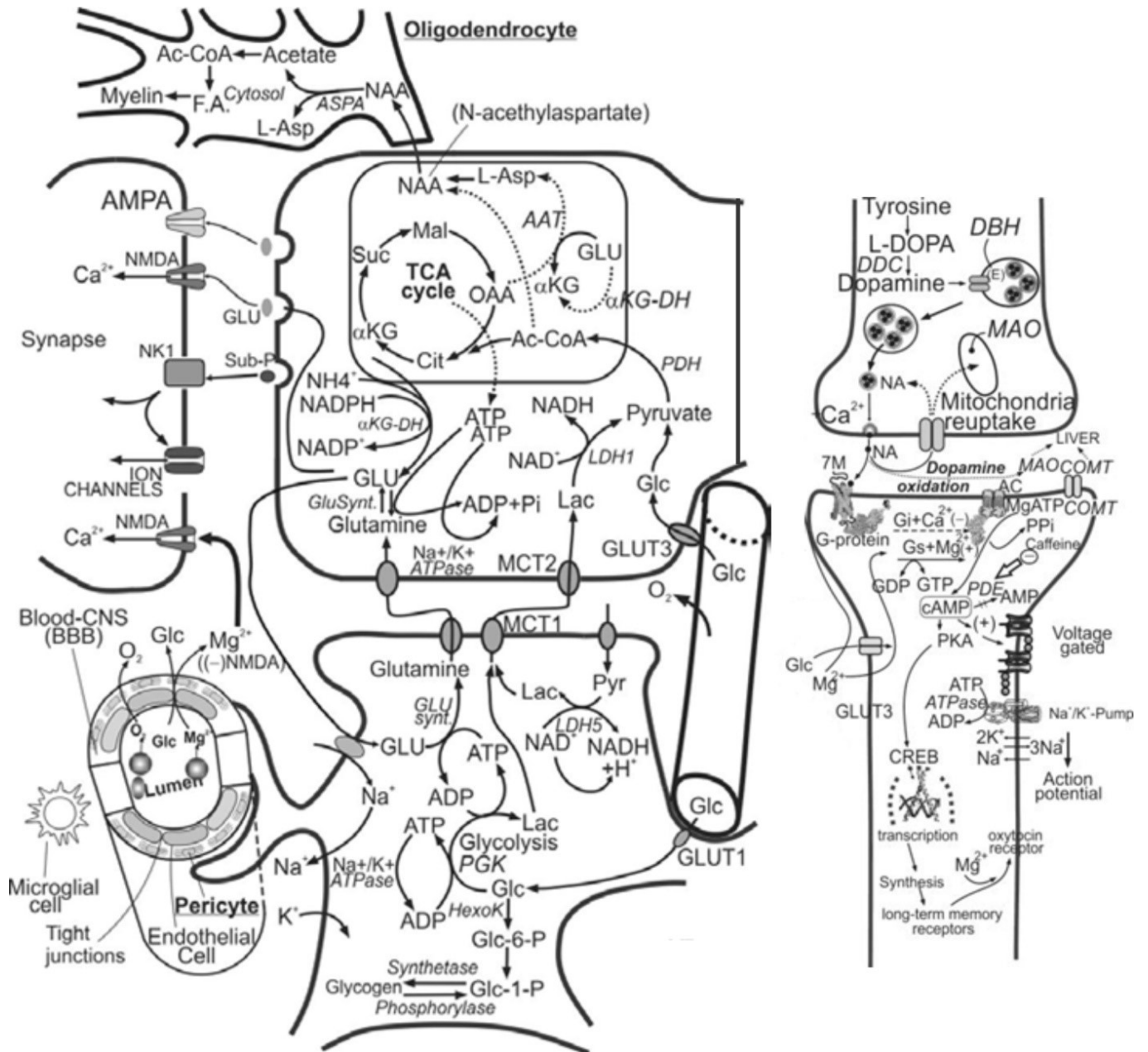


**Figure 6: Ionic-metabolic integrative coupling on the neuronal astrocyte-red cell system.** Neuron-astrocyte-BBB-(blood-brain-barrier) coupling on glutamatergic-(GLU)-neurotransmission. The neuronal mitochondria acetyl CoA and L-aspartate became the substrate to synthesizes N-acetylaspartate (NAA) a precursor with l-glutamate to form N-acetylaspartate-glutamate (NAAAG), which at the astrocyte could be broken by carboxypeptidase II, releasing L-glutamate and NAA. At the oligodendrocyte cells NAA by action of the enzyme aspartoacylase (ASPA) releases L-aspartate (L-Asp) and acetate.

The adrenergic system a G-protein-coupled receptor (GPCRs) exchanges binding of GDP inactive for GTP active (GDP/GTP-exchange) to conform a noradrenaline (NA) receptor coupled to adenylate cyclase (AC) at the *locus coeruleus* long axons synchronizing reality from all areas of the brain. The activatory signals of glutamic acid activated neuron conform well over 90% of the synaptic connections in the human brain, serving as the primary neurotransmitter for cerebellum granule cells.

Neuron uptake and stoichiometric cycling reversing the glutamate synthase reaction supports release of glutamate (Glu), activating the postsynaptic N-methyl-D-aspartate (NMDA) receptor.

Glutamate works not only as a point-to-point transmitter, but through spill-over synaptic crosstalk between synapses in which summation of glutamate released from a neighboring synapse creates extrasynaptic signaling/volume transmission. Glutamate regulates of growth cones and synaptogenesis during brain development.

At the astrocyte synaptically released GLU is co-transported with Na<sup>+</sup> by the Na<sup>+</sup>/K<sup>+</sup>-ATPase consuming one ATP in the exchange for extracellular K<sup>+</sup>.

The signaling mechanisms are complex because EPHRs (erythropoietin-producing human hepatocellular receptors) and ephrins can act simultaneously as receptors and ligands, leading to bidirectional – parallel or antiparallel – signaling hormonal axis [42].

A crucial step in the generation of long-term-memory (LTM) is consolidation, a process in which short-term-memory (STM) is converted to LTM. Hippocampus-dependent LTM depends on activation of Ca<sup>2+</sup>, Erk/MAP kinase (MAPK), and cAMP signaling pathways, as well as de novo gene expression and translation. One of the transcriptional pathways strongly implicated in LTM is the CREB/CRE (calcium, cAMP response element) transcriptional pathway. Interestingly, this transcriptional pathway may contribute to other forms of neuroplasticity including adaptive responses to drugs. Activation of the Erk1/2 MAP Kinase (MAPK)/CRE transcriptional pathway during the formation of hippocampus-dependent

memory depends on calmodulin (CaM)-stimulated AMP cycling to cAMP by AC [43].

The hydrophilic to hydrophobic direction could be designed as a little resistance parallel exergonic sense. A high Ca<sup>2+</sup> generating the dead-end inhibition of AC allow the anti-parallel high resistance of endergonic thermodynamics for the hydrophobic to hydrophilic direction at the supporting microtubules skeleton.

### Proline

The partially hydrated *nascent* Mg<sup>2+</sup> at the membrane activates the Na<sup>+</sup>/K<sup>+</sup>-ATPase in neuronal axons and by competition attracting water from Na<sup>+</sup>/K<sup>+</sup>-ions a size fitting  $\Delta$ -hydration shell dynamics to maintain the Proline-dependent torque (bending and sliding) of the amino acids chains of brain noradrenaline-adenylate-cyclase (NA-AC) could function in parallel vs antiparallel conformation.

The blood-plasma input the glucose and Mg<sup>2+</sup> crossing the choroid plexus allows the cerebrospinal fluid (CSF) to potentiate the enthalpy flow capable to support the conformational work required for the proline-dependent and H-bond breakdown of water cluster consumption coupled to the torque action over the NA-AC protein. Hence, forward sensorial (five senses) neurons to hypothalamic neuronal axis of hormonal activated secretion, reaching the brain. The emotional response of brain through a reversal axis of hormones expelled at the oral cavity.

Proline can only be stably accommodated within the first turn of  $\alpha$ -helix. When present elsewhere, proline disrupts the conformation of the helix, allowing a bending capable to produce sliding of two segmental chains of AC that between both acquire a sequential dynamic to conform the active inter-domains site. Hence, catalyze from an Mg<sup>2+</sup> in obligatory excess over MgATP to form in hydrophilic sequence the first product AMP and in a subsequent hydrophobic stage a Ca<sup>2+</sup>-dependent binding re-configuring R groups into a hydrophobic domain of the R groups of the chains catalyzing the endergonic AMP cycling to form cAMP.

The action potential firing at the inter-neuronal electric connection will release the NA containing vesicles to turn-off the dead-end inhibition of AC

by  $\text{Ca}^{2+}$  and activate the second stage of AMP cycling for cAMP second product release.

The  $\alpha$ -helix has a maximum number of H-bonds and Van Der Waals interactions formed between the oxygen of the peptide bond carbonyl and the hydrogen atom of the peptide bond nitrogen of the fourth residue down in the polypeptide chain secondary structure. The tightly packed twisting structure shows each  $\alpha$ -carbon with a phi angle of  $-57^\circ$  and a psi angle of  $-47^\circ$ . A complete turn of the helix contains an average of 3.6 aminoacyl residues, and 0.15nm pitch turn rise and R groups of each aminoacyl residue facing outward and  $\alpha$  turning helices as right-handed structures stabilizing transition states in the conformational dynamics of proteins. Conformational changes have an internal energy rich intermediate state, capable to sustain an activatory coupling by coordinative metal bonds and H-bond breakdown thermodynamics. The idea that allow conformational transition to substitute the covalent energy rich bond offered to biochemical problematic prevalent at the time, excluded from this single conjecture an energy transfer mechanism, that could be functional for electron transport chain transfer and connected its energy for coupling to ATP synthesis [44].

### **Dynamics interaction between adrenergic and glutamatergic pathways**

Neurotransmitter transporters limit spillover between synapses and maintain the extracellular neurotransmitter concentration at low yet physiologically meaningful levels and provide precursors for neurotransmitter biosynthesis. In many cases, neurons and astrocytes contain a large intracellular pool of transporters that can be redistributed and stabilized in the plasma membrane following activation of different signaling pathways. This means that the uptake capacity of brain areas in the nervous system composed of mostly unmyelinated axons, dendrites and glial cell processes that form a synaptically dense region containing a relatively low number of cell bodies (neuropil). Therefore, different neurotransmitters can be dynamically regulated over very short distances in the course of minutes to changes in

neuronal activity, blood flow, cell-to-cell interactions, etc. [45]

Oxytocin (OXT) neurons of the hypothalamus are at the center of several physiological functions, including milk ejection, uterus contraction, and maternal and social behavior. In lactating females, OXT neurons show a pattern of burst firing and inter-neuron synchronization during suckling that leads to pulsatile release of surges of OXT into the bloodstream to stimulate milk ejection. This pattern of firing and population synchronization may be facilitated in part by hypothalamic glutamatergic circuits, as has been observed in vitro using brain slices obtained from male rats and neonates [46].

### **Magnesium**

The free  $\text{Mg}^{2+}$  concentration was shown to change from 0.57mM to 1.9mM in between the change from oxygenated to deoxygenated cells, increasing the tendency from cells to release  $\text{Mg}^{2+}$  into the surrounding media.

The mean cerebrospinal fluid (CSF) magnesium level for the control group was  $2.56 \pm 0.19$  mg/dl (range 2.2 to 2.8 mg/dl). For the preeclamptic group who received intravenous magnesium sulfate, the mean CSF magnesium level was  $3.04 \pm 0.12$  mg/dl (range 2.9 to 3.2 mg/dl).

The partially hydrated *nascent*  $\text{Mg}^{2+}$  in membrane activates the  $\text{Na}^+/\text{K}^+$ -ATPase in neuronal axons to generate size fitting dynamics of the  $\Delta$ -hydration shell sequence of *nascent*  $\text{Mg}^{2+}$  competing for the hydration shell of  $\text{Na}^+$ .

Mutual exclusion between hydrophilic and hydrophobic domains allows vectorial kinetics, which bypasses microscopic reversibility, due to the enzymes turnover has only one sense the hydrophilic changing conformation to the hydrophobic one.

Mg-driven interaction of ion-hydration shells for the coupling of  $\text{Na}^+/\text{K}^+$ -ATPase and adenylate cyclase (AC). The  $\text{Na}^+$ -in channel and the  $\text{K}^+$ -out channel open as a function of changing potential  $\Delta V$ . MgATP breakdown by the ion pump-ATPase is required for releasing  $\text{Mg}^{2+}$ , which when in excess of substrate became activatory of basal and noradrenaline (NA) stimulated AC. The differential strength between the tendencies of ions to complete their hydration shells allows directional reactivity.

Moreover, the interactions of water depend of the different and variable stabilities for structuring H-bonds. Exclusion from hydrophobic regions of the

protein-lipid electrogenic membrane and the proteins themselves allow one-sided distribution of ligand water sites [47] [48].

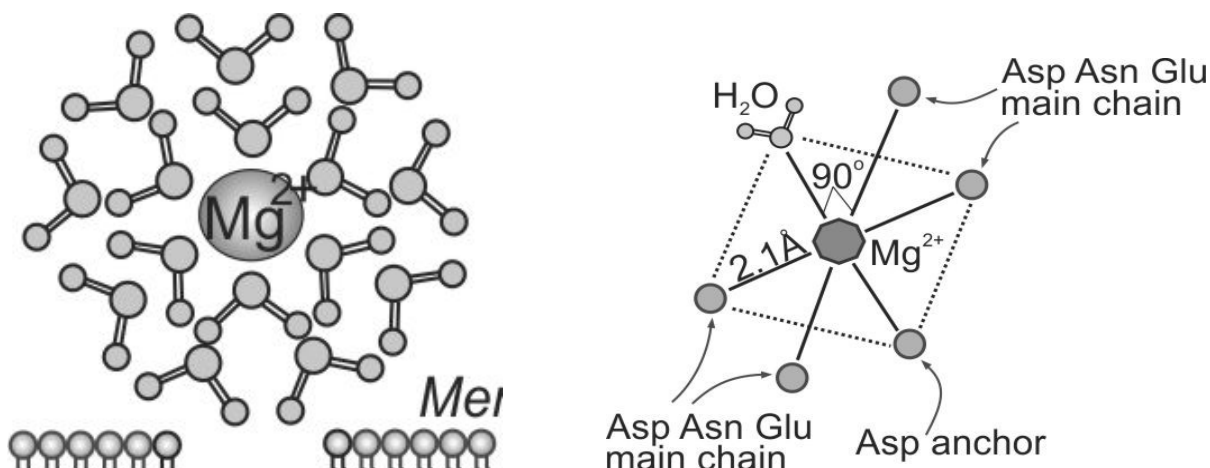


**Figure 7:**  $Mg^{2+}$  hydration shell is shown with two layers.  $Mg^{2+}$  was positioned with an apical 6<sup>th</sup> R-group to constitute an Asp-H<sub>2</sub>O axis.  $Ca^{2+}$  is shown with only one layer because the 2<sup>nd</sup> one usually does not participate in the fitting within a channel. In the conformational pathway from hydrophilic to hydrophobic state of AC by release of  $Ca^{2+}$  by CaM to a binding site configures a pentagonal-bipyramidal geometry, enclosing a hydrophobic domain for water exclusion in a highly endergonic configuration for cycling AMP into cAMP. The re-configuration by  $Ca^{2+}$  re-uptake by the free CaM involves the coupling of large mass action water cluster to obtain the initial hydrophilic state of AC and the release of single molecule of water that within the microtubules (MTs) by the coherence of magnetic attraction under the circulatory impulse  $\alpha\beta$ -tubulin usually involve in dissipative traction of entropy.

The divalent ions usually coordinate about two or higher R residual groups of a polypeptide chain to maintain quaternary structures of protein and usually configure parallel and anti-parallel dependence of phosphorylation by a tyrosine kinase analog of insulin receptor tyrosine kinase (IRTK). AQP4 is abundant in perivascular astrocyte end feet and where the astrocyte is in close apposition to neurons and is directed to an anti-parallel entropy dissipative pathway.

For  $MgCl_2$  saturation curves at constant total ATP concentration, the computer-generated curves based on the RARE BiBi model predict a change in the Hill cooperativity  $h$  from a basal value of 2.6, when  $Mg^{2+}$  is not obligatorily required, to 4.0 when the addition of hormones or neurotransmitters induces an obligatory requirement for  $Mg^{2+}$ .

The increase in  $Mg^{2+}$  level in the brain enhances memory and synaptic plasticity in vivo, acting in neurogenesis over neuronal differentiation of adult neural progenitor cells (aNPCs).  $Mg^{2+}$  in the tissue microenvironment promotes Schwann cells (SCs) synthesis and the regeneration of neuronal axons and myelinated nerve fibers.

Excessive  $Mg^{2+}$  concentration had been reported to inhibit SCs proliferation [49].

NPCs isolated from the dentate gyrus of adult C57/BL6 mice were induced to differentiate in a medium with varying magnesium concentrations (0.6, 0.8, and 1.0 mM) and extracellular signal-regulated kinase (ERK) [50].

The free divalent metals show an order of affinity for AC:  $K_{0.5}(Ca^{2+}) = 0.02$  mM,  $K_{0.5}(Mn^{2+}) = 3.8$  mM,  $K_{0.5}(Mg^{2+}) = 4.7$  mM, and an order of activity  $Mn^{2+}$  greater than  $Mg^{2+}$  greater than  $Ca^{2+}$ . The data indicate that  $Mn^{2+}$  and  $Mg^{2+}$  ions may compete for a regulatory site distinct from the active site and increase  $V_m$  without changing  $K_m(MgATP)$ ,  $K_m(MnATP)$ , or  $K_i(ATP^4)$  [51].

## Calcium

Biochemical receptors for glutamate fall into three major classes, known as  $\alpha$ -amino-3-hydroxy-5-methyl-4-isoxazolepropionic acid (AMPA) receptors, N-methyl-D-aspartate (NMDA) receptors, and metabotropic glutamate receptors. A fourth class, known as kainate receptors are similar in many respects to AMPA receptors, but much less

abundant. Many synapses use multiple types of glutamate receptors. AMPA receptors are ionotropic receptors specialized for fast excitation: in many synapses they produce excitatory electrical responses in their targets a fraction of a millisecond after being stimulated. NMDA receptors are ionotropic, but they differ from AMPA receptors in being permeable, when activated, to calcium. Their properties make them particularly important for learning and memory. Metabotropic receptors act through second messenger systems to create slow, sustained effects on their targets.

Hydrophobic  $\text{Ca}^{2+}$  released activates the glutamate neurotransmission. Serotonin (5-

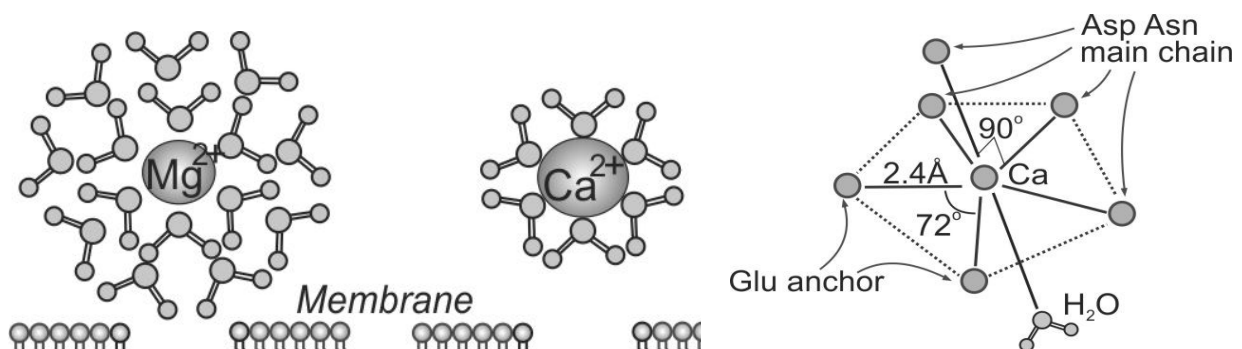


**Figure 8:**  $\text{Mg}^{2+}$  hydration shell is shown with two layers.  $\text{Mg}^{2+}$  was positioned with an apical  $6^{\text{th}}$  R-group to constitute an Asp- $\text{H}_2\text{O}$  axis.  $\text{Ca}^{2+}$  is shown with only one layer because the  $2^{\text{nd}}$  one usually does not participate in the fitting within a channel. In the conformational pathway from hydrophilic to hydrophobic state of AC by release of  $\text{Ca}^{2+}$  by calmodulin (CaM) to a binding site configures a pentagonal-bipyramidal geometry, enclosing a hydrophobic domain for water exclusion in a highly endergonic configuration for cycling AMP into cAMP.

The divalent ions usually coordinate about two or higher R residual groups of a polypeptide chain to maintain quaternary structures of protein and usually configure parallel and anti-parallel dependence of phosphorylation by a tyrosine kinase analog of insulin receptor tyrosine kinase (IRTK).

Under the stress state, the magnesium ion level decreases. Then the calcium ion channel opens massively, and the calcium ion flows inside, leading to cell swelling and into an apoptosis (dead state).

Thus, a supplementary magnesium ion can block the ion channel of NMDA receptor through the action of electric charge, thereby inhibiting the entry of calcium ion into cells.

The joint release of  $\text{Mg}^{2+}$ , glucose and  $\text{O}_2$  allows the matching of  $\text{O}_2$  release to that of glucose consumption rates, during brain aerobic glycolysis. The overall metabolic feedback by the in common dependence on free  $\text{Mg}^{2+}$  or  $\text{Mn}^{2+}$  of AC of brain,

hydroxytryptamine, 5-HT) produced in Raphe nuclei located in the brainstem, could induced  $\text{Ca}^{2+}$  increase and reduced the cAMP increase. Thus, indicating a cross-talk synchronizing between both the 5-HT-sensitive- $\text{Ca}^{2+}$  and the excess Mg-cAMP activated pathways. Ionic equilibrium controlled by  $\text{Ca}^{2+}$  effects, acting for a simultaneous dead-end inhibition of the adenylate cyclase (AC) by CaATP, AC inhibition and activation of the AMPA receptor, controls the glutamate receptor at the ion channel domain.

$\text{Ca}^{2+}$  could displace  $\text{Mg}^{2+}$  from mutual binding sites incrementing cytoplasmic  $\text{Mg}^{2+}$ .

fat cells and the insulin receptor tyrosine kinase (IRTK) in liver, allows homeostatic network integration.

The astrocyte manages water circuit turnover of cerebrospinal fluid (CSF) to maintain thermic and larger aggregates of water into homeostasis state. Within the open neuronal-astrocyte network system the smaller aggregates of water are released into venous blood and their exclusion from the body allows to prevent entropy increase interfering with the highly energy demanding neuronal processes.

The overall process requires preserving energy of activation and processing of information, separated by the neural lipid-protein membranes to proceed to its completion without reaching thermic homeostasis.

Thermic equilibrium is delayed in part by the astrocytes taking-out of the system the H-bonds

depleted water, which could be thereafter associated with air-water exhaled-out to drive heat/entropy to the outside as described for open systems [52].

Shedding their hydration shells  $Mg^{2+}$  and  $Ca^{2+}$  could fit into pore-regions of transporter proteins. The mechanisms are similar.

The energy released is larger for the smaller  $Mg^{2+}$ , which is surrounded by a more stable double hydration shell than  $Ca^{2+}$ .

A labile second layer is not usually involved in the mechanism of  $Ca^{2+}$  translocation.

The literature reports the calculated successive  $\Delta E$  kcal/mol in  $[Mg.(H_2O)_n]^{2+}$  by increasing the state of hydration by capturing of 1 molecule of  $H_2O$  and the Mg-O bond distances.

a)  $[Mg(H_2O)_4].(H_2O)^{2+}$ : Mg-O=0.194 nm,  $\Delta E=23.7$ .

b)  $[Mg(H_2O)_6].(H_2O)^{2+}$ : Mg-O=0.204 nm,  $\Delta E=18$ , c)  $[Mg(H_2O)_6](H_2O)_{12}^{2+}$ : Mg-O=0.207 nm,  $\Delta E=13.1$ .

The 1000/1 ratio for the cellular concentration  $Mg^{2+}$  vs  $Ca^{2+}$  that the transmembrane AC is closely located to the system  $Ca^{2+}/CaM$  for signaling transmission.

The ionic radii: 0.072 nm for  $Mg^{2+}$ , 0.067 nm for  $Mn^{2+}$  and 0.074 nm for  $Zn^{2+}$  in the octahedral and 0.060 nm in tetrahedral coordination. These divalent ions configure structure, which allow  $Mg^{2+}$  in Hb [53] up to six coordinative bonds, allowing hydrophilic structures a less stable configuration of higher water turnover than  $Ca^{2+}$ . The 0.1 nm  $Ca^{2+}$  allows a more stable configuration with a tendency to wraparound protein up to seven R groups for a hydrophobic water exclusion domain that need free CaM need for turnover.

$Ca^{2+}$  is present in the environment at much lower concentration than  $Mg^{2+}$ . Usually it is released from a  $Ca^{2+}$ -CaM turnover, which operates at a short distance of transmembrane AC.

A large release of  $Mg^{2+}$  could occur in the brain by oxyHb conversion into deoxyHb specie. In brain, this effect is desirable to reduce the rate of glycolysis. An uncomplexed ligand or buffer available to  $Mg^{2+}$  could be influenced by  $Ca^{2+}$ , pH, and other ions that bind to the same sites as  $Mg^{2+}$ .

### Nitric oxide and cyclic GMP

Hemoglobin carries nitric oxide (NO) in the globin part of the molecule. This improves oxygen delivery in the periphery and contributes to the control of respiration. NO binds reversibly to a specific cysteine residue in globin; the binding depends on the state (R or T) of the hemoglobin. The resulting S-nitrosylated hemoglobin influences various NO-related activities such as the control of vascular resistance, blood pressure and respiration. NO is not released in the cytoplasm of red blood cells but transported out of them by an anion exchanger AE1.

Cyclic guanosine monophosphate (cGMP) is a cyclic nucleotide derived from guanosine triphosphate (GTP). The cGMP acts as a second messenger much like cyclic AMP. Its activation of intracellular protein kinases in response to the binding of membrane-impermeable peptide hormones to the external cell surface [54] [55] [56] [57] [58] [59] [60] [61].

The Ras family of small GTP-binding proteins represents one of the main components of intracellular signal transduction required for normal cardiac growth, but is critically involved in the development of cardiac hypertrophy and heart failure.

The rapamycin mechanism has as a target formation of mTORC1, which controls cell growth and metabolism in response to nutrients, energy levels, and growth factors. It contains the atypical kinase mTOR and the RAPTOR subunit that binds to the Tor signaling sequence (TOS) motif of substrates and regulators. The mTORC1 is activated by the small GTPase RHEB (Ras homologue enriched in brain) and inhibited by PRAS40.

cGMP is a secondary messenger in phototransduction in the eye. In the photoreceptors of the mammalian eye, the presence of light activates phosphodiesterase, which degrades cGMP. The sodium ion channels in photoreceptors are cGMP-gated, so its degradation causes sodium channels to close. Hence, leads to the hyperpolarization of the photoreceptor's plasma membrane and ultimately to visual information being sent to the brain.

cGMP, like cAMP, gets synthesized when olfactory receptors receive odorous input, is produced slowly and has a more sustained life than cAMP, which has implicated it in long-term cellular

responses to odor stimulation, such as long-term potentiation. cGMP in the olfactory is synthesized by both membrane guanylyl cyclase (mGC) as well as soluble guanylyl cyclase (sGC). Studies have found that cGMP synthesis in the olfactory is due

to sGC activation by NO, a neurotransmitter. cGMP requires increased intracellular levels of cAMP and the link between the two second messengers appears to be due to rising intracellular calcium levels.

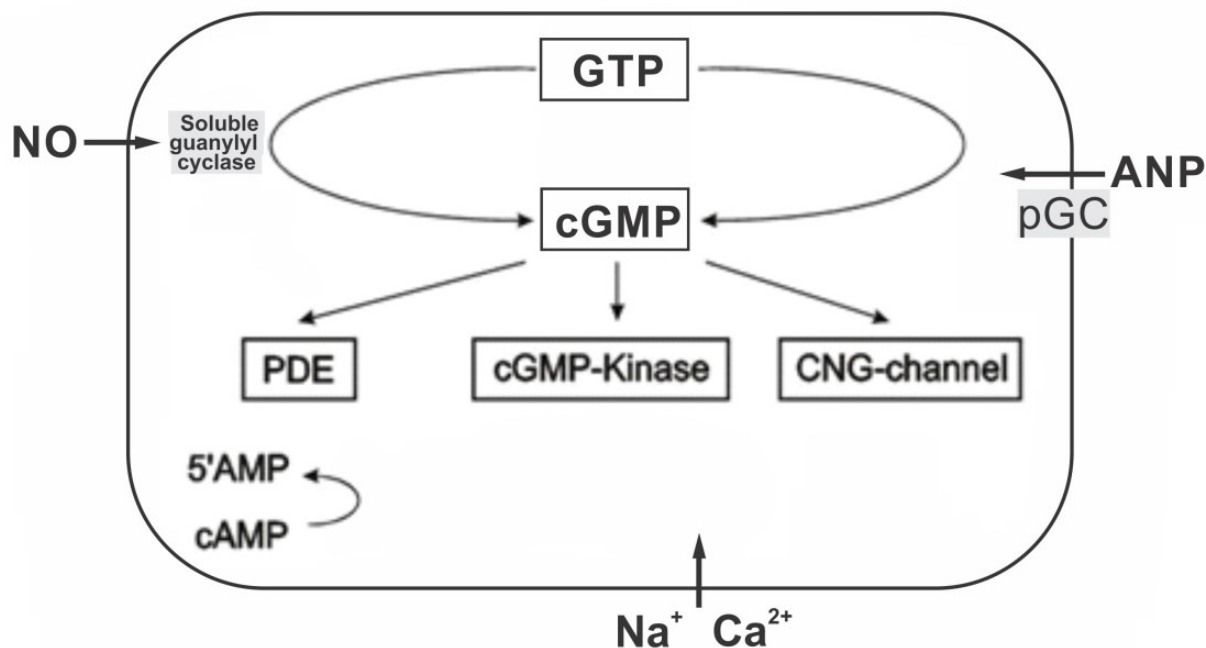


**Figure 9: cGMP is a common regulator of ion channel conductance, glycogenolysis, and cellular apoptosis.** It relaxes smooth muscle tissues. In blood vessels, relaxation of vascular smooth muscles leads to vasodilation and increased blood flow. At presynaptic terminals in the striatum, cGMP controls the efficacy of neurotransmitter release.

Numerous cyclic nucleotide phosphodiesterases (PDE) can degrade cGMP by hydrolyzing cGMP into 5'-GMP. PDE 5, -6 and -9 are cGMP-specific while PDE1, -2, -3, -10 and -11 can hydrolyze both cAMP and cGMP. Early consolidation only depends on cGMP, whereas late consolidation is mediated by cAMP [62].

Phosphodiesterase inhibitors prevent the degradation of cGMP, thereby enhancing and/or prolonging its effects.

The two differentiable pools of cGMP in both of which phosphodiesterase-1 (PDE1) and -2 (PDE2) are highly expressed for cGMP degradation in the hippocampus [63].

Guanylate cyclases represent a widely distributed family of enzymes that convert guanosine triphosphate to the second-messenger molecule cGMP. The 2 primary forms are the transmembrane-associated particulate guanylate cyclase, which functions as a receptor for natriuretic

peptides, and the soluble guanylate cyclase (sGC), which serves as a receptor for NO [64].

cGMP is the second messenger of 2 distinct signaling pathways: NO is produced by endothelial cells and binds to sGC in the target cell; and ANP and BNP, derived primarily from cardiomyocytes, stimulate GC-A, whereas CNP, secreted by endothelial cells, stimulates GC-B. cGMP signaling may be augmented by the use of NO mimetics such as nitrovasodilators; sGC activators or stimulators; increasing levels of natriuretic peptides; by inhibiting natriuretic peptide degrading enzymes; and inhibiting the activity of cGMP-hydrolyzing PDEs.

## Water

Changes in hydration shell of a protein occur because the tendency of the dipolar water molecules makes H-bonds with R-groups. The latter reactivity chelates ions like Mg<sup>2+</sup>. The tendency of a protein

tor form complexes depend on the number and strength of partial charge of the R groups of the polypeptide chain available on the surface of the protein.

Therefore a dynamics mechanism to form and break H-bonds allows proton-induced change in conformation of the protein that could relate to a  $\Delta pH$  inducing  $\Delta pK_a$ , like these of R histidine side chains.

The polarity of water molecules at room temperature and normal atmospheric pressure maintains an average  $n=3.4$  H-bonded between themselves. Water has a larger calorific capacity than other liquids, due to its capacity to absorb heat by decreasing the number of the molecules, linked into an average cluster structure  $(H_2O)_{n<3.4}$ . The entropy of the aqueous system of increases as the more highly ordered arrays of water molecules are replaced by the less orderly poorly H-bonded.

The H-bond breakdown allows the tendency  $n \rightarrow 1$  and became released into the astrocyte to be eventually conducted outside of the neuron system itself. Hence, the heat produced by ligand water breakdown during changes at the protein conformation [65].

The H-bond breakdown when released outside of the body, at cooler temperatures follow the direction  $(H_2O)_{n<3.4} \rightarrow (H_2O)_{\text{vapor}}$ . The overall effect limits entropy increase, allowing to sustain the homeostatic state of temperature, which characterizes brain. The overall thermodynamic changes has to be plotted again the scale of the endergonic direction. The expected change depends of the number of molecules of water loss per protein molecule during the ligand-protein transition. To evaluate thermodynamic change in  $\text{oxyHb}-(H_2O)_n$ ,  $n=60$  in transition to  $\text{deoxyHb}+60H_2O$ , has to be taken in account that even an small enthalpy change ( $\Delta H$ ) per molecule of water has to be multiplied by 60.

The transition between these differently ligand states of the protein allows for a sequential exergonic release of energy, decreasing equilibrium tendency at each of the ligand-protein complexes into a final equilibrium for predominance of the conformational changes.

The gases do not move in aquaporin by a simple diffusion but aquaporin (AQP) allows facilitated diffusion through which water,  $CO_2$  and

$NH_3$  moves through the endothelial cells of the neurovascular unit (NVU). AQP9 is found in the astrocyte cell body and control of water distribution within the brain and show associated fluid dynamics dysfunctions. AQP4 is abundant in perivascular astrocyte end feet and where the astrocyte is in close apposition to neurons.

### Hb conformational dynamics

The cooperative order for Hb involves a decrease from the 6, 4 and 2 in the coordinative of  $Mg^{2+}$  and its release, which allows His  $\beta_2$  to interact with the  $Fe^{2+}$  of the Heme and the release of  $O_2$  configuring the tetramer to the binding of 2,3-DPG into a single domain. Thus, both  $4O_2$  and  $2Mg^{2+}$  could cross blood brain barrier (BBB). The release of nascent  $Mg^{2+}$  into cerebrospinal fluid (CSF) saturates the obligatory activatory site of adenylate cyclase (AC).

The mutual exclusion in the dynamics of structural changes of proteins means that cannot simultaneously proceed the vectorial changes required in both directions of a molecular transition between two protein complex states. Thus, could not perform at the same time the parameter for decrease of oxy to deoxyHb with the opposite parameter for a simultaneous increase of deoxy to oxyHb, implicating that act by a time-dependent sense of the physics involved in momentum conservation.

The tendency of the water molecules to associate through H-bonds is outweighed by the energetic increase push toward vapor randomness. Differentiable ligand states of the same protein like oxyHb vs deoxyHb could complete a turnover cycle by thermodynamically balancing the exergonic with the endergonic senses [66].

The balancing could be provided by the change in the number of water molecules linked and release during transition from the R to T state of the protein conformation.

The H-bond breakdown between water molecules takes up energy from the system, requiring the input of energy from the surroundings.

Water molecules are not as highly oriented as those in cagelike shells around crystalline structures of nonpolar solutes and water, forming highly

ordered cagelike clathrates. Hence, the input of energy to dissolve hydrophobic compounds in water produces by the ordering of water reduces entropy. Long chain fatty acids have hydrophobic alkyl chains surrounded by a shell of ordered water molecules.

The number of ordered water molecules, and therefore the magnitude of the entropy decrease, is proportional to the surface area of the hydrophobic solute enclosed within the cage of water molecules.

Hb conformational dynamics: The tetramer arrangement of R groups between pairs  $\beta_2 \alpha_1$  and  $\beta_1 \alpha_2$  each coordinative  $Mg^{2+}$  allows 2,3-DPG conforming a single site for the 4 subunits in a mutual exclusion effect that confer the irreversible sequence or vectoriality. The transition oxy- to deoxyHb operates transport of cGMP.

This elucidation of Hb structure dynamics and mutual exclusion function allowed a new perspective for the transmembrane noradrenaline-adenylate-cyclase (NA-AC) that an hydrophilic active site could by conformational change by mutual exclusion became by an irreversible sequence became hydrophobic, allowing a vectorial transition to bypass the microscopic reversibility principle.

A protein hydrophilic active site could by mutual exclusion become hydrophobic, allowing this vectorial transition to bypass the microscopic reversibility principle.

Prigogine proposed a coupling between larger sources transfer of enthalpy to smaller ones allow an open system to operate life. However, his proposal lakes the mechanisms that allow transfer of energy ending with entropy release out of the system [67]. These systems are able to maintain vectorial kinetics and this separation between the systems maintain high enthalpy with tendency to constantly exclude entropy out of the system is basically an organized cosmos rather than one maintained by chaos [68].

Example: the order conservation in the energy flow from the sun is coupled to water cluster thermogenic H-bonds breakdown to vapor, during day time is cycled by heat dissipation by the cooling effect of night. Thus, the rain event operates a cycle in which constant input of enthalpy turnover do not equilibrates with entropy because is excluded. On the other hands the phenomenon of greenhouse

effect tends to maintain entropy within the enclosing environment of the earth when unable to radiate in space all the generated entropy, leading to a chaos environment. Hence, phenomenon capable to organize the structure of the space in the human body for energy fluctuations functional for exclusion of entropy structured by brain metabolic dominance over the body supplier of enthalpy could maintain high enthalpy because, organized an additional oral cavity pathway, allowing a high dissipative rate to entropy [69] [70].

The position of proline in a polypeptide chain allows sliding between segments, in the tertiary folding structure response to electrostatic attractions, could differentiate positive vs negative domains. Thus, bypass the microscopic reversibility principle, illustrated as a single door, vectorial kinetic only made possible by the jokingly Maxwell proposed: operator demons. The physiological function of Hb oxygenation by  $pO_2$  shows a microscopic thermogenesis biological vector, functioning by the enthalpy potential of the large mass action of surrounding air and releasing entropy. The mechanism shows the H-bonds breakdown required for changes in the structure-function levels by the proline mediated folding. The tense (T) to relax (R) forms shows vectorial microscopic dynamics, during Hb oxygenation. Thus involves a sliding by H-bonds breakdown, distancing between subunits  $\beta_2$  and  $\alpha_1$ . Thus, open a larger entrance to a fully hydrated  $Mg^{2+}$  to coordinate amphoteric and negative R groups characterizable to a hydrophilic site. The transition of R to T allows positive R groups to bind 2,3-DPG to form deoxyHb. Thus, a microscopic smaller entrance by decreasing its opening size does not allow entrance of the fully hydrated  $Mg^{2+}$ , but allow the exit of nitric oxide (NO) and a poorly hydrated  $Mg^{2+}$ , denominated nascent. This one acts for competitive hydration sieving on the shells of  $Na^+$ , which in terms take water from the  $K^+$  shell, potentiating a  $K^+/Na^+$ -translocation operating the electrogenic transmembrane potential. The deoxygenation in the reverse transition of R to T binds NO, protecting against a premature decrease of the chromosome's telomeres size by stressing factors such as depression, anxiety and physic traumatism, over endothelial cells delaying premature senescence. The arginine metabolism

produces NO, dilating blood vessels, improving the circulatory systems and the muscular recovery-development. A diet rich in arginine by producing a high sustainable level of NO may prevent the resistance to treatment by the consolidation of large vascular masses. The H-bonds donor potential by their breakdown leads to randomness (or entropy) decreasing the kinetic energy of solvation, scaling down the polarity on the thermogenic dissipation of oxy vs deoxyHb and choroid plexus epithelium on blood's plasma generation of CSF. The enthalpy of photosynthesis-metabolism releases CO<sub>2</sub>, whereas the water cluster mediated thermostatic function releases vapor. In both systems, the entropy release maintains a high potential of enthalpy. Hence, overcomes the thermic and electric noises by an irreversible dissipative kinetics, facilitating a clear development of a meditative level of reasoning and learning. Thus, the brain acquires an autonomous function, beyond behavioral genetic conditioning.

Crystals of RNA, DNA and proteins have tightly bound water molecules, which are not osmotically active, as is these were part of the structure itself, but with different properties than the bulk water.

Transition from the R to the T-form changes H<sub>2</sub>O association constant of Hb  $\Delta pK_a(H_2O)$ . Water molecules can be detected as ligands of a protein in solution by nuclear magnetic resonance, and/or water-glycerol equilibrium studies. It is proposed that the change in a protein hydration shell is essential, for many enzymes in the cycle enzyme-substrate transition to enzyme-product.

Conformational changes are driven by the formation of several differentiable ligand-protein complexes, involving the overall energy of activation (E<sub>a</sub>). A thermodynamic open-system allows a pattern for vectorial progress of deoxygenation in tissues to function without any significant reversibility until pO<sub>2</sub> at the lungs allows re-oxygenation of Hb.

The thermodynamic change by the breaking and re-arrangement of H-bonds within the molecule is not subject to thermic tendency of protein R groups to move without conserving the capacity of vectorial movement. Formation of complexes like the coordinative Mg<sup>2+</sup> or 2,3-DPG manifests capacity for spatial oriented microscopic behavior,

and therefore could function in terms of vectorial kinetics.

The exergonic change has to dominate in both direction sequences of Hb interconversion, T to R (in the lung), or its reverse R to T (in tissues). The energy potential reverses as a function of higher pO<sub>2</sub> and pH, at the lungs decreasing at the tissue level. The multiple equilibrium in deoxygenation involves dissociation of the ligands 4O<sub>2</sub>, 2 to 4Mg<sup>2+</sup> and 60H<sub>2</sub>O, and association of 2,3-DPG, and H<sup>+</sup>. The pK<sub>a</sub> of the R-form (oxyHb) changes from 6.6 to 8.2 in the T-form (deoxyHb).

The H<sub>2</sub>O became released as single molecules and tend to mix with water cluster decreasing its H-bond content. The water expelled-out from the body drives heat-dissipation, and therefore becomes a carrier of the increased in entropy of the surrounding water. This coupling changes the Hb system tendencies by H-bond number thermodynamic balancing of oxygenation vs deoxygenation. Water binding in the direction of facilitating the R state is exergonic. Release of water should be endergonic, but overall there are exergonic contribution of H<sup>+</sup> and 2,3-DPG binding. The tendency of the greater effective charge of Mg<sup>2+</sup> because leaves without a complete hydration shell allows this ligand to enter by subtracting water from Na<sup>+</sup>/K<sup>+</sup> to sequence organize the ions movement along the transmembrane action potential signal.

The extent of the protein hydration shell decreases by 60 ligands water molecules in the direction of oxy to deoxyHb and the Mg<sup>2+</sup> that in order to coordinate with the R-groups loss the associated 60 molecules of water [Mg.(H<sub>2</sub>O)<sub>6</sub>](H<sub>2</sub>O)<sub>12</sub>)<sup>2+</sup>. The Mg<sup>2+</sup> water loss leads to a nascent Mg<sup>2+</sup> in which has been decreased the water molecules in the second shell. In the deoxyHb (T form) the decrease of solvation leads to an entropy increase. The hydrophobic side chains of amino acid tend to cluster in a protein interior, and the H-bonds formed involve an endergonic process made exergonic by the much higher mass action of surrounded a 55.5M water cluster of 60 H-bond breakdown. To avoid a calculation that implies a large thermodynamics changes for the R to T forms in an irreversible vectorial sense with mutual exclusion.

The structural transition is irreversible and therefore was denominated mutual exclusion

because the R to T form could not exist at the same time.

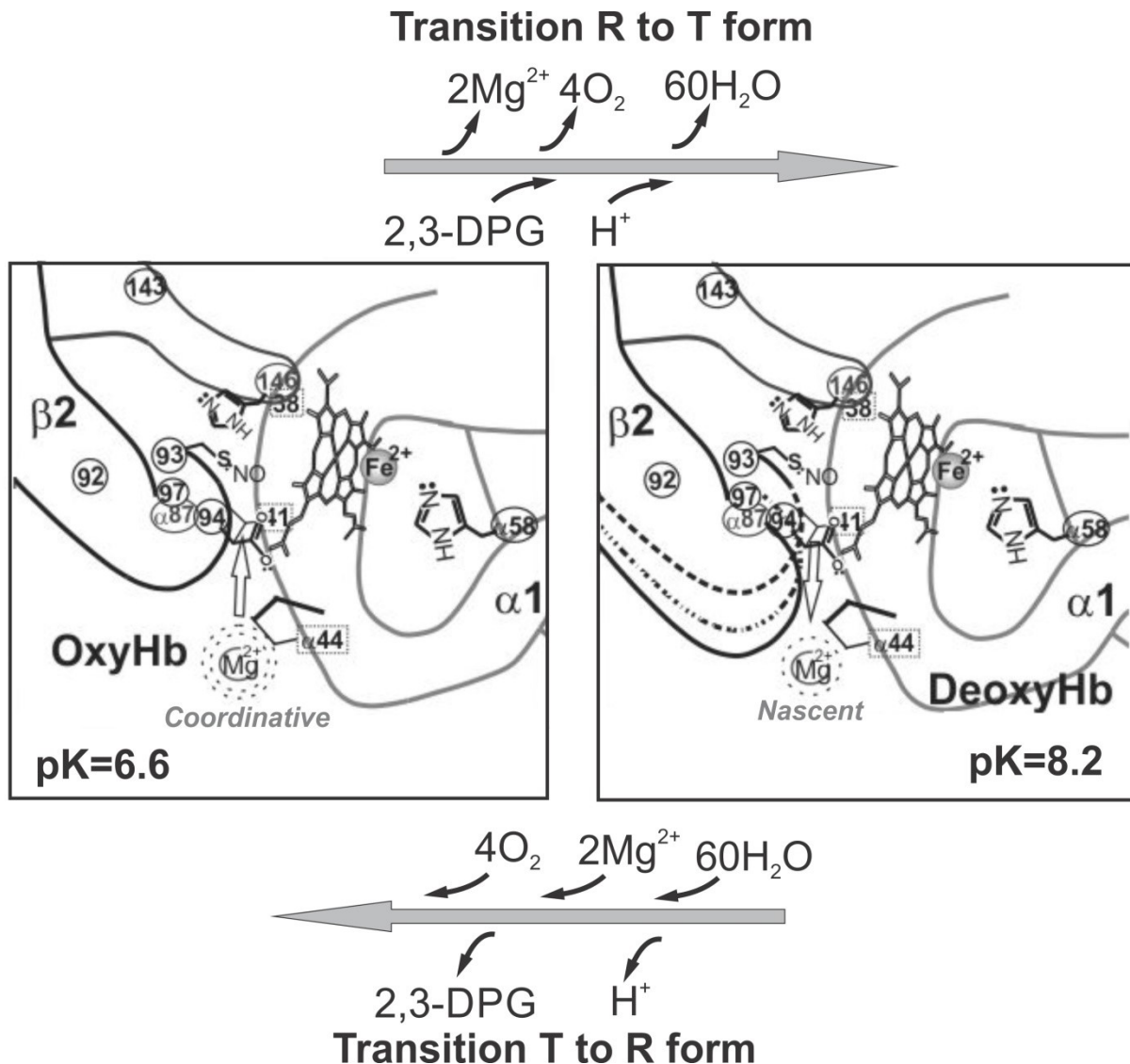


**Figure 10: Conformational dynamics of Hb.** In the  $\beta_2\alpha_1$  interface of oxyHb, the binding of 2,3-DPG forms deoxyHb plus  $\text{H}^+$  and dissociation of  $\text{Mg}^{2+}$  or  $\text{Zn}^{2+}$ . Structural symmetry allows an equivalent set of changes at the  $\beta_1\alpha_2$  interface. Peptide bonds are rigid and fixed in a plane in where two  $\alpha$ -carbons, 0.36nm apart, rotate 180 o over angles  $\phi$  (fi) and  $\psi$  (psi). The longitudinal lengths from  $\alpha$ -carbon to the coordinated negative R groups are: His=0.5nm, Cys=0.23nm and Asp=0.39nm; Magnesium Radius: atomic=0.150 nm and ionic ( $\text{Mg}^{2+}$  ion)=0.086 nm; Zinc radius: atomic=0.135 nm and ionic ( $\text{Zn}^{2+}$  ion)=0.088 nm; Iron radius: atomic=0.140 nm and ionic ( $\text{Fe}^{2+}$  ion)=0.077 nm.

The turnover depends of the group proline  $\alpha_1/\alpha_2$  44 for control of  $\text{Mg}^{2+}$  access to chelating-hydrophilic region. The lungs the deoxyHb conformational change to oxyHb involves the sliding of  $\alpha_2\beta_2$  vs  $\beta_1\alpha_1$ , which allow entrance of  $2\text{Mg}^{2+}$  ions fully hydrated into the hydrophilic region. The R-groups of oxyHb modify the cooperative state of the molecule by changing the coordinative  $\text{Mg}^{2+}$  order from 2 to 4 and 6 at the

lungs to reach a highly oxygenated state of Hb of arterial blood. This one decreases from each  $\text{Mg}^{2+}$  coordination state from 6 to 4 and 2 until its  $\text{O}_2$  discharge from the upper to the lower regions of the body until conducted by the venous system to return to lungs.

The quaternary structure of a protein is trapped in a latent/entropic state, in which side chains/R-groups move in random translational,

rotational, and vibrational kinetics equivalent to 0.7kcal/mol at 37°C. This latent/thermal-state in Hb could be overcome by Mg<sup>2+</sup> or by Zn<sup>2+</sup>. The latter ion shows a higher coordinative affinity for the R groups involved, when experimentally is used Zn<sup>2+</sup> instead of Mg<sup>2+</sup>

The  $\alpha_1\beta_2$  R-groups: His (histidine) 143, Cys (cysteine) 93, Asp 94, His  $\beta$ 146 and the R-group His  $\alpha$ 87, at the  $\alpha$ 1-Heme. The sum up of the symmetric structure of R-groups at the interphase  $\beta_1\alpha_2$  allows a more stable octahedron geometric configuration. The formation of an (4O<sub>2</sub>Heme)oxyHb(Mg<sup>2+</sup>)<sub>2</sub> complex with two Mg<sup>2+</sup> in the quaternary structure of Hb [71].

Hence, deoxygenation could follow a pattern of gradual release of O<sub>2</sub>, from the Mg<sup>2+</sup>-Hb or when experimentally the divalent metal coordinates with the Hb protein to form (Zn<sup>2+</sup>)<sub>2</sub>-Hb complex.

However, the augment of glucose level in blood in untreated diabetes induces in the erythrocyte an increase of sugar phosphates. These pathological metabolic states by releasing from coordination the Mg<sup>2+</sup> from its ligand state with decrease the molecular affinity of Hb for O<sub>2</sub>.

The multiplicity of complexes allows that deoxygenation could occur over an extended pH-range, than could be possible for any particular divalent metal complex of Hb. The pH of blood remains 7.4 but surroundings tissues allow increasingly lower pH from the trunk to the limbs.

The sliding displacement of R-groups allows for endogenous restructuration of coordinative bonds, overcoming thermic isotropic tendencies. The *mutual exclusion* between oxyHb vs deoxyHb allows Hb to be a carrier of O<sub>2</sub> plus the hydration shell of *nascent* Mg<sup>2+</sup> to tissues and brain demands for electrogenic action potential level. Kosmotropic tend to subtract water from the hydration spheres of proteins, to complete their own.

At the brain, oxyHb not only functions transporting O<sub>2</sub> for release in the synapses, but does the same for Mg<sup>2+</sup>. The conformational change associated to the quaternary structure transition of oxyHb from a relax (R) to a tense (T) form in deoxyHb, involves the quaternary structure of the protein to release 60H<sub>2</sub>O molecules. Thus, facilitating that Mg<sup>2+</sup> would be released with a decrease number of H<sub>2</sub>O molecules in its hydration shell. Effect facilitated by the increase of deoxyHb

pKa=8.2 to oxyHb pKa=6.6. The tendency to decrease H<sup>+</sup> dissociation reduces the tendency to bind Mg<sup>2+</sup>, which lacks water in its remaining hydration shell, pulls-out 60 water molecules from the protein hydration shell.

The conformational change decreasing affinity for O<sub>2</sub> leads the chelated R-His groups to release Mg<sup>2+</sup>. The mechanism involves an amphiprotic response by the displacing of Mg<sup>2+</sup> through the increasing affinity for H<sup>+</sup> changing pKa to 8.2, during the imidazole ring restructuring to imidazolium ( $-N:- + H+ \rightarrow =NH(+)-$ ). Hence, differentiating this nascent Mg<sup>2+</sup>, a denomination suggested by similitude with nascent chloride. The *nascent* Mg<sup>2+</sup> could be differentiated from total Mg<sup>2+</sup> by the smaller number of H<sub>2</sub>O coordinated to the ion, reducing its overall size. This increases the effective charge of the Mg<sup>2+</sup> ion released from its chelating interaction with the negative charged groups of the protein.

The sliding of the  $\beta_2\alpha_2$  vs  $\beta_1\alpha_1$  allows that proline  $\alpha_1/\alpha_2$  44 Hb by not having free C $\alpha$  rotation could be displaced to block access to the hydrophilic crevices within Hb molecular interior.

The sliding of the  $\beta_2\alpha_2$  vs  $\beta_1\alpha_1$  in the transition of T to R that displaces symmetrically the two Pro  $\alpha$  44 elongated distances to  $\beta$  94. This opens the access of fully hydrated Mg<sup>2+</sup> (enclosed within a second hydration shell) to the hydrophilic crevices.

In the R to T sense an Mg<sup>2+</sup> sliding allows closing the distance between Pro  $\alpha$  44 and the  $\beta$  chains, preventing that a full hydrated Mg<sup>2+</sup> could enter, but still allowing the *nascent* Mg<sup>2+</sup> to leave the crevices in the Hb molecule.

The interconversion of oxy to deoxy Hb creates, by the sliding of  $\alpha_2\beta_2$  vs  $\beta_1\alpha_1$  chains a modification of the proline  $\alpha_1/\alpha_2$  44 salt links in the path for ions, like Mg<sup>2+</sup>, to reach the hydrophilic multiple histidine configured space.

After mutual inclusion of O<sub>2</sub> and Mg<sup>2+</sup> stabilization of the conformational change into the R (relax) form [(O<sub>2</sub>)<sub>4</sub>Hb(Mg)<sub>2</sub>].(H<sub>2</sub>O)<sub>R</sub> reverse the sliding and in oxyHb two proline  $\alpha$  44 moves to close both gaps. This conformational change represents the less-reversible thermodynamic event for each sense of Hb turnover.

**The oxyHb to deoxyHb releases nascent  $Mg^{2+}$  competing for water shell sizing ions to fit the ion channels dynamics by the split of Mg-ATP by the  $Na^+/K^+$ -ATPase**

The lack of important changes in cytosolic free  $Mg^{2+}$  by oxyHb deoxygenation on demand of  $O_2$  and  $Mg^{2+}$  simultaneous release, at the transmembrane action potential for the competitive

uptake of water from the shells of sodium-potassium adenosine triphosphatase ( $Na^+/K^+$ -ATPase,  $Na^+/K^+$ -pump), to fit on the membrane and synaptic cleft channels. The high positive charge manifested by the poorly hydrated  $Mg^{2+}$  (*nascent*  $Mg^{2+}$ ) when it is release from its coordinative complex state with a protein, ensures that its high activity even at low concentration could overcome the poor activity of the  $Mg^{2+}$  when surrounded by a complete hydration shell [72].

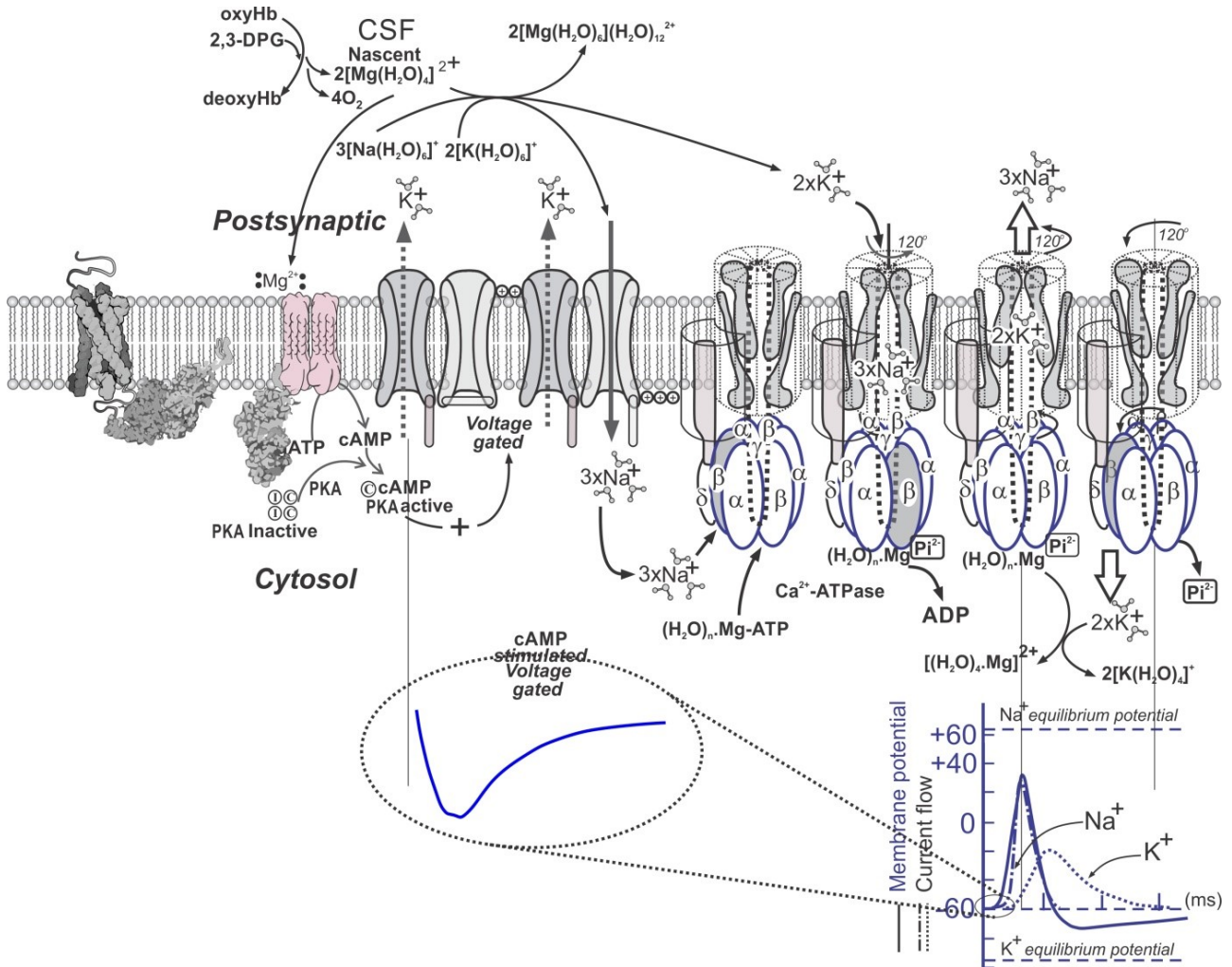


**Figure 11: Mg-driven Interaction of ion-hydration shells for the coupling of  $Na^+/K^+$ -ATPase and AC.** The  $Na^+$ -in channel and the  $K^+$ -out channel open as a function of changing potential  $\Delta V$ .  $Mg$ -ATP breakdown by the ion pump-ATPase is required for releasing  $Mg^{2+}$ , which when in excess of substrate became activatory of basal and NA stimulated AC. The differential strength between the tendencies of ions to complete their hydration shells allows directional reactivity. Moreover, the interactions of water depend of the different and variable stabilities for structuring H-bonds. Exclusion from hydrophobic regions of the protein-lipid electrogenic membrane and the proteins themselves allow one-sided distribution of ligand water sites.

The  $Na^+/K^+$ -pump has driven by the ATPase uses the energy of ATP for an electrogenic transmembrane for active transport, leading to a cycle of the protein residue phosphorylation (R-

aspartate), and the dephosphorylation with release of ADP. The conformational change operates, against the concentration gradient, of the higher affinity for  $3Na^+$  ions binding and exposes exported

to the extracellular region. The phosphorylated form of the pump has a low affinity for  $\text{Na}^+$  ions, so they are released; in opposite direction transfer the phosphorylated protein of higher affinity for  $2\text{K}^+$  imported the ions into the cell.

The neuronal adenylate cyclase (AC) in the  $\text{Na}^+/\text{K}^+$ -pump operated by  $\text{Na}^+/\text{K}^+$ -ATPase. Hb in red cells releases  $\text{O}_2$  and  $\text{Mg}^{2+}$  and glucose to the plasma crossing the choroid plexus and generating cerebrospinal fluid (CSF), allowing the release of glucose,  $\text{O}_2$  to generate Mg-ATP at nerve cells in the hypothalamus. The  $\text{Mg}^{2+}$  vs  $\text{Ca}^{2+}$  can compete in noradrenaline-(NA)-AC by moving as ligands between two domains of the protein to generate the  $\text{Mg}^{2+}$  obligatory activatory step to catalyze conversion of substrate Mg-ATP into AMP, by the hydrophilic conformational change of AC protein. A proline dependent binding allows sliding between two activatory domains for  $\text{Ca}^{2+}$  hydrophobic conformational change allowing AMP cycling into cAMP and this one dependents activation of Kinase-A and its role in Mg-cAMP unzipping of DNA (CREB).

The  $\text{Mg}^{2+}$  with octahedral geometry in the first and second hydric layers ( $12\text{H}_2\text{O}$ ). $[(6\text{H}_2\text{O})\cdot\text{Mg}^{2+}]$  is released from  $\text{Mg}_2(\text{O}_2)_4\text{Hb}$  as *nascent*  $\text{Mg}^{2+}$  shown as  $2[\text{Mg}(\text{H}_2\text{O})_2]^{2+}$  attracting water from  $3[\text{Na}(\text{H}_2\text{O})_6]^+$  to enlarge the number of water in its hydric sphere. The decreased hydration state of  $\text{Na}^+$  allows a smaller size capable to fit a gate through the neuron membrane. The capture by the smaller sized  $\text{Na}^+$  of water from hydration water of internal  $2[\text{K}(\text{H}_2\text{O})_3]^+$ , which allows the release of  $\text{K}^+$  to fit into a gate the exterior CSF. The ion exchanged across the membrane generates the electrogenic potential, advancing along the membrane. The  $\text{Na}^+/\text{K}^+$ -ATPase phosphorylate the membrane gates in the cytoplasmic side for the action potential consumption and release of Pi.

The  $\text{Na}^+/\text{K}^+$  pump controls neuron activity mode of cerebellar Purkinje neurons, accessory olfactory bulb mitral cells and probably other neuron types. The distribution of the  $\text{Na}^+/\text{K}^+$ -pump on myelinated axons in the human brain to be along the internodal axolemma, and not within the nodal axolemma as previously thought. Spin correlated in the nano-space-time and transmission velocity at nano-junction aligning crossing magnetic tunneling. Magnetic tunnel junction will low the nano-magnet

barrier allowing microtubule interconnected pathways to correlate conectomas circuits.

Cosmic entanglement applies to the quantum-nano-space-time of biological membrane structure determining relationship of vectorial thermodynamics for coherent-decoherent states as applied to life functional metric dimension [73]. Water trapped inside brain microtubules can undergo a spontaneous quantum phase transition [74] [75]. Hence, toward a macroscopic coherent quantum state in which water molecules oscillate in phase with an electromagnetic field, condensed from quantum vacuum, corresponding to a suitable electronic transition [76].

At the astrocyte synaptically released GLU is co-transported with  $\text{Na}^+$  by the  $\text{Na}^+/\text{K}^+$ -ATPase consuming one ATP in the exchange for extracellular  $\text{K}^+$ .

The  $\text{Na}^+/\text{K}^+$ -pump dysfunction has been tied to various diseases, including epilepsy and brain malformations.

The Jagendorf's Jump of ATP formation caused by acid-base transition of spinach chloroplasts [77] is an analogous mechanism of proton translocation, which function in the reverse coupling kinetics of  $\text{Na}^+/\text{K}^+$ -ATPase across the membrane [78]. Accordingly, when the mechanism could manifest reversibility is a parallel vectorial function, which does not respond to the principle of microscopic reversibility. This one is based in a static configuration of the active sites, which operates simultaneously in both senses according only to the mass action of the reaction.

The transmembrane enzymes operate by a dynamic of the structural function changes, breaking symmetry by mutual exclusion, because the conformational change involves the re-organization of the active site, usually involving H-bond breakdown in order to replace the structure by other configuration to allow a reverse of the reaction sense [79] [80] [81] [82].

A pump reversing flow is analogous with the  $\text{H}^+/\text{K}^+$ -ATPase mechanics, studied on fundic mucosa of rat's gastric tissue acid secretion, characterized by the effects of two inhibitors: thiocyanate ( $\text{SCN}^-$ ) and 2-methyl-8-(phenylmethoxy)-imidazo-[1,2-a]-pyridine-3-acetonitrile (MPIPA). Thus, unmask the secretion of  $\text{HCO}_3^-$  and the inhibition blocking basal distal to

second messenger activation of the acid formation process.

SCN<sup>-</sup> inhibit by becoming protonated under conditions of low luminal pH and inhibit the formation of H<sup>+</sup> by parietal cell H<sup>+</sup>/K<sup>+</sup>-ATPase and the associated fluxes of K<sup>+</sup>, Cl<sup>-</sup> and Na<sup>+</sup> show increases in the total secretion of HCO<sub>3</sub><sup>-</sup> an additive effect in K<sup>+</sup> concentration increase by the additive effect of both reagents. Chloride ions show a high degree of inverse correlation in the presence of SCN<sup>-</sup> alone and plus MPIPA. Sodium ions demonstrate an inverse correlation when the tissue response to SCN<sup>-</sup> alone. The effect showing competition with Cl<sup>-</sup>/Na<sup>+</sup> cotransports at Cl<sup>-</sup> channels associated with either the secretion of H<sup>+</sup> or an exchange site for HCO<sub>3</sub><sup>-</sup>.

Using an enzymatic to assay HCO<sub>3</sub><sup>-</sup> release was shown that in the absence of MPIPA, 10<sup>-2</sup>mM histamine, 10<sup>-1</sup>mM methacholine and 1mM dBcAMP (dibutyryl cyclic adenosine monophosphate) plus 1mM theophylline stimulate HCO<sub>3</sub><sup>-</sup> secretion. These effects were reduced by 10<sup>-3</sup>mM MPIPA.

Postincubation concentrations of Cl<sup>-</sup>, Na<sup>+</sup> and K<sup>+</sup> in the bathing media were determined and compared with those of the preincubation period.

Methacholine and dBcAMP plus theophylline inhibit HCO<sub>3</sub><sup>-</sup> secretion. The ability of the gastric fundic mucosa to respond to MPIPA for stimulation of HCO<sub>3</sub><sup>-</sup> secretion does not depend on the presence of HCO<sub>3</sub><sup>-</sup> or CO<sub>2</sub> in the bathing media.

Cl<sup>-</sup> and K<sup>+</sup> ion fluxes appear to be inversely related to the appearance of measurable HCO<sub>3</sub><sup>-</sup> secretion by MPIPA may be coupled to either or both of these ion fluxes.

The potent inhibitor effect over gastric acid secretion could be extrapolated for its potential pharmacological agent use by its cytoprotective activity against induced mucosal injury *in vivo*.

Isoproterenol by binding the β-adrenergic receptors on the cell surface activating AC. Renin released from rat renal cortical slices was measured under conditions desired to elevate intracellular cAMP and Ca<sup>2+</sup> [83]. Phenylephrine initiated Ca<sup>2+</sup> influx, which blocked accumulation of cAMP within the juxtaglomerular cell, thereby inhibiting renin release.

Enhanced Ca<sup>2+</sup> influx has been shown to increase the release of arachidonic acid and norepinephrine, endogenous factors known to stimulate renin release and suggests that an ordered sequence of events occurred in preference to random effects [84].

Redistribution of ions could modulate neuronal activity, given that voltage-gated ion channels are a key element in the progress of spikes at the axon. Neuronal firing is argued to be sensitive to the variation of as little as one millivolt across the cell membrane, or the involvement of a single extra ion channel. Transcranial magnetic stimulation is similarly argued to have demonstrated that weak EM fields can influence brain activity.

### **Blood brain barrier (BBB)**

The choroid plexus generating from plasma the cerebrospinal fluid (CSF) functions in the mutual exclusive vectorial kinetic according to a potential of hydrophilic-plasma to hydrophobic-CSF flow. Thus, conducts in a unilateral sense the flow for brain irrigation and entropy release.

The brain of the newborn enjoys a hormonal system development involving about 60% of total calories ingested, which became stabilized at adult age as 25% of total body energy. At maturity the H-bond energy contributions of the enzyme hydration vs dehydration turnovers adds to a thermogenic flow of energy that requires that the brain develops an autonomous cooling system. Thus, at the blood-brain barrier (BBB) (150ml CSF) are maintained permanently, and 0.3-0.4 ml/min CSF are renovated constantly to generate about 500ml/daily output. The equivalence H-bond contribution is (H<sub>2</sub>O)<sub>n=3.4</sub> for each water cluster configuration about 3.4×5kcal/mol=17kcal/mol.

In the brain, which is dependent on glucose and oxygen as the major source of energy, the glucose concentration is usually 4 to 6 mM (5 mM equals 90 mg/dL), but decreases to 2 to 3 mM when fasting. Confusion states occur below 1mM and coma at lower levels. The hypothalamic glucose binding nerve cells regulate the glucose levels of blood.

### **The RARE BiBi mechanism**

The RARE BiBi shows a second-order dependence on substrate concentration:  $Mg^{2+}$  has to bind first to activate the binding site for MgATP. Hence, the noradrenaline (NA) activated of the hypothalamic tissue is controlled by obligatory ions  $Mg^{2+}$  exceeding the substrate concentration. cAMP and calmodulin (CaM) release of  $Ca^{2+}$  determine signaling of the amplitude, phase and period of circadian rhythms. ATP<sup>+</sup> and chelating metabolites decreases CaATP, strongly activating an  $Mg^{2+}$  in excess of substrate for adenylate cyclase (AC) activation. Effect increases the cAMP-dependent activation of CREB pathways for memory affirmation.

$Ca^{2+}$  releases activate the glutamate neurotransmission. Serotonin (5-hydroxytryptamine, 5-HT) produced in Raphe nuclei located in the brainstem, could induced  $Ca^{2+}$  increase and reduced the cAMP increase, indicating cross-talk between the 5-HT-sensitive  $Ca^{2+}$  and cAMP pathways. Ionic equilibrium controlling  $Ca^{2+}$  effects for a simultaneous dead-end CaATP inhibition of AC. Thus, function for mutual exclusion activation of the  $\alpha$ -amino-3-hydroxy-5-methyl-4-isoxazolepropionic acid (AMPA) receptor, is an ionotropic transmembrane receptor for glutamate (iGluR) that mediates fast synaptic transmission in the central nerve system (CNS).

### **This hydrophilic configuration**

This hydrophilic configuration has to be mutually exclusive by H-bond breakdown (second door) to reconfigure a hydrophobic structure of positive R-groups to attract negatively charged molecules like  $ADP^{3-}$  and  $AMP^-$ . However, the endergonic product: cAMP, which could not be liberated from a hydrophobic close environment, which allows water exclusion for vectorial decrease in the cyclization energy. However, Mg-cAMP is released by the large mass action of water clusters and the increase in free  $Mg^{2+}$ . Turnover requires the mass-action of water cluster for additional H-bond breakdown, reconfiguring the obligatory Mg site characterizing the hydrophilic state.

These are transitions thermodynamically coupled between an exergonic reaction couples to drive the endergonic, sliding event by the H-bond

breakdown of the binding folding dissipative heat release.

The directionality would be given by mutual exclusion and this complementarity would be the conformational change of the protein, dependent on a breakdown of a small ratio of H-bonds of the total potential of the water cluster. A subsequent event depends on the exergonic uphill event of H-bond breakdown to recreate the hydrophilic domain (3th door). However, this step has the large contribution to the enthalpy of the system by a natural coupling to the high H-bond mass action of water clusters at molar level. The system operates with the remaining H-bonds within the water cluster. This is rather not detectable since at the test tube reactants and products are at  $\mu$ molar level. However, the water cluster involves the solvation energy of encompassing saturation surroundings.

Hence, the active site function should be equivalent to a mutual exclusion by the H-bond breakdown, required for the structural states (or change) related to the coupling to the electron transport system.

An endergonic state of the enzyme will depend on the number and strength of R-groups on the enzyme, within the membrane in transition from hydrophilic to hydrophobic state. The hydration changes depend of the tendency of the bipolar water molecules to organize H-bonds in a cluster  $(H_2O)_{n \approx 3,4}$ . Thus, allows energy conservation at the enzyme at the structure of the protein chain sliding of the pKa of the amphoteric R-group of histidine and the pKa of differentiated R-groups in the active site. Hence, the site became organized from hydrophilic to attract ADP and Pi in a mutual exclusion transition into a hydrophobic domain enclosing the substrates to optimize the environment for the synthesis of the products: ATP, plus the released  $H_2O$ .

The finding that  $CF_1$ -ATPase requires  $Mg^{2+}$  for binding to the membrane and reconstitution of allotropic properties implicates that vectorial response may depend from both conformational change at active site coupled to a conformational change displacing the topology of R-groups in the membrane from a hydrophilic to hydrophobic conformational domain.

Figuratively, the microscopic reversibility principle describes that a single microscopic door

allows transit in both senses, allowing only a closed thermodynamic system, which only allows changes by mass-action equilibrium. However, an irreversible open system do have vectorial kinetic as long that enthalpy input is continuous as light trapping by the chloroplast and the generated entropy is continuously dissipated.

Hence, to evade that incompatibility, it is possible to assume two inversely linked doors, mutually exclusive, one to be open when the other is closed. The conformational changes described are operating when one domain is hydrophilic and the other turns to become hydrophobic.

### **Folding dynamics twist depends of imidazole ring role proline**

Vectorial kinetics is conferred by the folding dynamics-dependent of a proline within the polypeptide. The H-bonds could be regarded as doors, when open attracts water cluster to the segment containing negative R-groups capable to coordinate  $Mg^{2+}$  (first door).

Secondary structure of polypeptide chain can fold  $\alpha$  helix coiled structure stabilized by intra chain H-bonds.

The polypeptide can change direction by making reverse turns and loops.

Tertiary structure for water soluble proteins folds into compact structures with tendency to form non-polar hydrophobic cores.

The H-bond dynamics on folding allows the peptide bond a resonance stabilized polar and planar structures. Two parallel  $\beta$ -pleated sheets with an intervening strand of  $\alpha$ -helix domains bends on the surface of globular proteins. This structure offers little steric hindrance to a modification in the direction of the polypeptide chain.

The imidazole ring, a five-membered ring of proline, allows a second residue to manifest a reverse turn.

Constructing mutual exclusion domains through H-bonds turnover allows the interaction between distant regions of a polypeptide chain. The hydrophobic effect drives protein folding in about  $10^{-1}$  to  $10^{-13}$  s to rotate around the C-C $\alpha$  and N-C $\alpha$  bonds of the polypeptide backbone to consolidate a hydrophobic core, which will tend to displace water out.

Required to bend, twists and folds the polypeptide sequence in its transition another structure level, by producing differential configurations by hydrophilic associations of cations ( $Mg^{2+}$ ,  $Ca^{2+}$ ,  $Zn^{2+}$ , etc.) and hydrophobic ones for  $Ca^{2+}$  and the anions (2,3-DPG<sup>5-</sup>, ATP<sup>4-</sup>, ADP<sup>3-</sup>, AMP<sup>2-</sup>, cAMP<sup>-</sup>, etc.).

### **Quantum physics of axonal function**

Both  $\alpha$ - and  $\beta$ - tubulin is composed of approximately 450 amino acids and in their sequence identity (approximately 40%), slight folding difference between  $\alpha$  and  $\beta$  forms can be observed. The two tubulins exhibit homology with a 40,000-MW bacterial GTPase, FtsZ, a ubiquitous protein in eubacteria and archeobacteria.

In eukaryotes, microtubules are long, hollow cylinders made up of polymerized  $\alpha$ - and  $\beta$ -tubulin dimers [85]. The inner space of the hollow microtubule cylinders is referred to as the lumen. The  $\alpha$  and  $\beta$ -tubulin 50 kDa subunits are ~50% identical at the amino acid level [86].

Tubulin polymerizes end to end, with the  $\beta$ -subunits of one tubulin dimer contacting the  $\alpha$ -subunits of the next dimer. In which one end will have the  $\alpha$ -subunits exposed while the other end will have the  $\beta$ -subunits exposed. The same polarity allows to assign a (-) and (+) ends, a bundle of protofilaments in parallel allows that (-) end has only  $\alpha$ -subunits exposed while the other has only  $\beta$ -subunits exposed. Microtubule elongation can occur at both the (+) and (-) ends, it is significantly more rapid at the (+) end [87].

In vitro assays for microtubule motor proteins: dynein and kinesin using a fluorescent tag of a microtubule fixed to a microscopic slide to observe their space displacement.

Dendrites receive input from many other neurons and carry those signals to the cell body (soma). If stimulated enough, a neuron fires an action potential, an electrical impulse that spreads to other neurons. The neurons in the brain incorporates dendritic inputs to fire the sum of action potential implicates for crosstalk communication.

Cosmological during a Dark Ages from 370,000 years until the emerging of stars, the only photons (electromagnetic radiation, or "light") in

the universe were those released during decoupling (visible today as the cosmic microwave background). The decoupled photons filled the universe, gradually redshifting to non-visible wavelengths after about 3 million years, leaving it without visible light, but the *21 cm radio emission by H atoms*.

A far-distancing emission as antenna to dendrites and spines reaching neurons into its tree shaped dendritic structure. With electronic spin signals emitting at the same frequency distributed in space along that branching structures from other neurons in the network.

The antenna operative at the quantum microtubules level are the H atom electron orbital spins, signaling *up* (higher energy) and *down* (lower energy), emitting 21 cm. A single common wavelength allows a coherence sum up to synchronize thousands of synaptic outputs into axon/membrane action potential (for each differentiable neurotransmitter: glutamatergic, catecholaminergic and adrenergic) for specific time functional brain's areas. Hence, allows electric neuronal circuit to operate with a *null noise* with an integrated crosstalk expression to reach an infant meaningful cognition to slowly replace the hormonal communication with the infant-progenitors.

The activity in the soma cell body was highly correlated with dendrite activity. When an action potential reaches a presynaptic terminal, it activates the synaptic transmission process. The first step is rapid opening of calcium ion channels in the membrane of the axon, allowing calcium ions to flow inward across the membrane. The resulting increase in intracellular calcium concentration causes synaptic vesicles filled with a neurotransmitter chemical to fuse with the axon's membrane and empty their contents into the extracellular space. The neurotransmitter is released from the presynaptic nerve through exocytosis. The neurotransmitter chemical then diffuses across to receptors located on the membrane of the target cell. The neurotransmitter binds to these receptors and activates them.

Inside the presynaptic terminal, a new set of vesicles is moved into position next to the membrane, ready to be released when the next action potential arrives. The action potential is the

final electrical step in the integration of synaptic messages at the scale of the neuron.

Extracellular recordings of axon action potential propagation are distinct from somatic action potentials in three ways. The signal has a shorter peak-trough duration ( $\sim 150\mu\text{s}$ ) than of pyramidal cells ( $\sim 500\mu\text{s}$ ) or interneurons ( $\sim 250\mu\text{s}$ ). The voltage change is triphasic. In recordings from freely moving rats, axonal signals have been isolated in white matter tracts including the alveus and the corpus callosum as well hippocampal gray matter.

The generation of action potentials in vivo is sequential in nature, and these sequential spikes constitute the digital codes in the neurons expressed as electric imaging and magnetic resonance imaging. Microtubules run along the length of the axon and provide the main cytoskeletal "tracks" for transportation.

The axoplasm is the equivalent of cytoplasm in the cell. Microtubules form in the axoplasm at the axon hillock. They are arranged along the length of the axon, in overlapping sections, and all point in the same direction – towards the axon terminals. This is noted by the positive endings of the microtubules. This overlapping arrangement provides the routes for the transport of different materials from the cell body. Studies on the axoplasm have shown the movement of numerous vesicles of all sizes to be seen along cytoskeletal filaments – the microtubules, and neurofilaments, parallel of both directions between the axon and its terminals and the cell body.

Outgoing anterograde transport from the cell body along the axon carries mitochondria and membrane proteins needed for growth to the axon terminal. Ingoing retrograde transport carries cell waste materials from the axon terminal to the cell body. Outgoing and ingoing tracks use different sets of motor proteins. Outgoing transport is provided by kinesin, and ingoing return traffic is provided by dynein. Dynein is minus-end directed. There are many forms of kinesin and dynein motor proteins, and each is thought to carry a different cargo. Kinesin walking on a microtubule. It is a molecular biological machine that uses protein domain dynamics on nanoscales. Kinesin and dynein are motor proteins that move cargoes in the anterograde (forwards from the soma to the axon tip) and retrograde (backwards

to the soma (cell body)) directions, respectively. Motor proteins bind and transport several different cargoes including mitochondria, cytoskeletal polymers, autophagosomes, and synaptic vesicles containing neurotransmitters.

The vast majority of axonal proteins are synthesized in the neuronal cell body and transported along axons. Some mRNA translation has been demonstrated within axons.

Quantum physics of neuron in the function of neurons depends of structures at the synaptic level, contributing to the electron spin differentiating up and down positions, with adapted angular momentum. The electrogenic membrane could allow organizing a non-polarized electron current to acquire polarity and the polarization of the current is maintained by alignment. Hence, the electrons that at the beginning do not manifest orientation are capable to reinforce electrical signals by passing through two layers of similar polarity and the signal power became decreased when magnetization has opposite senses.

Quantum mechanics at brain level were shown by spintronic success of Vowel recognition with four coupled spin-torque nano-oscillators were obtained by tuning their frequencies according to an automatic real-time learning rule. Thus, allows electrical pulse frequencies to develop a cross-talk between neuronal circuits, implicating the importance of language for coding and decoding information.

The electrogenic properties allow differential in the one neuron connective capability to maintain an average of  $10^4$  synapses. Hence, electric signals potentiation will decrease randomness by reinforcement of neuronal circuits. The information paths are organized in layers. Thus, signals combined as synaptic functions learned to interact and compare with experience. After iterative step a consent tendency indicates errors.

Microtubules regulate synaptic-vesicle, provides path for bi-directional transport between presynaptic terminals in exocytosis at sites of release [88] [89]. In dendritic spines the cytoskeletal of actin filaments originated in the dendrite shaft could enter the spine head morphology [90] [91] [92] [93].  $Ca^{2+}$  influx actin polymerization modulates changes in synaptic strength [94]. Stimulation of postsynaptic N-methyl-D-aspartate receptors. Microtubule

invasions, indicating that microtubules targeting into spines are sensitive to plasticity signals integrating plasticity, involved in both pre- and postsynaptic functions.

Microtubules at the cytoplasmic activation step could allow a configuration with a singular conjunction of nodes reinforcing electric signals and therefore eliminating noise random signals.

The dynamics of microtubules alternate phases of polymerization and depolymerization. These are modulated by GTP hydrolysis microtubule-associated proteins and various post-translational modifications of tubulin [95] [96], like the reversible removal of the C-terminal tyrosine residue of  $\alpha$ -tubulin at the external surface of subunits. The residue is cleaved off by specific tubulin carboxypeptidases. Detyrosinated depolymerize microtubules restored on disassembled  $\alpha$ -tubulin by tubulin tyrosine ligase (TTL) [97] [98] [99] [100] [101]. Differentiation between oppositely oriented microtubules controls polarized neuronal transport [102]. The magneto-resistance of the neuron turns modulations of electric current in voltage terminals of synaptic function. The magnetization of the outer membrane vs the inner one allows spin transference. The role of spin or angular momentum of electrons will depend on the capability to orient electric impulses into polarized structures of membranes conductivity.

$Mg^{2+}$  and  $Ca^{2+}$  could coordinate R-groups in a membrane of differentiable polarity, assimilable to hydrophilic for negative R-groups coordinating hydrated  $Mg^{2+}$ , with  $H_2O$  molecules, configuring folding. The latter, responds by sliding when nascent  $Mg^{2+}$  is released allow the exposing of positive R-groups capable to respond to  $Ca^{2+}$  and/or the binding of negative molecules. Hence, allows sequential coupling that in humans become especially reinforced by myelination.

There is some similitude for the  $Na^+/K^+$ -ATPase pump to create polarity and action potentials by differences on access to channels and building-up of polarity, allowing the emergence of Cartesian wavelongs of differentiable wavelengths to consolidate long-term memories.

How much current actually flows across the membrane over the course of an action potential?

A typical nerve cell contains  $100Na^+$  channels per square micrometer. At a membrane potential of

+20mV, each channel conducts  $10^7$  ions per second. Assuming a cell surface  $10^4\mu\text{m}^2$  (volume of  $10^4\mu\text{m}^3$ ) corresponds to an increase in the  $\text{Na}^+$  concentration of less than 1%. A stronger action potential results very small change in the distribution of charge. Its efficient allows long distance signaling and rapid repetition rates.

The failure in regulating the tyrosination/detyrosination cycle occurs as a result of aging [103].

The tubulin carboxypeptidases VASH1 and VASH2, resulted in perturbed neuronal migration in the developing neocortex, microcephaly and cognitive defects, including mild hyper-activity, lower anxiety and impaired social behavior.

The most prominent Alzheimer's disease clinical symptom are progressive memory loss and decreases in synaptic density and cognitive impairment [104] associated to elevated amounts of

oligomeric amyloid- $\beta$  peptide (1–42) ( $\text{oA}\beta$ ) [105] that when oligomerize form disruptive plaques in the brain.

### Hydrophobic

The molecular kinetics synchronization that prevents microscopic reversibility, because could not be conceptually assimilated to the principle of microscopic reversibility requiring a single door, which could allow transit in both senses.

Coordinative binding of normally induces a conformation change, which allows for exposure of the hydrophobic core of human cardiac troponin C (cTnC). It requires a large thermodynamics expense for exposing R groups of this hydrophobic domain.  $\text{Ca}^{2+}$  binding in the cycling reaction of AMP into cAMP is highly endergonic process, which requires a higher  $\text{Mg}^{2+}$  concentration to compete

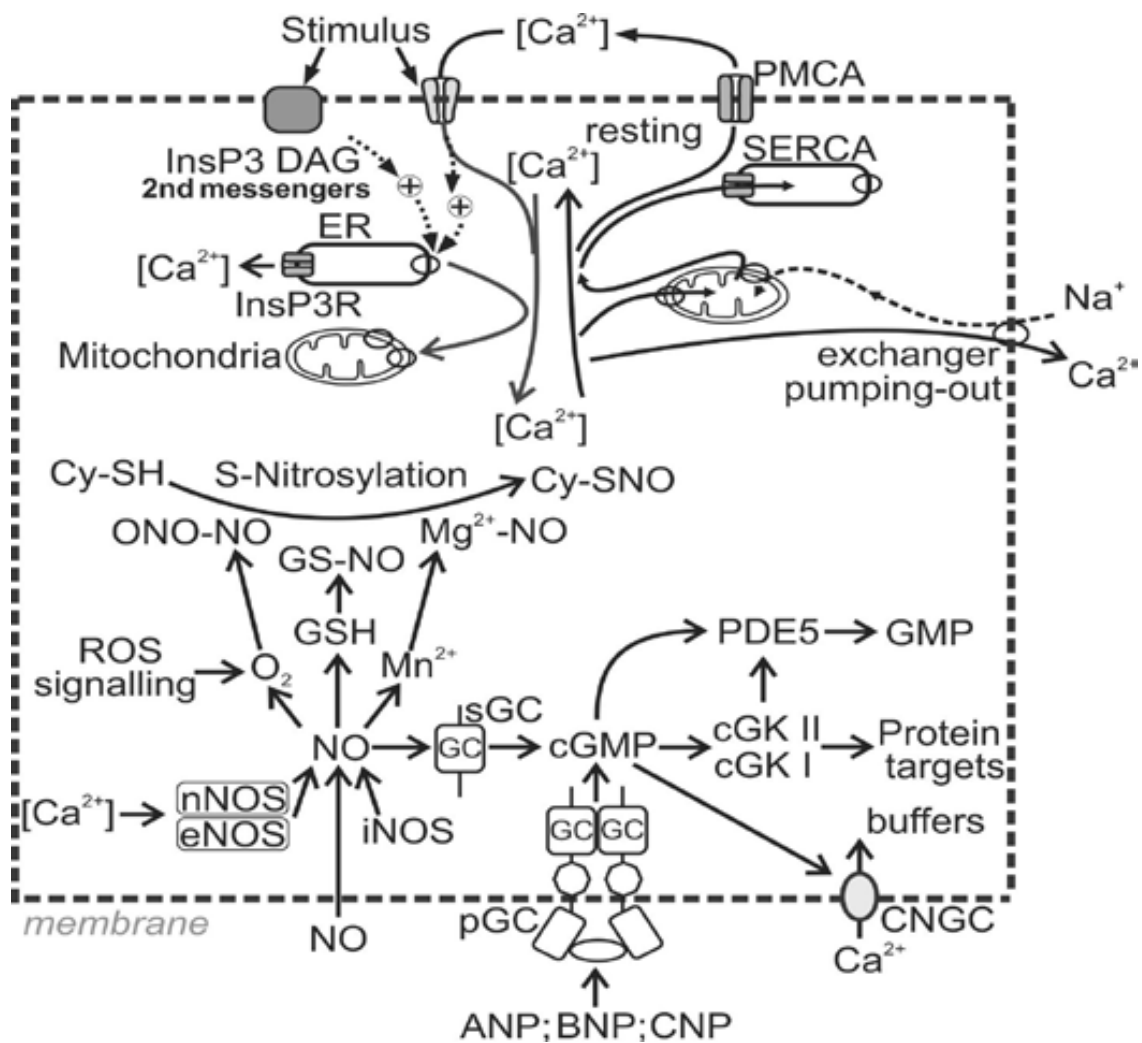


**Figure 12:  $\text{Ca}^{2+}$  signaling mechanisms.** A Nitric oxide (NO) paracrine signal could act by diffusion from other cells within the cell itself could be produced by different NO synthases (NOSs).

The cells to reach the resting state activate the mitochondrial reuptake and the pumping of  $\text{Ca}^{2+}$  out of the cytoplasm. Nitric oxide (NO) can stimulate soluble guanylyl cyclase to form the messenger cGMP signaling pathways to activate the cyclic nucleotide-gated channels (CNGCs).

The cells cytoplasm maintain 100nM  $[\text{Ca}^{2+}]$ , but after a stimulus the entrance of  $\text{Ca}^{2+}$  from channels or from the endogenous endoplasmic reticulum (ER) rises to 500nM the  $[\text{Ca}^{2+}]$ . The entering ions bind mostly into the cytoplasm buffers calbindin D-28k (CB) and parvalbumin (PV), and taken-up by mitochondria. The  $\text{Ca}^{2+}$  entry phase is terminated in a sequential manner by the  $\text{Na}^+/\text{Ca}^{2+}$ -exchanger, and the  $\text{Ca}^{2+}$  pumps: plasma membrane  $\text{Ca}^{2+}$ -ATPase (PMCA), sarco/endoplasmic reticulum  $\text{Ca}^{2+}$ -ATPase (SERCA) for the termination of the action spike.

The  $\text{Ca}^{2+}$  signaling include entry channels controlling the uptake from the outside and from internal stores, as well as the  $\text{Ca}^{2+}$  release to the outside. Buffers control operation range to prevent  $\text{Ca}^{2+}$  level leading to cell death. The  $\text{Ca}^{2+}$  pump and exchangers remove it from the cytoplasm to return in the internal stores. CNGC Signaling function requires  $\text{Ca}^{2+}$  sensors and effectors.

CNGCs activate either  $\text{Ca}^{2+}$  entrance or cyclic guanosine monophosphate (cGMP)-dependent protein kinase (cGK) and reactive oxygen species (ROS) signaling. cGMP is formed by a plasma membrane guanylyl cyclase (pGC), which is part of the single membrane-spanning receptor activated by a variety of peptides.

$\text{Ca}^{2+}$ /calmodulin-dependent protein kinases (CaMKs), calcineurin, phosphorylase kinase, and myosin light chain kinase (MLCK),  $\text{Ca}^{2+}$ -promoted ras inactivator (CAPRI). Atrial natriuretic factor (ANP), C-type natriuretic factor (CNP) guanylin, brain natriuretic factor (BNP).

Time domains: for exocytosis,  $\mu\text{s}$ ; for contraction, ms; for metabolism, sec and for gene transcription, min.  $\text{Mn}^{2+}$ ,  $\text{Zn}^{2+}$  and  $\text{Mg}^{2+}$  could not activate CaM, the latter ion affects the specificity of CaM and its distribution among targets.

Calreticulin (CRT) is a low-affinity  $\text{Ca}^{2+}$ -binding protein that is located within the lumen of the endoplasmic reticulum (ER) and homologous proteins calnexin and calmeglin have an acid C-terminal domain with a large number of low-affinity

$\text{Ca}^{2+}$ -binding sites. CRT terminates in the Lys-Asp-Glu-Leu (KDEL) sequence as an endoplasmic reticulum protein retention receptor 1, by their continual retrieval from the cis-Golgi or a pre-Golgi compartment, responsible for its binding retaining CRT into the ER lumen, binding capacity 20-30 mol of  $\text{Ca}^{2+}$ /mol of protein.

The buffer calbindin D-28k (CB) in enabled neurons for highly localized  $\text{Ca}^{2+}$  events, which occur in spines, this ones have volume, which increase as a function of lack of  $\text{Ca}^{2+}$ -buffers. The spines increase the numbers of their synaptic connections and this neuronal miniaturization greatly enhances the signal processing capacity of the brain.

The calcium affinity of neural cell adhesion molecule (NCAM) has functional roles during nervous system development and in the adult after injury and in synaptic plasticity. It shows a closed-domain apo-like conformation, isothermal titration calorimetry shows that two metal binding sites of N-CaM are occupied by  $\text{Ca}^{2+}$ ,  $\text{Mn}^{2+}$  and  $\text{Mg}^{2+}$  at two metal binding sites, but the  $K_d(\mu\text{M})$   $\text{Ca}^{2+}$  5.6 is half the  $K_d$  for  $\text{Mn}^{2+}$  that binds much more strongly than  $\text{Mg}^{2+}$   $K_d=450$ .

The  $\text{Zn}^{2+}$  ions do not bound to the  $\text{Ca}^{2+}$ -binding loops of N-CaM in a position normally occupied by  $\text{Ca}^{2+}$ .  $\text{Mg}^{2+}/\text{Ca}^{2+}$  competition allows  $\text{Mg}^{2+}$  to switch-off CaM, when  $\text{Ca}^{2+}$  decreases to resting levels, because the titration curve for  $\text{Ca}^{2+}$  shift to higher  $\text{Ca}^{2+}$  concentration and the extent of activation will be inversely related to the  $\text{Mg}^{2+}$  tendency to occupancy of N-CaM.

### **CREB unzipping of DNA**

cAMP response element-binding protein (CREB) regulates transcription of genes: c-fos, Brain-derived neurotrophic factor (BDNF), tyrosine hydroxylase, numerous neuropeptides (somatostatin, enkephalin, VGF, corticotropin-releasing hormone), and genes involved in the mammalian circadian clock (PER1, PER2).

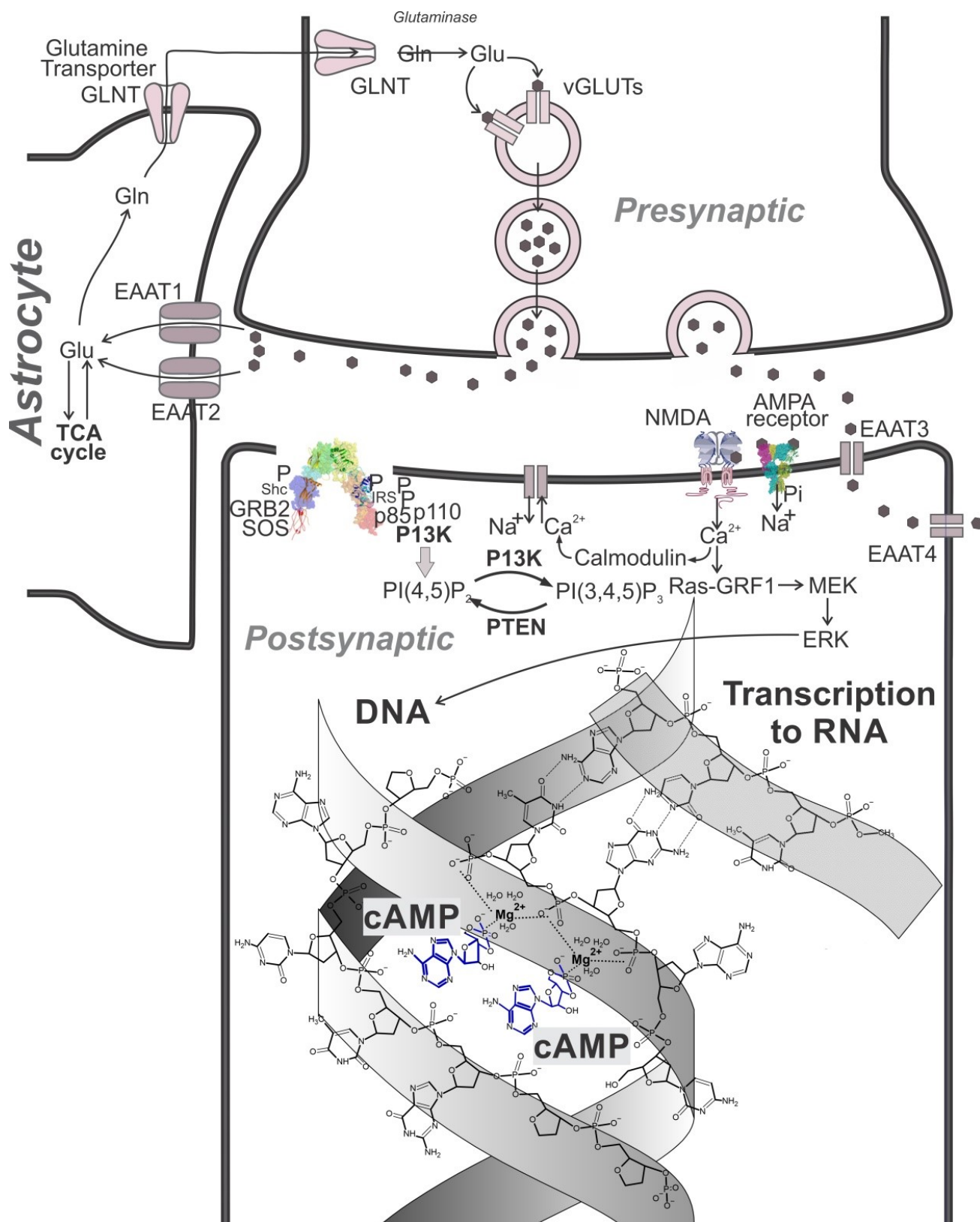


**Figure 13: Physiological mechanism for Mg-cAMP fitting into the double strands of DNA for physiological reversible unzipping at 37°C.** Base sequence of the two chains attracted to match in a double stranded binary rotational symmetry of DNA. Mg-cAMP unzipping mechanism opens the double-stranded DNA structure positioning the outside purines and pyrimidines bases to transcription mechanism leading to protein synthesis. The biological mechanism allows CREB expression plasticity by turning on/off, involving the breakdown of H-bonds.

Mg-cAMP inserted in DNA domain allows a switch-on by  $Mg^{2+}$  and -off by  $Ca^{2+}$ . A dynamic mechanism to activate gene expression in CREB by inducible gene response to dopamine phosphorylation via G protein coupled receptor. Thus, acting to synthesize brain derived growth factor, a regulator during neuronal development and synaptic plasticity.

The triplex-helix structure of DNA dynamics during transition of the opening unzipping mechanism is analogous to the triplex-helix structure that appears to correspond and demonstrated to bind single-stranded DNA (which in the unzipping mechanism appears as Mg-cAMP) involved in triplex formation.

In the proposal of antiparallel triplexes [106], the third strand composed of purine bases, reflex the purine, adenine in the Mg-cAMP operating in CREB function. The unzipping mechanism of Bennun, in which the DNA opening, allows a parallel and the antiparallel, as templates for the gene expression of the father and mother contributions to the double helix and the reverse transition of zipping to the close state the double strands of DNA restores the original H-bonds. Thus, preserved the tendency by separation of cAMP as if the CREB mechanism described as operative a reversible of cAMP function by zipping coupled to the water cluster  $(H_2O)_{n=3,4}$  breakdown. Hence, a contribution to the energy by H-bond replacement to produce dimers  $H_2O \sim OH_2$ , maintained in circulation by the pressure exerted when contained by microtubules, to finally lead to entropy dissipation oral cavity lead to outside of the system.

It is inferred that the smaller size of dimers allows entering into the microtubules circulation, can exclude the larger sizes of water cluster. Thus, provides a perspective to an operative entropy pathway. The latter, is functional to conservation of its much larger concentration, which sustains the mass action of water cluster, by its exclusion from the entropy conducting microtubules.

H-bonds play integral roles in biological structure, function, and conformational dynamics, fundamental to life. The non-physiological heating treatment technic for the strands separation of DNA at  $65^\circ C$  has been in use. Hence, a technical test tube approach has led to bypass the proposed

unzipping for DNA expression as a plasticity mechanism, which allows a brain homeostatic preservation at the  $37^\circ C$  (figure 13) [107].

Transcriptional processes determine whether or not a gene is expressed and at what level. The activity of the promoter, the action of enhancers (and repressors), as well as the overall epigenetic landscape surrounding the gene are all involved in this regulation.

### The water pair hydrophobic structure

The interaction  $(H_2O \sim OH_2)$  from two H atoms of 2s and 2p orbitals allows a tetrahedral of  $104.5^\circ$  angles from of positive charge, potential energy barrier to rotation of one of the water molecules with respect to the other.

O-H results from the 1s orbit bond strain with oxygen (O) to form a sp orbital. The H-bond of two water molecules, the partially positive hydrogen atom  $\delta^+$  attracts the partially  $2\delta^-$  negative charge of one O to the other. The result in a dipole-dipole attraction mediated by the in between H-bonded distance  $H-O-H-(OH_2)$  0.177nm the polarity strength in water 104kcal/mol. The same H covalently to oxygen atom distance of 0.1nm is about 110kcal/mol. An N-H and  $C=O-H-N$  as between complementary pairs cytosine attracted to guanine separated by 0.27 to 0.3nm spontaneously attracted to form  $H-O$  or  $N-O$  by the unshared N or O electrons pairs. The water molecules detached from these intramolecular bonds within a protein become H-bonded between them, in bulk water. The dipolar state can induce transitive dipoles in other close molecules. Liquid state of water clusters shows a half-life  $10^{-8}$  s to  $10^{-11}$  s. The average number is  $(H_2O)_{n=3,4}$ . From liquid state (0.54kcal/g) a large number of H-bonds have to be broken to become vapor.

However, heat homeostasis at cerebrospinal fluid (CSF) hydrophobic medium at the pressure present in astrocytes, is able to maintain the release of single molecule of water by H-bonds breakdown and the hydric affinity disappears and allow a little polar state to manifest aggregated by non-polar interactions of  $H_2O::OH_2$ , indicating energy configuration:  $(H_2O \sim OH_2)$ , between both oxygen atoms. Thus, circulates within the astrocytes network in a metastable state of high oscillatory

tension between the oxygen orbitals, between surrounding hydrogen atoms tending to maintain covalent stability. Water dimer is the most widely examined water cluster. The turnaround angle differentiates six different isomers of water dimers. Hereby, RP isomers are illustrated in figure, the potential planar resonance states, orbital-5  $E_{orb}=-15.15\text{eV}$  and orbital-9  $E_{orb}=-8.90\text{eV}$ , with oscillatory potential  $\Delta E=-6.25\text{eV}$ .

Thus, determines several possible states of coherence. Hence, kinetic energy accumulates by resonance amplification. However, in the CSF the absence of  $\text{O}_2$  and  $\text{N}_2$  allows coherence and their

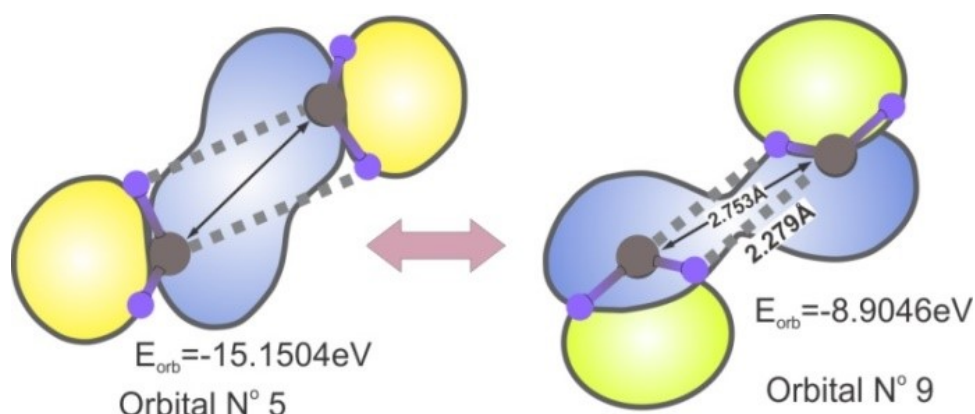


**Figure 14: Two oppositely charged ions, however, can form an ion pair.** The free energy change for transfer of two oppositely charged residues from water to the monopolar interior of a protein is about  $-1\text{kcal/mol}$ . When the ion pair forms, the water molecules in the solvation sphere of each ion are released to the bulk. Each ion therefore loses its free energy of solvation, driving their force for ion-pair formation the increase in the entropy of water clusters, during formation of the ion pair.

The microwave regions of the electromagnetic spectrum are radio waves, based in hydrogen level 1s orbital that has in energy difference of polarization change spin flip, dividing in two the energy barriers or electron density on the orbital motion. Pauli exclusion to energy density level allows movement only between tunneling is exchanges in the two pair of the H-bond donating and accepting water monomers ( $\text{H}_2\text{O}\sim\text{OH}_2$ ).

A more rigorous statement is that, concerning the exchange of two identical particles, the total (many-particle) wave function is antisymmetric for fermions, and symmetric for bosons.

This means that if the space and spin coordinates of two identical particles are interchanged, and then the total wave function changes its sign for fermions.

In the dimers has been determined to begin to flip of the acceptor monomer followed by  $180^\circ$

presence in the air induce a randomness decoherence, into the oral cavity, generates the exhaled vapor to the outside, decreasing entropy of the organism and allows brain to operate electrical impulses by the enthalpy potential of dissipative entropy, approaching the kinetic irreversibility of an open-system.

Ion pairs can form in the hydrophobic interiors of globular proteins. The free energy of solvation of an ion is so large (about  $60\text{kcal/mol}$ ) that an isolated charged residue is never found in the hydrophobic interior of a globular protein.

rotation about oxygen-oxygen bond. The interchange orbital exclusion could be assimilated to the Pauli's exclusion resulting between energy level (barriers).

The vibrational position results from intrinsic magnetic dipole movements as carried to the hydrogen spin. These jump interactions increase in energy parallel and decrease with anti-parallel (spin flip). The frequency ( $\nu$ ) of the quantum relationship  $E=h\nu$  detectable by this transition  $\lambda=hc/E$ .

A water dimer is capable to expand Doppler shifts and became a much broader H spectrum when cooling CSF.

In dimers when the position of the 4H became parallel (relative positions for H-bonds with differential frequency emission). The magnetic movements are antiparallel (spin flip) create harmonics in resonances kinetic energy trapped within the dimer structure. The wave function of

electron and proton overlaps because  $d_e$  encompasses partially the proton location. The structure could expand the energy content by vibration absorbing kinetic energy, trapping in resonance maintaining coherence under limit of pressure (microtubules) and temperature.

The dimers exhibit three distinct low barriers to kinetic pressures over orbital displacement. This resistance results in vibrational states, stabilized by resonance.

Analysis of H atomic closeness distance for electron and proton leads to a Pauli's resistance to configure the same quantum state and explain a vibrational state shared at H atoms, forced to partially share microscopic space at differential time to elude the exclusion. Since the magnetic dipoles unstable state represents the possibility to emit tiny electric current loops, structuring the high energy reached by the dipoles, within water pairs.

### **The oscillatory mechanism between the two states of the pairing**

Single water molecules could not have a liquid state at  $(H_2O)_{n=0}$  because lacks H-bonds, suggesting the emergence of other structures in the interior of the cell.

Entangled by H orbitals superposition has resonance effects that participates in structure function system for thermic maintenance from muscles (tremor affecting hypothermia) a brain pulsations, etc. In perspective the rapid loss of the corporal temperature produces by death lead to speculations about the meaning, that at the time of death, there is an instant decrease in body weight of 26g.

Entangled by the complementary pairing between the hydrogen atoms of each water-water pair of molecules as shown:  $(OH_2 \sim \sim H_2O)$ , results in repulsion between the atoms of oxygen. Similarly, in the complementary oscillatory state of the pair, is shown entanglement between both oxygen atoms:  $H_2O \sim \sim OH_2$ , and distancing between the hydrogen atoms.

The molecular entanglement surges from the tendency to relate both vibrational configurations by not breaking the water identity. Hence, it is sustained in the first configuration by each H atom participating in vibrational state with the other

opposite electron orbital to reach oscillatory a complementary tendency to have tendency to configure some but insufficient stability at the two electrons resembling the orbital connections of molecular hydrogen. The participation of only two electrons out of the six in each oxygen share entanglement by its partial orbital attraction for pairing to only approach stability. Thus, lacking a complete mutual sharing of orbitals, which occur when both oxygen atoms could acquire a molecular bonding, because each atom attractions surge from its orbitals space: "s" and "p". These allow tetrahedral geometry  $2s$   $2p$  and hybrid orbitals:  $4 \times sp^3$ , in which two could be share, but the other two could not. Thus, a changing attraction between orbitals of oxygen could explain an oscillatory attraction state by the loss of oxygen entanglement present in the hybrid transition:  $(OH_2 \sim \sim H_2O)$  vs the gain of entanglement:  $H_2O \sim \sim OH_2$ , providing transition states between two differential symmetries, allowing the breaking of the attraction strength in one of them.

These instable configurations of two single molecules of water could be entangled when interact, or share spatial proximity in a way such that the quantum state of each molecule of the group cannot be described independently of the state of the others. Entanglement has been shown between the rotational states of a  $40CaH^+$  molecular ion and the internal states of a  $40Ca^+$  atomic ion.

Substantial interdisciplinary attention due to an intimate entanglement of spin and orbital degrees of freedom which may give rise to a novel spin-orbital insulating behavior and exotic quantum spin liquid phases.

Hence, water in molecular pair entanglement, allows the hidden of the polarity affinity for ions, etc., which characterizes polymeric water configurations for hydration shells of ions and could allow differential properties in between the hydrophilic phase and the hydrophobic one. This is so because the hidden polarity entanglement allows unidirectional way to cross the membrane from the outside of the membrane to its inside.

Decomposition of the pairing yields a non-accumulative state (or dissipative function) allowing non-reversibility to the system thermodynamics, because the dissipative effect by loss of mass action.

The connection with quantum mechanics is made through the identification of a minimum packet size, a photon, for energy within the electromagnetic spectrum. The identification is based on the theories of Planck and the interpretation of those theories by Einstein. The correspondence principle then allows the identification of momentum and angular momentum (spin).

The energy conservation function relates of the inertial response in the energy spectrum gap from the ground state to first excited state. As the number of particles increased, the additional contribution to the ground state energy got closer and closer to zero, leading to a material that was always gapless.

The evolution of the energy-space within differential locus is modulated by the differential rates of enthalpy vs entropy, by maintaining flatness, conservation Euclid's metric, preventing deviations that could modify the cosmic curvature.

The approach originality allows thermodynamics analysis of the neuronal structure and functional responses by environmental relationships like the 24hs cycle control by the time relative level of  $Mg^{2+}$  vs  $Ca^{2+}$  are capable to modify the functional level of adenylyl cyclase (AC).

The AC turnover involves an exergonic phase dependent on an excess of free  $Mg^{2+}$  over the substrate  $MgATP$ , with hydrophilic function binding of single molecules of water at the expense of the breakdown of H-bonds, structuring water clusters. Thus, the energy input for a conformational change, involving the  $Mg^{2+}$  coordinative relationship between the R groups of the enzymes. Thus, disturb a time dimension of a quantum mechanics vibration system. Hence, these groups could manifest a kinetic energy output that could propagate by tunneling from the inside of AC to its location on the membrane to signal as a molecular antenna other enzyme molecules for synchronized activation chain for this phase of the reaction. The subsequent restructuring of the new conformational structure of the active sites required for the highly endergonic reaction to produce cAMP. Hence, the active site reconfigure as a hydrophobic domain, which releases  $Mg^{2+}$  and its coordinated water molecules (Nascent  $Mg^{2+}$  will integrate the AC system with the ATPase system by

modifying hydration shell of the  $Na^+/K^+$  ions, during turnover of the pump). The AC hydrophobic domain by the H-bonds breakdown of the coupled water clusters and exit of the single molecules of water from the system drives an irreversible kinetic sense. The insignificant reduction by the isolated water concentration in water cluster concentration 55.5M, allows the cluster to act as a reactant to saturate the protein. Accordingly, prevents any reverse of the kinetic sense of turnover powering its cycling in the absence of the equilibrium (irreversible kinetics) to recreate the  $Mg^{2+}$  activatory site of AC, which precedes the binding of substrate:  $MgATP$ , and therefore to overcome the microscopic reversibility principle.

The  $Mg$ -cAMP unzipping of DNA could activate CREB to originate the RNA transcription involves in the proteins synthesis to support the plasticity process involved in the creation of neuronal circuits. Infants are born with an incomplete development of the brain, and the human species has the mammalian olfactory bulb, atrophied into an olfactory epithelium, which creates a large period incapacitating the expression of genes related to motor activities in which the development of brain at begin consume near 70% of total body ingested calories.

It has been shown by the studies of infant's behavior a functional amygdala and hippocampus when they still have an under-developed frontal brain.

This period is strongly linked to learning: behavior, language, family integration, motor and integrative that individualizes social responses in an emotional memory related by 40% to experience rather than genetic responses. Henceforth, human characterizes their social achievement as the expression of free will.

### **The change of the membrane potential between the external hydrophilic face vs internal hydrophobic environment by dissipative entanglement**

Brain function is inextricably coupled to water homeostasis. The main volume between neurons is occupied by glial cells.

Sensory stimuli cause changes in cytosolic  $\text{Ca}^{2+}$  levels that are detected by a family of  $\text{Ca}^{2+}$ -binding proteins and neuronal calcium sensor (NCS).

Cosmic entanglement applies to the quantum-nano-space-time of biological membrane structure determining relationship of vectorial thermodynamics for coherent-decoherent states as applied to life functional nano metric dimensions. Water trapped inside brain microtubules (MTs) can undergo a spontaneous quantum phase transition. Hence, toward a macroscopic coherent quantum state in which water molecules oscillate in phase with an electromagnetic field, condensed from quantum vacuum, corresponding to a suitable electronic transition.

However, the potential energy surface (PES) of water is too complicated to represent it with an analytical function, even for the water dimer. Despite this difficulty in the functional representation of the PES, there are some useful and successful effective two body potential energy functions (PEFs) that can be used for molecular simulations [108] [109].

For the water dimer the interaction energy is about 5kcal/mol while the water monomer energy cancels by a sum of the two around 1kcal/mol.

Differentiable affinities between the bipolar state of polymeric water with the hydrophilic side of membranes and that of entangled pairs with the hydrophobic side regions allows coupling at the junction between neurons releasing the cerebrospinal fluid (CSF) containing pairs. Hence, the greater diffusion capability into the hydrophobic of the pair for the astrocytes environment, allows rapid circulation. Hence, the continuous flow of pairs allows capturing heat by increasing the oscillatory kinetic of the pairs, allowing their discharge into the oral cavity and reach the vapor state at the physiological temperature of 36.6°C. The vapor by reaching the surface of a mirror spontaneously returns to the liquid state, usually used to detect life. Water cluster  $(\text{H}_2\text{O})_n$  allows maintaining polarity and surrounds metallic ions in soluble state vs  $\text{H}_2\text{O}\sim\text{H}_2\text{O}$  with hidden polarity, which results in  $(\text{H}_2\text{O})_{n=3,4}$  could not transit across the double layered membrane to the hydrophobic environment.

Thus, water cluster will require specific channels modulatory controls which by modulating

its opening and closing state by the membrane structure functions to support ion translocation.

Discussion of these events CSF (containing entangled pairs) on the astrocytes, during circulation as liquid transitional state from liquid to vapor could be characterized by supporting an excess of the kinetic energy (vibrational, rotational and translational), the pairs increased solubility into hydrophobic regions.

Thermodynamics of the structure vectorial function by turnover of the tubulin  $\alpha/\beta$  heterodimer hidden polarity confers the possibility to a pairing state  $\text{H}_2\text{O}\sim\text{H}_2\text{O}$  to modify the  $\text{K}^+$ ,  $\text{Na}^+$ ,  $\text{Mg}^{2+}$  hydrated structures of ions, allowing differential states between both flow senses as required to maintain oscillatory MTs oscillatory potentials.

The tunneling nanotubes (TNTs) are membranous bridges between neighboring cells, for the transport of intracellular organelles and cytoplasmic molecules. TNTs, which can contain MTs, transmit electrical signals through calcium waves between cells.

The surface of the MT bundle would behave as an ion-selective barrier, capable of generating highly synchronized, self-sustained electrical oscillations. These electrical oscillations would generate highly dynamic electric fields emanating from the entire MT structure.

The MT wall could be envisioned as a structural sandwich of negative charges on either side facing adsorbed ions (space charge) from the bulk solution, several transmural capacitors in series would have to be charged properly to allow ions through.

A positive gate voltage relative to ground would force bulk cations to be injected into a buffer zone “de-doping” the gate by attracting counter ions on the opposite sense, allowing trans-MT electro diffusional currents.

Glutamate and NMDA receptors bind tubulin, and the connection between cardiac L-type  $\text{Ca}^{2+}$  channels and mitochondria is mediated by MTs [110].

The density change of entangled water modifies the solvation state of hydrophilic molecules like metal ions ( $\text{Mg}^{2+}$ ,  $\text{Na}^+$ ,  $\text{K}^+$ ), during transport across the membrane could accelerate an increase the membrane potentials [111].

The hydrophilic outside of membrane vs the hydrophobic inside could configure a vectorial sense to water, as a carrier of entropy.

The free energy of the membrane potential between its external hydrophilic face vs internal hydrophobic environment requires dissipative entropy.

The basic functional spectral part of the generated field is assumed to occur in the UV region and the periodic structure of a microtubule

(MT) enables a combination of in-phase signals (differing by  $2\pi$  or its multiples) to produce a coherent signal. Nonlinear properties of MTs enable the generation of the electromagnetic spectrum at lower frequencies. Oscillations in the MT cavity can transfer power of oscillations along the MT and provide additional synchronization of frequency. The excitation of electromagnetic field in the MT cavity seems to provide energy transfer along the MT to adjust frequency.

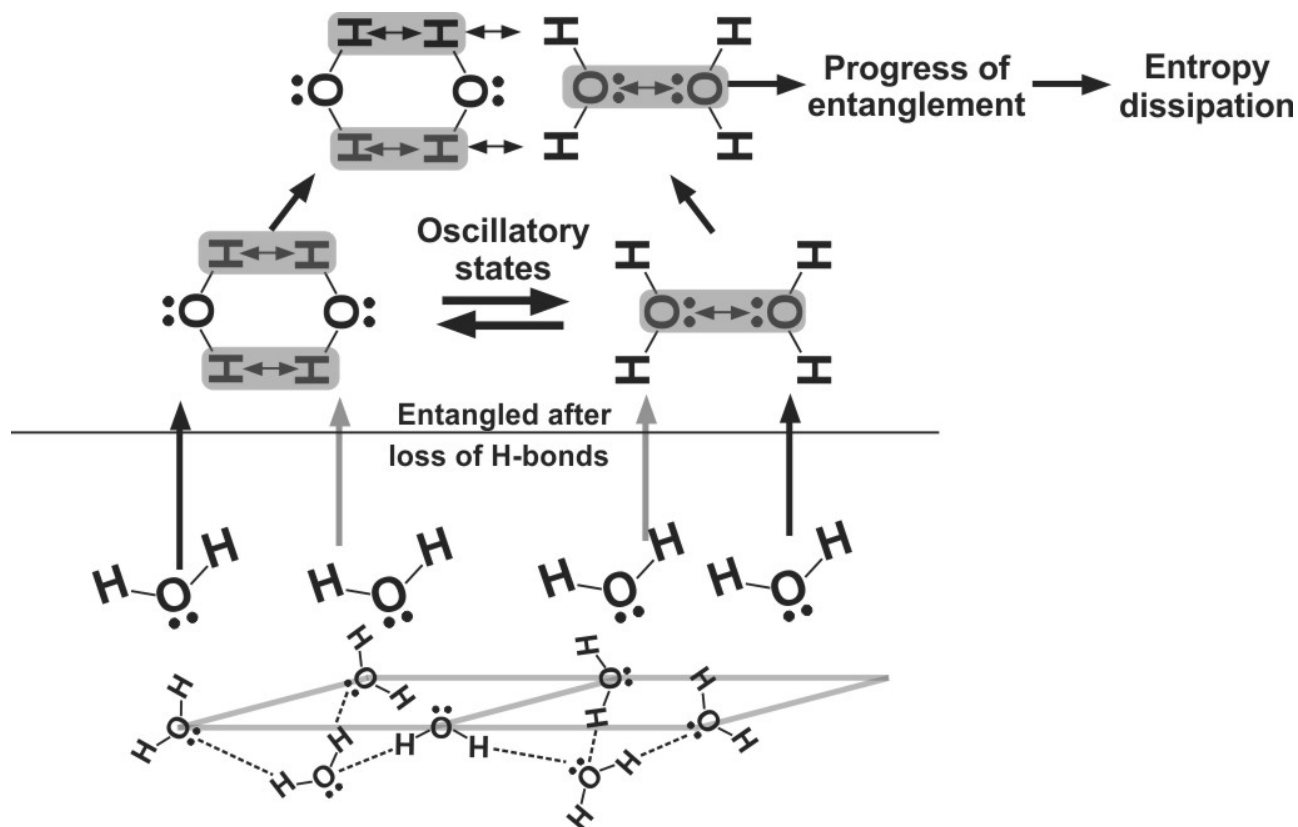


**Figure 15: Molecules in coherent resonance** capable by entanglement to contain energy in a latent state as liquid, when in the circulatory astrocyte system and to reach quantum decoherence as vapor at **36.6°C**, when reaching the oral cavity. Directional entanglement could be calculated to progress at about a rate of  $10^{15}$  molecules per nano-second, for the involved dissipative function of 500 ml CSF per day.

The generation of electromagnetic field is based on a dipole oscillation system with a classical dipole moment and near-field relations. Interaction of the electromagnetic field between dipoles is assumed to occur along the helix and along the axis of a MT. Due to different distances the frequencies in both directions can be different. The tubulin heterodimers are individual units whose properties should be equivalent. Each dipole is formed by  $^{18}\text{Ca}^{2+}$  ions which may occupy a significant space of

the circular heterodimer cross section and may be shifted along the axis.

Coherent oscillations of MTs in the frequency region from the radio frequency bands up to the UV region are about 1015 to about 1017 Hz. The corresponding propagation phase velocities about 106 m/s and  $2.9 \times 10^8$  m/s. The nonlinear properties of MTs enable electromagnetic activity at lower and higher frequencies in the range from the acoustic to the UV region [112].

Differentiable affinities between the bipolar state of polymeric water with the hydrophilic side of membranes and that of entangled pairs with the hydrophobic side regions allows coupling at the junction between neurons releasing the cerebrospinal fluid (CSF) containing pairs. Hence, the greater diffusion capability into the hydrophobic of the pair for the astrocytes environment, allows rapid circulation.

Thus, water cluster will require specific channels with modulatory control for opening and closing states by the membrane structure functional support of ion translocation.

CSF (containing entangled pairs) on the astrocytes, during circulation as a liquid transitional state from liquid to vapor could be characterized by supporting an excess of the kinetic energy (vibrational, rotational and translational) and the pairs increased solubility into hydrophobic regions.

Thus, the hidden polarity confers the possibility to a pairing state  $H_2O \sim H_2O$  to modify the  $K^+$ ,  $Na^+$  and  $Mg^{2+}$  hydrated structures of ions. Thus, allows differential states between both flow senses as required to maintain oscillatory membrane potentials.

Moreover, the density change of entangled water modifies the solvation state of hydrophilic molecules like metal ions ( $Mg^{2+}$ ,  $Na^+$ ,  $K^+$ ). Thus, during transport across the membrane could maintain the turnover of membrane potentials.

In this scheme the hydrophilic outside of membrane vs the hydrophobic inside could configure a vectorial sense to water, as a carrier of entropy that is released out of the system.

### **Tubulin and microtubule**

The tubulins are a multi-gene family that encode for the constituents of microtubules (MTs), and have been implicated in a spectrum of neurological disorders. The functional properties of the microtubule cytoskeleton dependent on the cell type, developmental profile and subcellular localization.

MTs are complex cytoskeletal protein arrays that undergo activity dependent changes in their structure and function as a response to physiological demands throughout the lifespan of neurons. Many factors shape the allostatic dynamics of MTs and

tubulin dimers in the cytosolic microenvironment, such as protein–protein interactions and activity-dependent shifts in these interactions that are responsible for their plastic capabilities and its role in behavioral and cognitive processes in normal and pathological conditions.

Myelinating Schwann cells (or neurolemmocytes) wrap around axons of motor and sensory neurons to form the myelin sheath. These are involved in peripheral nerve biology for the conduction of nervous impulses along axons nerve development and regeneration, trophic support for neurons, production of the nerve extracellular matrix, modulation of neuromuscular synaptic activity, and presentation of antigens to T-lymphocytes.

Dendrites are often highly branched to increase their receptive field. Microtubules the axo-ciliary synapse hair-like appendages found on the surfaces of neurons [113]. The myelin sheath appears to canalize biophotons.

Tubulin dimers bound to GTP bind to the growing end of a microtubule and subsequently hydrolyze GTP into GDP.

The diameter size of the neuron's axons microscopic tunnels do not allow water clusters to circulate, but do accommodate the smaller dimers.

Two magnetic fields could either show attraction or repulsion. At the tubulin molecular level its bilayer micro-structure in order to isolate the configuration of microtubule inner magnetic atoms conducting channel it is surrounded by juxtapositional arrangement of an upper strata to function as a static deviation, which could prevent the magnetic field transmission to the exterior by the metrics dynamics of exposing the Minus-End (-) of  $\alpha$ -tubulin GDP-Lattice, responding to the hydrolysis of 7.5kcal/mol GTP-Cap Plus-End (+).

Electrons that transit from  $\alpha$  to  $\beta$  interface (Minus (-) to Positive (+))  $\alpha$ -tubulin spin polarity and  $\beta$ -tubulin would show the opposite polarity along the axon.

The magnetization can be destabilized and begin the auto-oscillate at the lowest energy spin. The mode of the spin grows exponentially in amplitude until a new steady state characterized by density at the particulate frequency. Spin correlated in the nano-space-time and transmission velocity at nano-junction aligning crossing magnetic tunneling.

Magnetic tunnel junction will low barrier nano-magnet are interconnected with correlate circuits.

The non-collinear (*parallel and antiparallel*)  $Mg^{2+}$  vs  $Ca^{2+}$ , hydrophilic vs hydrophobic, sliding distancing vs contracting the enzyme molecular response changes the spin densities. Classification of signaling at microwave frequencies synchronizes the spin-torque nano-oscillator.

*Sources of functional specification for the tubulins.*

Functional specification for the tubulins can arise at a transcriptional (A), translational (B) and post-translational level (C). (A) Transcriptional: enhancers, promoters, intronic sequences, and the general genomic environment differ between tubulin isoforms, influencing the expression of transcripts spatially and temporally. (B) Translational: mRNA stability, mRNA localization, secondary structure, miRNA binding sites and the interaction with RNA binding proteins all contribute to translational efficiency of tubulin genes.

MT function in the intracellular response to insulin stimulation and subsequent glucose transport by glucose transporter 4 (GLUT4), which resides in specialized storage vesicles that travel through the cell. Before GLUT4 is inserted into the plasma membrane for glucose transport, it undergoes complex trafficking through the cell via the integration of cytoskeletal networks. MT elements in insulin action in adipocytes through a summary of MT depolymerization, MT-based GLUT4 movement, molecular motor proteins

involved in GLUT4 trafficking, as well as MT-related phenomena in response to insulin and links between insulin action and MT-associated proteins.

Microtubule associated protein (MAP) originally the “extracellular signal-regulated kinases” a target for phosphorylation by MAPK were later found, and the protein was renamed “mitogen-activated protein kinase” (MAPK), known to be phosphorylated by ERK.

Tyrosinated microtubules newly formed at highly dynamics. Detyrosination of tubulin may promote stability by protecting microtubules from the depolymerizing activity of kinesin-13 motors [114]. Thus, inhibiting cytoplasmic linker proteins and dynein loading onto microtubule plus ends [115] [116]. In neurons regulate the trafficking of cargos, axon outgrowth and branching. Kinesin-1 moves along detyrosinated microtubules [117] forming mitochondria trafficking [118] to  $\alpha$ -amino-3-hydroxy-5-methyl-4-isoxazole-propionic acid (AMPA) receptors to dendrites [119] ant to mediated synaptic transmission [120].

The levels and degree of phosphorylation are significantly higher in paired helical filament (PHF)-derived tau than in normal adult tau. The non-proline directed kinase MARK in PHF-tau phosphorylation, the phosphorylated Ser262 epitope on PHF-tau as assessed by fluorescence resonance energy transfer. In Alzheimer disease the main structural components are neurofibrillary tangles [121].

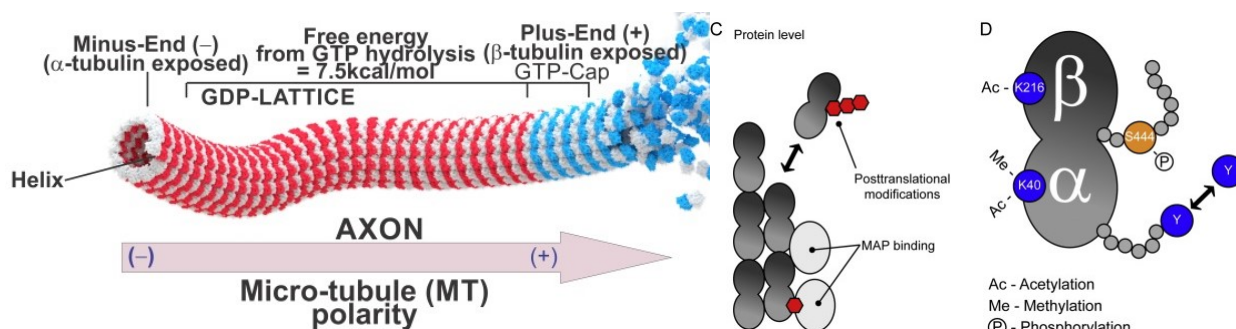


**Figure 16: Microtubule polarity.** MTs are highly charged electrically polarized polymers, where their  $\alpha\beta$  tubulin heterodimeric units have a high electric dipole moment structures, highly sensitive to both electric fields *in vitro* and *in vivo*. Although differences in the oscillatory regimes were often found, the fundamental frequency of 39 Hz was confirmed by Fourier transformation. 3D phase portraits constructed with the time delay method showed monoperiodic limit cycles. The organized oscillations, however, shifted spontaneously to chaotic periods with more complex behaviors.

Thermodynamics of the structure vectorial function by turnover of the tubulin  $\alpha/\beta$  heterodimer is 110kDa (molecular weight) polymerize assembled into microtubules of a 400 amino acids chain length into the 14nm hollow, 25nm of diameter microtubules by juxtapositional arrangement.

The assembled haired 13 protofilaments left-handed 3-start helix with a helical pitch per microtubule,  $5\mu\text{m}$  (highly variable). 1600  $\alpha/\beta$ -tubulin heterodimers per  $1\mu\text{m}$  microtubule length of a pushing force  $\approx 3\text{-}4$  pN (pico Newton) and pulling force  $\approx 30\text{-}65$  pN, which shrinkage rate  $\approx 20\text{-}30$   $\mu\text{m}/\text{min}$ , association rate constant  $\approx 2\text{-}10$   $\mu\text{M}^{-1} \text{ s}^{-1}$ , persistence length  $\approx 5.2\text{mm}$ , critical concentration  $\approx 0.1\text{-}2$  mg/ml.

The re-configuration by  $\text{Ca}^{2+}$  re-uptake by the free calmodulin (CaM) involves the coupling of a large mass action by water cluster to obtain the initial hydrophilic state of adenylate cyclase (AC).

Addition of monovalent cations  $\text{Na}^+$  and  $\text{K}^+$  stimulates MT assembly until a saturating concentration is reached, after which an inhibitory effect is observed. The presence of  $\text{Na}^+$  has been observed to stabilize tubulin sheets for a long time.

The presence of  $\text{Mg}^{2+}$  and  $\text{Mn}^{2+}$  increase MT stability, while additionally leading to the formation of GDP- $\alpha$ -tubulin ‘rings’ in solution.  $\text{Ba}^{2+}$ ,  $\text{Mg}^{2+}$  and  $\text{Mn}^{2+}$  are modeled to interact non-specifically with the tubulin dimer, lowering the electrostatic repulsion between the C-termini tail and tubulin body. The shielding effect is modeled to bias the C-termini towards a kinked conformation, stabilizing the overall MT structure. But, not all divalent cations have this effect; the presence of  $\text{Zn}^{2+}$  or  $\text{Co}^{2+}$  leads to the formation of polymeric, two-dimensional tubulin sheets instead of cylindrical MTs.

The electromagnetic field is supposed to be generated by MTs composed of identical tubulin heterodimers with periodic organization and containing electric dipoles. A classical dipole theory of generation of the electromagnetic field allows analyzing the space–time coherence. The structure of MTs with the helical and axial periodicity enables the interaction of the field in time shifted by one or more periods of oscillation and generation of coherent signals. Inner cavity excitation should provide equal energy distribution in a microtubule [122].

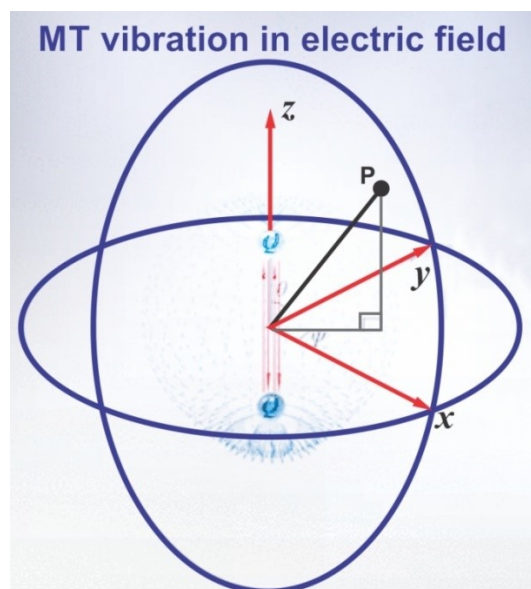


**Figure 17: electric field (EF) generated by a Hertzian dipole in a spherical polar coordinate system and its vector directions at the locations where the MT was placed.** The myelin sheath appears has the capacity to canalize biophotons. Design of microtubule (MT)-based biosensors requires an alternating EF by an electronic device (represented by a dipole) and used to excite the vibration of individual MTs distancing away from the electronic device [123]. The distance  $r = 0.1$  m between the dipole and microtubules (MTs) to demonstrate such a design of the MT-based biosensor. The frequency shifts of MTs. The amplitude of time-dependent EF should be large enough to excite forced vibration energy absorption of MTs with sufficiently large amplitude.

In the case of an alternating electric field, the direction of the electric field reverses after the half period of the field. When the recombination does not occur, the process becomes a non-sequential ionization. Formalism for the ionization rate above the Bohr radius and Hydrogen atom ionization energy are given by  $\alpha_0 = \frac{4\pi\epsilon_0\hbar^2}{me^2}$ ,  $E_{ion} = R_H = \frac{me^4}{8\epsilon_0^2\hbar^2}$  where  $R_H \approx 13.6\text{eV}$ . Tunneling from Hydrogen orbitals can be operative [124]. Electric field  $E_a$  for the ordinary Hydrogen atom is about  $5.1 \times 10^3 \text{MV/cm}$  and the characteristic frequency:  $\omega_a \approx 4.1 \times 10^4 \text{THz}$ , transition of the electron from the ground state of the atom (Volkov states) of free electron in the electromagnetic field.

The qubits are based on oscillating dipoles forming superposed resonance rings in helical pathways throughout lattices of MTs.

*Intermolecular* force that mediates interaction between molecules (London forces), including the electromagnetic forces of attraction or repulsion, which act between atoms and other types of neighboring particles. London forces are weak relative to *intramolecular* forces – the forces which hold a molecule together.

MTs form bundles, which are particularly prominent in neurons, where should define axons, dendrites and spines. Sealed MT bundles displayed spontaneous electrical activity consistent with self-sustained electrical oscillations that responded directly to the magnitude of the stimulus. MT bundles were initially voltage-clamped at a holding potential of zero mV.

Highly polarized cells such as neurons present two structurally and functionally distinct domains, namely a single long, thin axon and multiple shorter dendrites that either transmit or receive electrical signals, respectively. MT stability is at the center of the polarization process of neurons, which is fundamental to their development and plasticity. Parallel arrays known as bundles in axons and dendrites are required for the growth and maintenance of neurites in neurons.

MTs are thought to generate oscillatory electric fields at expense of elasto-electrical vibrations, driven by a permanent electrical polarization from local asymmetries in the ionic distributions between the intra- and extra-MT environments and

consistent with the periodic open-contracted switching of the nanopores.

Holding potentials as small as 1 mV induced large changes in the cytoskeletal conductance.

The electrical response of the MT bundles depended on both, the magnitude and the polarity of the electrical stimulus.

MT bundles elicited highly synchronized trains of current oscillations that mimicked the response observed with action potentials.

Coherent oscillations of these C-terminal tails are modeled to generate solitonic pulses of mobile charge along the outer surface of a MT, creating ionic currents along its length. Ions from the bulk solution are modeled to be pumped into the hollow MT lumen through nanopores across its wall, resulting in charge accumulation inside the cylindrical MT over time. The permeability of the MT lumen allows free movement of selective ions  $\text{Na}^+$  and  $\text{K}^+$ .

The hydrogen atoms possess a property known as nuclear spin. The Doppler Effect broadening of spectral lines is that there is a range of macroscopic velocities, from emission from regions moving away from and towards the observer in a rapidly rotating accretion disk [125]. Autocorrelation functions through a driven damped harmonic oscillator analog for light scattering [126].

$\text{Ca}^{2+}$  and  $\text{Mg}^{2+}$  ions could not penetrate through the membrane due to their higher electrostatic attraction to the electrostatically negative external surface and their larger hydration shells. However, the concentration of  $\text{K}^+$  inside the lumen increased in response to a pulse of  $\text{Ca}^{2+}$  ions travelling along the outer MT surface.

The oscillations are either electric, due to charge separation from London forces, or magnetic, due to electron spin and possibly due to nuclear spins (that can remain isolated for longer periods) that occur in gigahertz, megahertz and kilohertz frequency ranges. The hypothetical orchestration process by connective proteins as microtubule-associated proteins (MAPs), influence the qubit state by modifying the space-time-separation of superimposed states.

Neurons generate patterns in the electromagnetic field, which in turn modulate the firing of particular neurons. A conscious proposition in the sense that the field or its

download to neurons is conscious, but the processes of the brain themselves are driven by deterministic electromagnetic interactions [127].

The instability process is controlled by GTP hydrolysis and would be an energy-consuming process that varies depending on the isoforms of  $\alpha$ - and  $\beta$ -tubulin incorporated into the MTs, their posttranslational modifications, and their interaction with MAPs. Despite being constantly changing structures, MTs have sufficient longevity to be substrates for tubulin modifying enzymes for tyrosination, detyrosination, acetylation, D2 modification, glutamylation, glycation, palmitoylation, and phosphorylation. These posttranslational modifications modulate their binding to particular MAPs, motor proteins, or proteases. They dynamically interact with other cellular proteins and organelles. MAPs bind and stabilize MTs in a phosphorylation-dependent manner and their alterations disrupt brain function.

Actomyosin a contractile ring is a prominent structure during cytokinesis required for nucleokinesis, acts perpendicular to the axis of the spindle apparatus. MTs are not uniformly arranged and both plus- (+) and minus-ends (-) can be found at the distal tip of the neurite. This arrangement results in dynein motor proteins transporting cargo towards the soma, whereas plus-end directed kinesin family proteins are responsible for transport towards the developing growth cone during development (and the axonal bouton following differentiation).

Vesicular cargoes move relatively fast in nano-space (50–400 nm/day) whereas transport of soluble (cytosolic) and cytoskeletal proteins takes much longer (moving at less than 8 nm/day) [128].

The movement of cytoskeletal “slow” cargoes is actually rapid but unlike fast cargoes, they pause frequently, making the overall transit rate much slower (“Stop and Go” model) of slow axonal transport on the cytoskeletal protein neurofilaments [129].

MT network in  $\beta$  cells has unique morphology with several distinct features, which support granule biogenesis (via Golgi-derived MT array), net non-directional transport (via interlocked MT mesh), and control availability of granules at secretion sites (via submembrane MT bundle). This array is parallel to the plasma membrane and serves to withdraw

excessive granules from the secretion hot spots, is destabilized and fragmented downstream by high glucose stimulation. The capacity to remodel MT network is regulated by glucose.

Besides the MT network itself, it is important to consider the interplay of molecular motors that drive and fine-tune insulin granule transport. Importantly, activity of kinesin-1, which is the major MT-dependent motor in  $\beta$  cells, transports insulin granules.

Tiny, rod-like structures of MTs in the insulin-producing cells of the pancreas help control when and where insulin is released [130].

$Zn^{2+}$  interacts at the N-terminal of each tubulin monomer, causing protofilaments to align in an antiparallel orientation to one another. Prolonged exposure to a solution of  $Zn^{2+}$  can lead to sheets ‘wrapping up’ to form >300 nm diameter macrotubes, indicating the importance of electrostatics in the determination of the polymorphic structure of tubulin. Interestingly,  $Ca^{2+}$  has the opposite effect, causing MT disassembly through acceleration of GTP hydrolysis.

Tumor-treating fields (TTFields) are a cancer treatment modality that uses alternating electric fields of intermediate frequency (~100-500 kHz) and low intensity (1-3 V/cm) to disrupt cell division. According to the standard model, TTFields, which are 10-300 kHz, 1-3 V<sub>rms</sub>/cm a.c. electric fields, inhibit cancer-cell proliferation by interacting with the large dipole moment of tubulin, which causes MT alignment along TTField-generated electric field lines leading to a disruption of the mitotic spindles.

The receptor tyrosine kinases (RTKs) show inhibitory activity on the dual tubulin assembly of MT. MT is crucial in multiple cellular functions including mitosis, cell signaling, and organelle trafficking, which makes the microtubule an important target for cancer therapy.

Neuronal parallel magnetization signals a low resistance for a propagation of a signal qualifying as a positive one. The anti-parallel magnetization means high resistance or null. *Nascent*  $Mg^{2+}$  is partially hydrated is able to restore the ionic and electric imbalance by reactivating the sodium/potassium pump and by reducing the calcium overload.

The thermodynamics relationship between structure and function requires an astrocytes network for circulation after breakdown of H-bonds. The water cluster exhausted the H-bonds by the transition of hydrated R-groups in proteins in mutual exclusion direction with the dehydrated ones in oxyHb to deoxyHb, and plasma to cerebrospinal fluid (CSF). Dimers integration by non-polar superposition of orbitals into a transitory state of single molecules of water as a liquid state is maintained by a kinetic resonance of excess energy.

Receptor tyrosine kinases (RTKs) are transmembrane cell-surface proteins that act as signal transducers. They regulate essential cellular processes like proliferation, apoptosis, differentiation and metabolism.

AMPA-sensitive glutamate receptors are crucial to the structural and dynamical properties of the brain, to the development and function of the central nervous system and to the treatment of neurological conditions from depression to cognitive impairment.

The contribution of the cytoskeletal MT is associated protein 1B (MAP1B) to the pathway-specific internalization of AMPARs. Although interfering with protein synthesis using short interfering RNA (siRNA) to eEF2 kinase (eukaryotic elongation factor 2 kinase) blocked the dendritic MAP1B increase by both pathways, it selectively blocked the DHPG- and not the NMDA-induced AMPAR endocytosis [131].

Insulin secretion from pancreatic  $\beta$ -cells is initiated through channel-mediated depolarization, cytoskeletal remodeling, and vesicle tethering at the cell membrane, all of which can be regulated through cell surface receptors. Receptor tyrosine kinases (RTKs) promote  $\beta$ -cell development and postnatal signaling to improve  $\beta$ -cell mass and function, yet their activation has been shown to initiate exocytotic events in  $\beta$ -cells. The pathways that control insulin release and the potential interplay between c-Kit and IR signaling are discussed [132].

The endocrine cells of the pancreatic islets of Langerhans secrete hormones that are responsible for the minute-to-minute regulation of glucose homeostasis, with the  $\beta$ -cells composing the majority of islet cell mass in mammals. Upon stimulation,  $\beta$ -cells release insulin that binds to

insulin receptors (IRs) in peripheral tissues (skeletal muscle, adipose tissue and liver) to stimulate glucose uptake and storage. Biphasic insulin release from  $\beta$ -cells is initiated with glucose-stimulated closure of ATP-sensitive voltage-gated potassium ion channels. Calcium leading to increased exocytosis from insulin granule by the activation of select membrane receptors found on  $\beta$ -cells a factor that can influence insulin secretion. The G protein-coupled receptor (GPCR) glucagon-like peptide-1 receptor (GLP-1R) is one of the well-established roles of  $\beta$ -cell receptors, increasing insulin secretion through increased levels of intracellular calcium and reduced voltage-gated potassium ion channel activity.

### Pattern recognition in associated memory

The connection of neuronal circuits as conectomas manifest Doppler Effect by the magnetic resonance imaging (MRI) a long microtubules (MTs). Accordingly, neuronal circuit encoded learning by pattern recognition imaging develop from hormonal associative of the infant memories.

The thermodynamics functional analysis is neuronal maintenance of the optimal enthalpy level occurs by an anatomic structure for an oscillatory microscopic opening of the system. Hence, the mass and energy input allowed by the “Nodes of Ranvier” structure, allowing the enthalpy increase by water clusters, and other H-bonds integrated structures when are coupled for their breakdown. The generated single molecules of water organize by their polarity in dimers configuration:  $2\text{H}_2\text{O} \rightarrow \text{H}_2\text{O} \sim \text{OH}_2$ , circulating within MTs. This dissipative pathway allows the randomness of entropy to be incorporated into the kinetics resonance of dimer structures and circulation through MTs to exit outside the system at the oral cavity.

This favors microscopic magnetic tunneling unions for water dimers could manifest at the H atom level the up and down-spin of electrons, turning around the oxygen-oxygen orbitals superposition. Thus, function as antenna for emission signaling at the 21cm line, connecting neuronal network. Thus, the input for enthalpy incorporation generates a dissipative flow of

differentiable frequencies signaling other neurons in a quantum space-time level for near simultaneous

integration from a basal to vectorial sequence of the excited states.

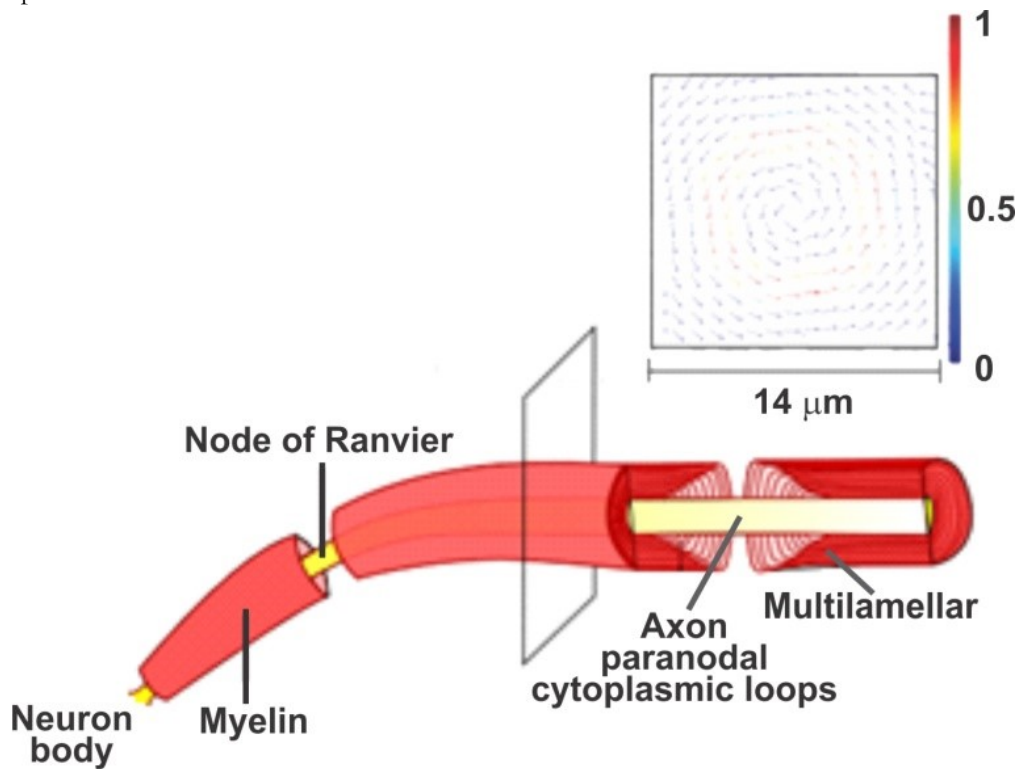


**Figure 18: optical properties of myelinated axons.** The average 2mm length of brain axons were shown to transmit from 46% to 96% of biophotons entering into the myelinated structure from the terminal direction to the opposite axonal cone, accordingly the capacitance  $10^9$  photons per second (1% of  $10^{11}$  brain neurons) large enough to allow optical channels of information bits communication.

### Engineering protecting in space to damage by galactic cosmic rays

Engineering scintillator's reactive shielding for protection of dendritic spines involved in learning and memory. Neuron small branches of the main dendrite shaft or protrusions denominated dendritic spines-small less than one micron a fraction of the human have width contain synaptic connection to receive neuronal signals. Accordingly, has been related by branching areas and number to act as receptors from other neurons. A source of great concern to NASA is the effect of the high sensitivity to damage by galactic cosmic rays (GCR) the charged atomic nuclei flying at near velocity of light that pervade the cosmos at remnants of the death of stars and traversing the astronauts is a dangerous level of ionized hydrogen atoms emitted by the sun. The effect may prolong because the particles leaves in the cells a quantity of excess of energy ionizing the atoms by removal of electrons

of the different tissues, creating free radicals. The typification of radiation linear energy dose (LET) affecting hippocampal, settled memory and cortical learning and seeking function necessary for the astronaut's performance. An evaluation of an interplanetary dose rate or milligray (mGy) a day: about 0.5mGy could be accumulated according to large time of exposition, such as required for navigation to reach the planet Mars, even further for colonization project.

The problem was first approached by engineering a heavy material shielding like thick lead covering. A publish use of scintillation crystals specified a methodology for absorption of radiation that hereby has been tabulated as possible reactive shield protection for use as cover for the astronaut suits, areas and the spacecraft with a scintillation crystal painting. The non-radioactive isotopes of Sr were used at the earlier time of TV manufacturing to protect people by the absorption of the radiation from TV screens [133].

**Table 1: Scintillators.**

Radiation	Scintillators
Alpha	CsI(Tl), ZnS(Ag); CaF <sub>2</sub> (Eu)
Beta	NaI(Tl); CsI(Tl); BGO; BaF <sub>2</sub> ; CaF <sub>2</sub> (Eu); ZnS(Ag); CaWO <sub>4</sub> ; CdWO <sub>4</sub>
Gamma	CaWO <sub>4</sub> ; CdWO <sub>4</sub>

Several desirable properties of high stopping power a fluor is suspended in the base, a solid polymer matrix. Wavelength shifters can sometimes be used, an index of refraction near that of glass. Ruggedness and good behavior under high temperature may be desirable where resistance to vibration and high temperature is necessary. One or more layers should be tested to obtain optimal combination [134].

### Discussion

In order to moderate the rate of entropy increase in a dynamics cosmos with gravitational waves exteriorizing the dynamic limit of expansion, and inward inner differentiated space as voids is required between open and closed curvatures, preserving this balance as flatness by a gyroscopic effect when the linear velocity of light ( $c$ ) could reach its maximum redshift. Thus, in order to prevent the associated momentum leading to unble infinite mass and increases in angular momentum acts as a feedback signal.

The cosmological space-time generates the thermodynamics function of entanglement correlation for H electron spin coherence and decoherence at the macro and micro scales of terrestrial life

The bosons do not respond to the Pauli exclusion's principle, which allows these maximal nodes of energy to occupy the same quantum state. Thus, in opposition to the fermions allowed localizing into singular multi-levels of energy. The result is an overlapping bosons interconnected along one dimension of the space by the hierarchical expression of convergence vs decoherence.

After the Dark Ages not only thermal photons emitted by kinetic energy, which lack response to gravity, but at the cosmos surged the light produced by internal nuclear fusion of hydrogen into helium, radiated by the stars, formed under gravitational attraction [135].

The thermodynamic model of an inwardly open system emerging from primordial entangled Planck bosons evolved from the primordial state by

a decoherence function, according the chronology of the universe. Thus, imprint the cosmos with the density fluctuations of its pressure-sound measured by the baryonic spectroscopic oscillations project (eBoss). These vibrations are preserved over the chronology expansion distance since emitted and are present in the light emitted by the most distant quasars.

A Dark Ages started when the cosmos cooled from 4,000K to 60K. The neutral hydrogen atoms formed released the 21 cm line without elongation, showing that an open flow of enthalpy existed between atoms and the impulse of the expansion.

Further cooling allowed a Dark Ages lasting 200-500 million years where the up/down-spin of electrons allowed the 21cm wavelength line emission, without significant emission elongation, indicating that the emission potency was frozen, by the at this movement present a very low temperature, allowed a cosmos, without transfer of excitation energy from the Universe expansion to the atoms themselves.

Ordered water layers result of charge organization that predicted a coherent phase of liquid water and coherent oscillation of water molecules between ground and excited state. Strong forces acting between water molecules at charged surfaces correspond to binding forces in metals. These points out that energy of random fluctuations cannot disturb the ordered water layer and the noise level in a microtubule is low.

The excitation by energy of photons has to be accounted for by a quantum mechanical assessment of denominated biophotons produce by mammals with wavelength with 200nm near infrared and 1300nm UV. Infrared is understood to encompass

wavelengths from around 1 millimeter (300 GHz) to the nominal red edge of the visible spectrum, around 700 nm (430 THz). Longer IR wavelengths (30  $\mu\text{m}$ -100  $\mu\text{m}$ ) are sometimes included as part of the terahertz radiation range.

Optical characterization of myelination axons to centimeter distances could disperse or transmit photons by axons appear to canalize visible wavelength could be expected to function as mechanisms capable of encoding, receiving and processing quantum information.

These hydrogen atoms possess a property known as nuclear spin. Medically Magnetic resonance imaging (MRI) detected from Doppler distancing imaging of spectral lines, which operate over a range of macroscopic and microscopic a nano dimensional senses or velocities. These ones result from emission from regions moving away from and towards the observer in a rapidly rotating accretion disk. This relationship allows to associate spin to the antenna effect, required for photon quantum vectorial emission to reach a coherence response to the excitatory input of energy.

Magnetic resonance imaging visualizes organs by detecting hydrogen atoms using superconducting magnets, particularly those tissues attached to water and fat molecules.

The 21 cm line emission at cosmological Dark Ages is characterized as an atomic transition domain of an electron at hydrogen 1s orbital, when spin-flip from up to down position, in which release the excess energy as a vectorial radio emission.

Energy storage released from the quantum states of electrons, the polarization of molecules and structures allows the transfer of particles between low and high energy states. Ionization may occur, excitation of electrons into the conduction band which causes temporary conduction and produces an energy pulse. If the supply of energy continues the resonant system may be destroyed. A complete description of the field generation partially in the UV region would enable analysis of various biophysical mechanisms occurring in living cells and tissues, in particular utilizing resonant effects. Electromagnetic resonance of filamentous structures at neural branches level can speed, the respond processes control. A fast evaluation in microseconds of different pathways precedes the occurrence of the comparatively slow result in

milliseconds ionic transmission. Such a mechanism can explain the enormous decision-making capability of the brain, compared to a strong computational power of silicon technology.

However, its detection could show elongation coupled to the Universe expansion *lookback on time*, not decreasing emission frequencies by the atoms themselves but occurring by the expansion distancing the positions of the hydrogen spin generators, according to redshifting by the Doppler Effect.

Accordingly the undergoing space-time dynamics could not release energy from atoms until the spatial distention reached a slow but significant accumulation of the baryonic mass and the associated increase in entropy. The process eventually leading to star formation, associated to the entropy location of slowly emergence of voids.

Thus, relating an enthalpy location increase to flow of entropy creating in the *voids* a dissipative location and conforming open thermodynamics, which supply enthalpy for the  $\Delta G$  for galaxies emergence. The gyroscopic *feedback* from a cosmos rotational state controls the expansionary flatness by the total angular momentum conservation and the one sense borders of primordial gravitational waves, their rate it the velocity of  $c$  constricting the space expansion.

Computer would make use of entanglement, a phenomenon unique to quantum systems. With entanglement, a particle's properties are affected by what happens (through coherence/decoherence) to other particles with which it shares intimate quantum connections. These connections give chemistry and many branches of materials science a complexity that defies simulation on chemical computers.

Quantum systems such as particles' spin and polarization can be inextricably tied together. Hence, could manifest a new effect: spin transfer. When the electrons of the electric current pass through a nano-magnet of the junction, their spin interacts with that of the electrons of that layer, and this causes the spin of the electrons of the current to polarize and align with the magnetization of the layer.

Magnetic tunnel junctions can serve as under levels for synapses and neurons, explaining how magnetic textures, such as domain walls and

topologically stable field configuration (skyrmions) could imitate the function of neurons in computational processing of data.

The human brain executes highly sophisticated tasks, such as image and speech recognition, with an exceptionally low energy and much more efficiently than supercomputers.

The long axons  $6 \times 10^4$  neurons at the locus coeruleus synchronize the five senses perception from different areas of the brain to locate the individual in a single perception of surrounding reality [136].

Brain function inspired spintronics by the implementation of nonlinear magnetization dynamics and stochastic nanoscale process.

Penrose and Hameroff [137] (they dubbed Orch-OR: orchestrated objective reduction) have argued that consciousness is the result of quantum effects in microtubules [138] [139]. Has been calculated [140] that the time scale of neuron firing and excitations in microtubules is slower than decoherence time by a factor of at least  $10^{10}$  to allow free will implementation by  $10^{11}$  neurons as the calculated required input of their very large presence at microtubules. Biologically, free will (*software*) is 40% indirectly resulting from the neuronal DNA (*hardware*) programmed behavior, from hormonal communication of mother and child.

Stress mediated by NA activation of AC induce alterations in neuronal molecular structures of R groups of enzymes thermally, responding to a nano space-time under quantum dynamics by a coordinative divalent metal ( $Mg^{2+}$ ,  $Ca^{2+}$ , etc.) the chelated R group, could function as an enzyme metal complex became vectorial organize for active site dynamics transition of the enzyme protein conformation.

The continuous flow of pairs allows capturing heat by increasing the oscillatory kinetic of the pairs. The vapor by reaching the surface of a mirror spontaneously returns to the liquid state, usually used to detect life. Polymeric state of water  $(H_2O)_{n=3,4}$  allows maintaining polarity and surrounds metallic ions in soluble state vs  $H_2O \sim H_2O$  with hidden polarity, which results in  $(H_2O)_{n=3,4}$  could not transit across the double layered membrane to the hydrophobic environment

and therefore operate specific gates to open the system interior to the exterior.

## Conclusions

The initial state of primordial universe by Planck bosons [141] involves gravitational waves or space-time vibrations of unidirectional sense, which at velocity of light ( $c$ ) adds an arrow of time for energy decoherence function under vectorial dynamics. A decoherence stage allowed separation of forces: strong and electroweak from a boson's entanglement state.

Enthalpy separation from entropy, entanglement influence over quantum dynamics, energy density decreasing by stretching down the frequency and enlarging space by decreasing located energy, based in the Compton volume.

Thus, scales from a higher frequency of blue color and ultraviolet to penetrate into the electron volume.

The much larger volume of the yellow or infrared could not be encompassing by the electron sphere. The emergence of quantum mechanics precedes the dominance of gravity indenting from  $H_2$  aggregation by the fusion reaction from hydrogen to helium igniting for atoms formation within stars, forming galaxies. Expansion shows a redshift separating each other the stars and blue shift when decreasing the space separating stars or galaxies.

Expansion a decoherence stage prevailed over gravity until the near end of Dark Ages characterized by 21cm line emission by the electron spin up and down from orbital positions around the proton in the H atoms.

The description of primordial stages is vectorial underforth chaos [142] [143] results from event of decreasing enthalpy and subsequent stage space-time expansion, allowing localization of entropy into void/vacuum by separation from enthalpy involved in stars formation [144] [145].

Doppler Effect manifestation is a phenomenon than may be detected at the psychological level by the human body, increasing his resistance to lower temperatures, when a train takes the individual an away from home and decreasing resistance when coming back to home. Multiple layers of space-time allow a conditioning

by the scale dimension of the electron spin-flip of the hydrogen atom when function as an antenna at the nano level of microtubule.

Life as a vectorial process could be characterized by several thermodynamic axis as an example the vector by a vector of hydrophilic to hydrophobic sense, in which a single polypeptide of adenylate cyclase (AC) could not show reversibility because a mutual exclusion operate for the two C1 and C2 protein domains at the events reconfiguring by bending and sliding into a variable configuration of the active site, allowing transition time organized flow of energy that may reverse direction by H-bond breakdown coupling, increasing the enthalpy therefore enthalpy into entropy is conserved. The relation of a photon splitting enlarge space is one direction and when two photons of lower energy could fuse into one of higher energy is the opposite, but directionality is conserved in both senses, without chaos, according to symmetry of the momentum conservation.

Mathematically, in dynamic systems theory, chaotic behavior is an aperiodic deterministic behavior that is very sensitive to initial conditions and the flatness in the cosmos preserves a pattern of directional axis from the initial conditions.

In a first stage the amino acids residues (R groups) of AC, coordinating the ions conform an active core for  $Mg^{2+}$ .

A proline at the AC polypeptide chain allows bending and sliding, to replace the first stage R groups for other ones sliding to bind  $Ca^{2+}$ . Additionally, interaction with the protein kinase C (PKC) by phosphorylation of the hydroxyl groups of threonine amino acid residues (R groups), differentiating structure and function pathways by the sliding steps, involved in the protein or enzyme folding sequence.

Coupling H-bond breakdown allows non-reversible events. But substitution at other sites or for turnover depends on the access to the reactive site of the mass action saturation by water cluster pools, leading to hydrophilic state.

Devices for monitoring and measuring simultaneously regional brain activity temporal vs spatial resolution in magnetic resonance imaging (MRI) could differentiate woman and man conectomas, because the image created by scanning brain Doppler Effect. Medically could be applied to

measure the nurturing child response to learn oral communication by the process of looking observation the muscle mouth movement of speaking people. Hence could discover and register by imaging the crosstalk structure and function between neuronal circuits. An analogy was created by Neuromorphic spintronics technical conversion of electric circuits to oral sound, may lead to pattern recognition by the developing of the nurture child of an associative memory [\[146\]](#).

$Mg^{2+}$  coordinated by negative R groups in oxyHb hydrophilic state, characterizes by mutually exclusion of hydrophobic state of the deoxyHb. The release of  $O_2$  jointly with kosmotropic  $Mg^{2+}$ , which by competition for the hydration shells of  $Na^+/K^+$ , maintains the action potential across membrane. The  $6 \times 10^4$  neurons of the locus coeruleus with NA-AC long axons reaching almost all brain regions. The latter, explains the integration of the five senses inputs, during significant emotional impact. The brain hypothalamic-7-TM-NA-AC can mobilize nutritional reserves, without activating a feedback response by the body's adrenaline. The latter could not cross the blood-brain barrier (BBB).

At the cell physiological level NA-AC and insulin receptor tyrosine kinase (IRTK) responsiveness to hormones could be modulated by the concentration of chelating metabolites because the adrenergic receptors in response to insulin, which act by phosphorylation captures cations. Thus, produce the release of free  $ATP^+$ , a negative modulator of AC and the  $Mg^{2+}$  activated IRTK. Thus, allows an integration of the hormonal response of both enzymes by ionic controls. This effect could supersede the metabolic feedback control by energy charge. Accordingly, maximum hormonal response of both enzymes to high  $Mg^{2+}$  and low free  $ATP^+$  allows a correlation with the known effects of low caloric intake increasing the level of free ions could elevate the average life expectancy.

Medical MRI visualizes organs particularly those attached to water and fat molecules by detecting hydrogen atoms using superconducting magnets.

These hydrogen atoms possess a property known as nuclear spin. Cause for Doppler broadening of spectral lines is that there is a range

of macroscopic velocities resulting from emission from regions moving away from and towards the observer in a rapidly rotating accretion disk. The same relationship at the nano space-time allows to associate spin-flip to the antenna effect, required for photon quantum emission to reach a coherence response.

The excess of  $Mg^{2+}$  activates NA-AC in an obligatory step to configure a hydrophilic active site for the water attack by water cluster  $(H_2O)_{n=3,4}$  of the MgATP and releases PPi and AMP. The H-bond breakdown configures by mutual exclusion a hydrophobic domain, in response to calmodulin release of  $Ca^{2+}$ . The opening of the hydrophobic active site allows release water to cycle the phosphoryl group of AMP into E-cAMP.

$Mg^{2+}$  releases cAMP and hydration shell after  $10^{-15}s$  to become mixed with water cluster and depolarized into hydrophobic dimers  $(H_2O \sim OH_2)$ . The dimers transit a route created from hydrophilic plasma, depleted from hormones, into the synaptic cerebrospinal fluid (CSF). 7TM-hormonal receptors coordinated to dendrites at the oral cavity allow the hypothalamic-NA-AC with axons across the BBB to modulate the HTPA axis secretions into the capillary arterioles irrigating the oral cavity.

The atrophy of the mammalian olfactory bulb lead humans into motor and re-adaptive brain needs. Thus, saliva transitional hormonal communication of infants allows the brain itself to improve velocity by myelination of axons. This close system reorganizes at the "Nodes of Ranvier" into a nano open system in order to recreate the enthalpy potential and entropy became dissipated out of the system.

After three years infants show a functional amygdala and hippocampus, but still have under developed parts of the frontal brain. The CREB characterizes implementation of transcription by an Mg-cAMP to opening of the double stranded DNA to form triple strand architecture. This physiological mechanism allows a switch on/off for transduction into RNA synthesis. Insulinotropic CRH inactivated due to a reduced ATP and cAMP, and loss of intracellular calcium oscillations. Emotional learning allows to bypass genetic constrains of the non-mature brain to obtain a self-cognition, which adapts the individuals for family and social links at the unconscious level.

The system allows directionality propagation to the uniformly entangled pairs allows by the hierarchical of the initial effect. At a dissipative forming rate of  $1.6E16$  pairs per ms allow a liquid state to water within the astrocytes. Individual molecules were operated by entanglement to allow a physiological function of cooling the body by releasing heat as vapor, at body temperature. Energy-consuming processes in the Brain by vasoactive intestinal peptide (VIP), adrenaline in tissues AC, and NA activated AC in brain. The glycogenolysis actions and the adenylate-cyclase cascade, coupled to the release of vapor out of the system. These create an open system preventing any metabolic reversibility even by a short time to the functional brain.

Paired do at a rate of  $1.6E16$  pairs per milliseconds (ms), greater that AC operational turnover. The water paired structure could oscillate between two states, one entangled by two oxygen atoms in the pair, and the other, by two structures of two entangled hydrogen atoms in the pair.

A mechanism by a switch on/off by  $Mg^{2+}$ -cAMP coordinative insertion to open DNA in a 3 helix transitory structure with bases pointed externally. The molecular of water without structure is 55.55M but water cluster  $(H_2O)_{n=3,4}$  after H-bonds breakdown leading to randomness/entropy. Energy of solvation when water is coordinated to  $Mg^{2+}$  is released jointly with oxygen in the mutual exclusion at the transition of oxyHb to deoxyHb. The low-polar states tend at the internal pressure of microtubules to generate a coherence water superposition as dimers  $(H_2O \sim OH_2)$ , with kinetic energy release exhaled as a 5% vapor in the oral cavity.

The mass action of water clusters restores the core site to the hydrophilic structure conferring vectorial kinetics to *turnover*.

Applying microscopic physics cluster-quantum-dynamics modify atomic polarity response to the H-bonds integrating structures of DNA, proteins and water by a magnetic coherence/decoherence response to their biological role in molecular dynamics by changing from hydrophilic to hydrophobic state.

The principle of microscopic reversibility responding to the thermodynamics that do not had dynamic of changing molecular structure and

function and only generates changes in concentration by affinity on equilibrium. Accordingly the paradox had been approached by analogy treatment as single inert door open and closes to the two directional senses incapable to generate vectorial kinetics. The latter is possible by synchronized movement of several doors.

*Quantum* dynamics operates transitions in the internal space-time of molecules and encompass *quantum* re-organization of dynamics function of orbitals. The hydrogen electron orbital spin up and down positions emit 21cm line that connect by the one sense magnetic rotation motion. A one sense of magnetic rotation is functional to modulate magnetic spin-antenna for mutual signaling concerted activation of neuronal network. This oscillation signals for concerted activation of the AC network modifying by a *nascent* Mg<sup>2+</sup> release, supplying MgATP to the Na<sup>+</sup>/K<sup>+</sup>-pump-ATPase and the Mg<sup>2+</sup> role over Na<sup>+</sup>/K<sup>+</sup> transit translocation by modifying their forward and reverse hydration shell sizes.

The *quantum* conservation of information operates in the lung arteriole system for enthalpy influx of glucose, during the oxyHb state of the erythrocyte. The thermodynamics operates as open by coupling the release of oxygen to the entropy gain by 2,3-DPG binding modifying Hb structure to deoxyHb state *mutual exclusion* irreversibility circulation on the venous lung blood CO<sub>2</sub> exchange on the entropy dissipation stages.

Thus, the brain meninges operates as a near autonomous blood circulatory system, supporting the functional structure dynamics of H-bond breakdown in DNA, proteins and water clusters in neuronal glial of operative configuration of circuit network. The internal pressure within connecting the microtubules glial axis could conserve the circulation in the liquid state of the generated by H-bond breakdown, generating isolated molecules of water that lack H-bond by their residual orbital electron function for oscillate attraction under water state as dimers (H<sub>2</sub>O~OH<sub>2</sub>). Hence, this resonance corresponds to an increase in the level of randomness, incremented during the course of entropy dissipation. Hence, the enthalpy contribution to brain function could be measured by the heat transition from 36.6°C over by the

dissipation according to a 1°C increase per 1ml = 1cal.

The thermodynamics relationship:  $\Delta G = \Delta H - T\Delta S$  acts as a law of energy conservation still capable to produce work after subtraction of the remnant entropy within a close system. The potential between levels could increase when the system allows a large enthalpy (*H*) and excludes its entropy (*S*) by its dissipation out of the system. Thus, preventing equilibrium by maintaining the flow of entropy by its excretion out of the system if not the cellular system would become dead.

Also the system structure and function could be compartmentalizable, for example: the cell structure could maintain at a lower level the entropy, within a nuclear membrane than in the cytoplasm by interconnecting microtubules channeling into differentiable senses entropy conserved separated in a *vesiculae* until release out of the body.

Transmembrane AC is involved in the regulation of multiple brain processes such as synaptic plasticity, learning and memory. They synthesize intracellular cAMP following activation by G-protein coupled receptors.

In the human brain the quantum physiology of the electrogenic action potential along myelin-sheath gaps requires recovery of voltage. Hence, at the uninsulated "Nodes of Ranvier" (exposed to the extracellular space) operate as nano open systems (for mass and energy) structuring the *capacitance* through ions channels recovering the Na<sup>+</sup>/K<sup>+</sup> concentration by the *inductor* ion (*nascent* Mg<sup>2+</sup>) of action potential. The functional analogy for the quantum technology of memory uses the term *memristor* - a word contraction for memory and resistor. A circuit records of the last variable *commutative* resistance during the electric power flow.

At the physiological neurons lead *inductor* signals the need of an enthalpy gain, even if creates a delay on the flow from one node to the next along the axon. The relationship between inflow and outflow of enthalpy vs entropy preserve the information of the sinusoidal curves registering frequency.

For inter-trial phase consistency, clusters of strong associations were found in the temporal and frontal lobes, especially in the bilateral auditory and pre-motor cortices. Higher phase-locking values

corresponded to higher cortical thickness in the frontal, temporal, occipital and parietal lobes [147].

Neuron phase synchronization effect realized by glial cells could allow harmonics between widely separated regions by synaptic firing signaling and decreasing the tendency to noise interference, mapping of the probabilistic spiking nature of pyramidal neurons in the cortex, which could relate function to learning and cognition.

The quantum technology [148] shows that spin torque nano oscillator could control a differentiable frequency of wavelength for vowel recognition, predicting a correlation applied to language acquisition [149]. An inferred analogy to magnetic resonance function of creating image [150]: would be that water dimers could function as physiological nano oscillator at the microtubules level, by the spin up and down of the orbital electron of the hydrogen atom by their antenna function as an emitter of 21 cm radio waves, avoiding noise. Hence, adapt the commutative resistance to the recognition of specific electromagnetics Doppler Effects, creating an intramolecular magnetic field around an atom in a molecule changing the resonance frequency, thus giving access to details of the electronic structure of a molecule and its individual functional groups, acting over neuronal circuit distancing. The extent of excitation can be controlled with the pulse width, typically ca. 3-8  $\mu$ s for the optimal 90° pulse.

NMR is useful for investigating nonstandard geometries such as bent helices, non-Watson-Crick base-pairing, and coaxial stacking. It has been especially useful in probing the structure of natural RNA oligonucleotides, which tend to adopt complex conformations such as stem-loops and pseudo-knots. NMR is also useful for probing the binding of nucleic acid molecules to other molecules, such as proteins or drugs, by seeing which resonances are shifted upon binding of the other molecule

The 21 cm line has a frequency that falls below the microwave region of the electromagnetic spectrum and it is observed frequently in radio astronomy because those radio waves are opaque to visible light.

The microwaves of the hydrogen line come from the atomic transition of an electron between the two hyperfine levels of the hydrogen 1s ground

state of spin-flip transition that have an energy difference of 5.87  $\mu$ eV =  $9.41 \times 10^{-25}$  J.

The strongest hydroxyl radical spectral line radiates at 18cm and atomic hydrogen at 21cm line. These combine to form water, are widespread in interstellar gas, which means this gas tends to absorb radio noise at these frequencies. Therefore, the spectrum between these frequencies forms a relatively “quiet” channel in the interstellar radio noise background, which is used as a characteristic life signal on the Universe. Water molecules can also be detected as ligands of a protein in solution by nuclear magnetic resonance, and/or water-glycerol equilibrium studies [151].

## References

- [1] Harris, R.H., Cruz, R. and Bennun, A. The effect of hormones on metal and metal-ATP interactions with fat cell adenylate cyclase. *Biosystems*, 11, 29-46 (1979).
- [2] Schuler A.L., Ferrazzi G., Colenbier N., Arcara G., Piccione F., Ferreri F., Marinazzo D. and Pellegrino G. Auditory driven gamma synchrony is associated with cortical thickness in widespread cortical areas. *Neuroimage*. 255, 119175 (2022 Jul 15).
- [3] Sengupta A, Panda P., Wijesinghe P., Kim Y. and Roy K. Magnetic Tunnel Junction Mimics Stochastic Cortical Spiking Neurons. *Sci Rep*. 7, 46894 (2017 Aug 29).
- [4] Harris R. and Bennun A., Hormonal control of fat cells adenylate cyclase, *Molecular & Cellular Biochemistry*, 13, 3, 141-146 (1976).
- [5] Bennun A. The noradrenaline-adrenaline-axis of the fight-or-flight exhibits oxytocin and serotonin adaptive responses. *International Journal of Medical and Biological Frontiers*. Volume 21, Issue 4, pages: 387-408 (2015). ISSN: 1081-3829. Nova Publishers. [http://www.novapublishers.org/catalog/product\\_info.php?products\\_id=56216](http://www.novapublishers.org/catalog/product_info.php?products_id=56216)
- [6] Brydon-Golz, S., Ohanian, H. and Bennun, A., Effects of noradrenaline on the activation and the stability of brain adenylate cyclase, *Biochem. J.*, 166, 473-483 (1977).
- [7] Brydon-Golz S. and Bennun A. Postsynthetic stabilized modification of adenylate cyclase by metabolites, *Biochemical Society Transactions*, 3, (1975), 721-724.

- [8] Ohanian H., Borhanian K. and Bennun A. The effect of manganese on the regulation of brain adenylate cyclase by magnesium and adenosine triphosphate, *Biochemical Society Transactions*, 6, 1179-1182 (1978).
- [9] Ohanian, H., Borhanian, K., De Farias, S. and Bennun, A., A model for the regulation of brain adenylate cyclase by ionic equilibria, *Journal of Bioenergetics and Biomembranes*, 13, 5/6, 317-355 (1981).
- [10] Bennun A. NA-Overstimulation of the Hypothalamic-Pituitary Adrenal Axis Turns-On the Fight-or Flight Response but Adrenaline Lacks a Negative Feedback which Could Normalize Psychosomatic Dysfunctions. Chapter 2, pp 13-70, (2014) in “Adrenaline: Production, Role in Disease and Stress, Effects on the Mind and Body”, Nova Biomedical, Endocrinology Research and Clinical Developments, Book Editor: Bennun A.. ISBN: 978-1-63321-084-4. Nova Publishers.
- [11] Fetterly T.L., Oginsky M.F., Nieto A.M., Alonso-Caraballo Y., Santana-Rodriguez Z. and Ferrario C.R. Insulin Bidirectionally Alters NAc Glutamatergic Transmission: Interactions between Insulin Receptor Activation, Endogenous Opioids, and Glutamate Release. *J Neurosci*. 41(11), 2360-2372 (2021 Mar 17).
- [12] Bennun, A. Membrane-bound vectorial enzymes structure the brain's open system potentiating enthalpy by entropy's dissipation. Editorial: Amazon (26 Mayo 2022) <https://www.amazon.com/-/es/Alfred-Bennun-ebook/dp/B0B2J4DFS9>
- [13] Laurent C.E., Delfino F.J., Cheng H.Y. and Smithgall T.E. The Human c-Fes Tyrosine Kinase Binds Tubulin and Microtubules through Separate Domains and Promotes Microtubule Assembly. *Mol Cell Biol*, 24(21), 9351-8 (2004 Nov).
- [14] Acevedo-Rodriguez A., Kauffman A.S., Cherrington B.D., Borges C.S., Roepke T.A. and Laconi M. Emerging insights into hypothalamic-pituitary-gonadal axis regulation and interaction with stress signaling. *J Neuroendocrinol*. 30(10), e12590 (2018 Oct).
- [15] Saxton R.A. and Sabatini D.M. mTOR Signaling in Growth, Metabolism, and Disease. *Cell*. 168(6), 960-976 (2017 Mar 9).
- [16] Liu G.Y. and Sabatini D.M. mTOR at the nexus of nutrition, growth, aging and disease. *Nat Rev Mol Cell Biol*. 21(4), 183-203 (2020 Apr).
- [17] Efeyan A., Zoncu R., Chang S., Gumper I., Snitkin H., Wolfson R.L., Kirak O., Sabatini D.D. and Sabatini D.M. Regulation of mTORC1 by the Rag GTPases is necessary for neonatal autophagy and survival. *Nature*. 493(7434), 679-83 (2013 Jan 31).
- [18] Breussa M.W., Lecab I. and Gstreinb T., Hansenbc A.H., Keays D.A. Tubulins and brain development – The origins of functional specification. *Molecular and Cellular Neuroscience*. 84, 58-67 (October 2017).
- [19] Vicario P.P., Saperstein R. and Bennun A. Role of divalent metals in the activation and regulation of insulin receptor tyrosine kinase. *Biosystems*. 22(1), 55-66 (1988).
- [20] Vicario P.P., Saperstein R., Katzen H. and Bennun A. Metabolic interactions of insulin receptor tyrosine kinase, *Annals of the New York Academy of Sciences*. 529, 92-95 (1988).
- [21] Casciano C. and Bennun A. A characterization of two inhibitors of H<sup>+</sup>, K<sup>+</sup>-ATPase in gastric tissue. *Biochemical Society Transactions*. 16, 27-29 (1988).
- [22] Vicario P.P. and Bennun A. Interaction of MnATP and peptide substrate with insulin receptor tyrosine kinase. *Society Transactions*, 16, 896-897 (1989).
- [23] Hallberg B. and Palmer R.H. Mechanistic insight into ALK receptor tyrosine kinase in human cancer biology. *Nat Rev Cancer*. 13(10):685-700 (2013 Oct).
- [24] Xiao X., Luo Y. and Peng D. Updated Understanding of the Crosstalk Between Glucose/Insulin and Cholesterol Metabolism. *Front Cardiovasc Med*. 9, 879355 (2022 Apr 29).
- [25] Qin Fu, Qian Shi and Yang K. Xiang. Cross-talk between insulin signaling and GPCRs. *J Cardiovasc Pharmacol*. 70(2), 74-86 (2017 August).
- [26] Fetterly T.L., Oginsky M.F., Nieto A.M., Alonso-Caraballo Y., Santana-Rodriguez Z. and Ferrario C.R. Insulin Bidirectionally Alters NAc Glutamatergic Transmission: Interactions between Insulin Receptor Activation, Endogenous Opioids, and Glutamate Release. *J Neurosci*. 41(11), 2360-2372 (2021 Mar 17).

- [27] Yang H., Jiang X., Li B., Yang H.J., Miller M., Yang A., Dhar A. and Pavletich N.P. Mechanisms of mTORC1 activation by RHEB and inhibition by PRAS40. *Nature*. 552(7685), 368-373 (2017 Dec 21).
- [28] Carroll B., Maetzel D., Maddocks O.D., Otten G., Ratcliff M., Smith G.R., Dunlop E.A., Passos J.F., Davies O.R., Jaenisch R., Tee A.R., Sarkar S. and Korolchuk V.I. Control of TSC2-Rheb signaling axis by arginine regulates mTORC1 activity. *Elife*. 5, e11058 (2016 Jan 7).
- [29] Condon K.J. and Sabatini D.M. Nutrient regulation of mTORC1 at a glance. *J Cell Sci*. 132(21), jcs222570 (2019 Nov 13).
- [30] Bennun, A. Characterization of the norepinephrine-activation of adenylate cyclase suggest a role in memory affirmation pathways. Overexposure to epinephrine inactivates adenylate cyclase, a casual pathway for stress-pathologies. Ed: Elsevier, *BioSystems* 100, 87-93 (2010).
- [31] Greene S.J., Gheorghiadu M., Borlaug B.A., Pieske B., Vaduganathan M., Burnett Jr. J.C., Roessig L., Stasch J.P., Solomon S.D., Paulus W.J. and Butler J. The cGMP Signaling Pathway as a Therapeutic Target in Heart Failure With Preserved Ejection Fraction. *Journal of the American Heart Association*. 2, e000536 (2013).
- [32] Bennun, A. The Metabolic-Psychosomatic Axis, Stress and Oxytocin Regulation (September 2017). Book: *Biology Research Summaries (With Biographical Sketches)*. Volume 2. Series: *Biology Research Summaries*. Editor: Bernard Olson. Nova Science Publishers, Inc.
- [33] Harris R.H., Cruz R. and Bennun A. The effect of hormones on metal and metal-ATP interactions with fat cell adenylate cyclase. *Biosystems*. 11, 29-46 (1979).
- [34] Bennun A. The Metabolic-Psychosomatic Axis, Stress and Oxytocin Regulation Nova Publishers (2016) Serie: *Biochemistry and molecular biology in the post genomic era*. <https://novapublishers.com/shop/the-metabolic-psychosomatic-axis-stress-and-oxytocin-regulation/>
- [35] Vicario P.P. and Bennun A. Separate effects of Mg<sup>2+</sup>, MgATP and ATP<sup>4-</sup> on the kinetic mechanism for insulin receptor tyrosine kinase. *Archives of Biochemistry and Biophysics*, 278, (1990), No.1, 99-105.
- [36] Vicario P.P. and Bennun A. Regulation of insulin receptor tyrosine kinase by metabolic intermediates. *Biochemical Society Transactions*. 17, 1110-1111(1989).
- [37] Vicario, P.P. and Bennun, A. Interaction of MnATP and peptide substrate with insulin receptor tyrosine kinase. *Biochem. Soc. Trans.* 17(6), 1108-9 (1989 Dec).
- [38] Vicario, P.P., Saperstein, R. and Bennun, A., Regulation of insulin receptor tyrosine kinase by divalent metal cations, metal-ATP substrate and free ATP, *Biochemical Society Transactions*, 16, (1988), 40-42.
- [39] Vicario, P.P., Saperstein, R. and Bennun, A., Role of divalent metals in the kinetic mechanism of insulin receptor tyrosine kinase, *Archives of Biochemistry Biophysics*, 261, No. 2, 336-345 (1988).
- [40] Vicario, P.P., Saperstein, R. and Bennun, A. Interrelationships of peptide substrate and metal-ATP with insulin receptor tyrosine kinase, *Biochemical Society Transactions*, 16, (1988).
- [41] Gutiérrez D.A., Chandía-Cristi A., Yáñez M.J., Zanolungo S., Álvarez A.R. c-Abl kinase at the crossroads of healthy synaptic remodeling and synaptic dysfunction in neurodegenerative diseases. *Neural Regen Res*. 18(2), 237-243 (2023 Feb).
- [42] White M.F. Receptor Tyrosine Kinases and the Insulin Signaling System. *Principles of Endocrinology and Hormone Action*, 121–155 (2018).
- [43] Xia Z. and Storm D.R. Role of signal transduction crosstalk between adenylate cyclase and MAP kinase in hippocampus-dependent memory. *Learning & Memory*. 19 (9), 369-74 (2012).
- [44] Bennun A. Hypothesis for coupling energy transduction with ATP synthesis or ATP hydrolysis. *Nature New Biology*. 233(35), 5-8 (1971).
- [45] Ryan R.M., Ingram S.L. and Scimemi A. Regulation of Glutamate, GABA and Dopamine Transporter Uptake, Surface Mobility and Expression. *Front Cell Neurosci*. 15, 670346 (2021 Apr 13).
- [46] Leithead A.B., Tasker J.G. and Harony-Nicolas H. The interplay between glutamatergic circuits and oxytocin neurons in the hypothalamus and its relevance to neurodevelopmental disorders. *J Neuroendocrinol*. 33(12), e13061 (2021 Dec).

- [47] Bennun A. The unitary hypothesis on the coupling of energy transduction and its relevance to the modeling of mechanisms. *Annals of the New York Academy of Sciences*. 227, 116-145 (1974).
- [48] Bennun A. The dynamics of H-bonds of the hydration shells of ions, ATPase and NE-activated adenylyl cyclase on the coupling of energy and signal transduction. <https://arxiv.org/abs/1208.5673> [q-bio.OT] (2012).
- [49] Zhang J., Zhang B., J. Zhang, Lin W. and Zhang S. Magnesium promotes the regeneration of the peripheral nerve. *Front Cell Dev Biol*. 9, 717854 (2021 Aug 11).
- [50] Liao W., Jiang M., Li M., Jin C., Xiao S., Fan S., Fang W., Zheng Y. and Liu J. Magnesium elevation promotes neuronal differentiation while suppressing glial differentiation of primary cultured adult mouse neural progenitor cells through ERK/CREB activation. *Frontiers in Neuroscience*. 11, 87 (23 Feb 2017).
- [51] Bennun A. Chapter 1: Molecular mechanisms integrating adenylyl cyclase responsiveness to metabolic control on long-term emotional memory and associated disorders. Book: *Long-Term Memory: Mechanisms, Types and Disorders*. Editors: Arseni K. Alexandrov and Lazar M. Fedoseev. Series: *Neuroscience Research Progress, Perspectives on Cognitive Psychology*. Nova Science Publishers, Inc., (2012), pp. 1-44.
- [52] Bennun A. The coupling of thermodynamics with the organizational water-protein intra-dynamics driven by the H-bonds dissipative potential of water cluster. <https://arxiv.org/abs/1303.6993>
- [53] Bennun A. The imidazole ring of proline allows a polypeptide folding dynamics by H-bonds breakdown sliding for a vectorial exergonic hydrophilic to an endergonic hydrophobic configuration for Hb and active site functions. [vixra.org](https://vixra.org) > *Biochemistry* > [vixra:2201.0182](https://vixra.org/abs/2201.0182). <https://vixra.org/abs/2201.0182> (2022-01-26).
- [54] Bennun A., Seidler N. and De Bari V.A. Divalent metals in the regulation of hemoglobin affinity for oxygen, *Annals of the New York Academy of Sciences*, 463, 76-79 (1986).
- [55] Bennun A., Needle N.A. and De Bari V.A. Stimulation of the hexose monophosphate pathway in the human erythrocyte by  $Mn^{2+}$ : Evidence for a  $Mn^{2+}$  dependent NADPH peroxidase activity. *Biochemical Medicine*. 33, 17-21 (1985).
- [56] De Bari V.A., Needle N.A. and Bennun A. Catalase as a manganese-dependent NADPH peroxidase. *Biochemical Society Transactions*, 13, 125-127 (1985).
- [57] Bennun A., Needle N.A. and De Bari V.A. Infrared spectroscopy of erythrocyte plasma membranes. *Biochemical Society Transactions*, 13, 127-128 (1985).
- [58] Bennun A., Seidler N. and De Bari V.A. A model for the regulation of haemoglobin affinity for oxygen. *Biochemical Society Transactions*. 13, 364-366 (1985).
- [59] De Bari V.A., Novak N.A. and Bennun A. Cyclic nucleotide metabolism in the human erythrocyte. *Clinical Physiology and Biochemistry*. 2, 227-238 (1984).
- [60] Novembre P., Nicotra J., De Bari V.A., Needle N.A. and Bennun A. Erythrocyte transport of cyclic nucleotide. *Annals of the New York Academy of Sciences*. 435, 190-194 (1984).
- [61] De Bari V.A. and Bennun A. Cyclic GMP in the human erythrocyte. Intracellular levels and transport in normal subjects and chronic hemodialysis patients. *Clinical Biochemistry*. 15(4), 219-221 (1982).
- [62] Argyrousi E.K., Heckman P.R., Van Hagen B.T., Muysers H., Van Goethem N.P and Prickaerts J. Pro-cognitive effect of upregulating cyclic guanosine monophosphate signaling during memory acquisition or early consolidation is mediated by increased AMPA receptor trafficking. *J Psychopharmacol*. 34(1), 103-114 (2020 Jan).
- [63] Giesen J., Mergia E., Koesling D. and Russwurm M. Hippocampal AMPA- and NMDA-induced cGMP signals are mainly generated by NO-GC2 and are under tight control by PDEs 1 and 2. *Eur J Neurosci*., 55(1), 18-31 (2022 Jan).
- [64] Greene S.J., Gheorghide M., Borlaug B.A., Pieske B., Vaduganathan M., Burnett Jr. J.C., Roessig L., Stasch J.P., Solomon S.D., Paulus W.J. and Butler J.. The cGMP Signaling Pathway as a Therapeutic Target in Heart Failure With Preserved Ejection Fraction. *Journal of the American Heart Association*. 2, e000536 (2013).
- [65] Bennun A. The Human Oral-Cavity-NA-AC-Hypothalamic Axis on the Developing of Emotional Intelligence, Creativity and Innovation. [vixra.org](https://vixra.org) > *Biochemistry* > [vixra:2111.0157](https://vixra.org/abs/2111.0157) (2021-11-29).

- [66] Bennun A. Dynamics of the Hydrophilic to Hydrophobic Proteins and Enzymes Turnover in A. Bennun's Biochemical-Physics Neurotransmission Model for the Glycerol Assay of the Hydration Shell Dynamics on the Hydrophilic Structure of the Active Site of CF1-ATPase" Book Title: Advances in Chemistry Research (James C Taylor Editor) in Volume 47 Chapter 5, pages: 165-182. January 2019. <https://novapublishers.com/shop/advances-in-chemistry-research-volume-47/>
- [67] Bennun A. The Thermal Radiation as the Expansionary Force Required by the Cosmological Constant. viXra.org > Relativity and Cosmology > viXra:2101.0103 <https://vixra.org/abs/2101.0103> (2021-01-15).
- [68] Prigogine, Ilya; Stengers, Isabelle (1984). Order out of Chaos: Man's new dialogue with nature. Flamingo. ISBN 0-00-654115-1.
- [69] Bennun A. Estructura y función termodinámica del cerebro como sistema abierto autónomo. Casanchi. (19 septiembre, 2020) <http://casanchi.org/ref/cerebro01.htm>
- [70] Bennun A. Transición Cuántica Del Agua de Estado Líquido a Vapor Por Entrelazamiento Fisiológico. viXra.org > Physics of Biology > viXra:2106.0094 <https://vixra.org/abs/2106.0094> (2021, June 16).
- [71] Bennun A. A coupling mechanism to interrelate regulatory with haem-haem interactions of haemoglobin, Biomed. Biochim. Acta. 46(2/3), 314-319 (1987).
- [72] Bennun A. Book: Molecular Aspects of the Psychosomatic-Metabolic Axis and stress. Series: Neurology - Laboratory and Clinical Research Developments. Editorial: Nova Science Publishers, 2015. ISBN: 978-1-63463-912-5.
- [73] Bennun, A. Inflation-Expansion Characterized by Relativistic Space-Time-Velocity Plus the Quantum-Dimensioning Parameters of CMB-Elongation. viXra.org > Relativity and Cosmology > viXra:2008.0156 <https://vixra.org/abs/2008.0156> (2020-08-21).
- [74] Bennun, A. The Vomeronasal Organ Functions in Entropy Dissipation, the Communication by Pheromones for a Feedback by the Pituitary Over Brain Plasticity and the Development of the Unconscious. viXra.org > Biochemistry > viXra:2002.0143 <https://vixra.org/abs/2002.0143> (2020-02-07).
- [75] Bennun, A. A protein hydrophilic active site could by mutual exclusion become hydrophobic, allowing this vectorial transition to bypass the microscopic reversibility principle. viXra.org > Physics of Biology > viXra:2205.0073 (2022-05-13).
- [76] Caligiuri L.M. QED Coherence and Super-Coherence of Water in Brain Microtubules and Quantum Hypercomputation. Rhythmic Advantages in Big Data and Machine Learning. 225–262 (10 January 2022).
- [77] Jagendorf A.T. and Uribe E. ATP formation caused by acid-base transition of spinach chloroplasts. Proc Natl Acad Sci USA. 55(1), 170-177 (1966 Jan).
- [78] Hans-Jürgen Apell. Finding Na, K-ATPase II - From fluxes to ion movements. An International Journal of the History of Chemistry. 3, 1.-S.19-41 (2019).
- [79] Casciano C. and Bennun A. Effect of Li<sup>+</sup> on the secretion of HCO<sub>3</sub><sup>-</sup> in rat fundic tissue, Biochemical Society Transactions. 17, 1111-1112 (1989).
- [80] Casciano C., Kaminska G.Z. and Bennun A. Investigations on the cytoprotective mechanism of thiocyanate in rat gastric mucosa, Biochemical Society Transactions. 17, 1113-1114 (1989).
- [81] Casciano C. and Bennun A. A characterization of two inhibitors of H<sup>+</sup>, K<sup>+</sup>-ATPase in gastric tissue, Biochemical Society Transactions. 16, 27-29 (1988).
- [82] Casciano C. and Bennun A. Characterization of the interrelationship of the secretory activities of gastric tissue. Annals of the New York Academy of Sciences. 529, 246-249 (1988).
- [83] Sulner J. and Bennun A. Ca<sup>2+</sup>-dependent control of renin release. Biochemical Society Transactions. 13, 363-364 (1985).
- [84] Emma J.E., Cervoni P., Sulner J.W. and Bennun A. KCl-stimulated renin release. Annals of the New York Academy of Sciences. 463, 281-283 (1986).
- [85] Weisenberg RC. Microtubule formation in vitro in solutions containing low calcium concentrations. Science. 177 (4054), 1104-5 (September 1972).
- [86] Desai A. and Mitchison T.J. Microtubule polymerization dynamics. Annual Review of Cell and Developmental Biology. 13, 83-117 (1997).

- [87] Walker R.A., O'Brien E.T., Pryer N.K., Soboeiro M.F., Voter W.A., Erickson H.P. and Salmon E.D. Dynamic instability of individual microtubules analyzed by video light microscopy: rate constants and transition frequencies. *The Journal of Cell Biology*. 107(4), 1437-48 (October 1988).
- [88] Parato J, Bartolini F. The microtubule cytoskeleton at the synapse. *Neurosci Lett*. 753, 135850 (2021).
- [89] Waites C., Qu X. and Bartolini F. The synaptic life of microtubules. *Curr Opin Neurobiol*. 69, 113-123 (2021).
- [90] Qu X., Kumar A., Blockus H., Waites C. and Bartolini F. Activity-dependent nucleation of dynamic microtubules at presynaptic boutons controls neurotransmission. *Curr Biol*. 29(24), 4231–4240.e5 (2019).
- [91] Guedes-Dias P., Nirschl J.J., Abreu N., et al. Kinesin-3 responds to local microtubule dynamics to target synaptic cargo delivery to the presynapse. *Curr Biol*. 29(2), 268-282.e8 (2019).
- [92] Guillaud L., Dimitrov D. and Takahashi T. Presynaptic morphology and vesicular composition determine vesicle dynamics in mouse central synapses. *eLife*. 6, e24845 (2017).
- [93] Piriya Ananda Babu L., Wang H.Y., Eguchi K., Guillaud L. and Takahashi T. Microtubule and actin differentially regulate synaptic vesicle cycling to maintain high-frequency neurotransmission. *J Neurosci*. 40(1), 131-142 (2020).
- [94] Mitsuyama F., Niimi G., Kato K., et al. Redistribution of microtubules in dendrites of hippocampal CA1 neurons after tetanic stimulation during long-term potentiation. *Ital J Anat Embryol*. 113(1), 17-27 (2008).
- [95] Gadadhar S., Bodakuntla S., Natarajan K. and Janke C. The tubulin code at a glance. *J Cell Sci*. 130(8), 1347-1353 (2017).
- [96] Moutin M.J., Bosc C., Peris L. and Andrieux A. Tubulin post-translational modifications control neuronal development and functions. *Dev Neurobiol*. 81(3), 253-272 (2021).
- [97] Barra H.S., Rodriguez J.A., Arce C.A. and Caputto R. A soluble preparation from rat brain that incorporates into its own proteins [<sup>14</sup>C]arginine by a ribonuclease-sensitive system and [<sup>14</sup>C]tyrosine by a ribonuclease-insensitive system. *J Neurochem*. 20(1), 97-108 (1973).
- [98] Baas P.W. and Black MM. Individual microtubules in the axon consist of domains that differ in both composition and stability. *J Cell Biol*. 111(2), 495-509 (1990).
- [99] Bré M.H., Kreis T.E. and Karsenti E. Control of microtubule nucleation and stability in Madin-Darby canine kidney cells: the occurrence of noncentrosomal, stable detyrosinated microtubules. *J Cell Biol*. 105(3), 1283-1296 (1987).
- [100] Kreis T.E. Microtubules containing detyrosinated tubulin are less dynamic. *EMBO J*. 6(9), 2597-2606 (1987).
- [101] Prota A.E., Magiera M.M., Kuijpers M, et al. Structural basis of tubulin tyrosination by tubulin tyrosine ligase. *J Cell Biol*. 200(3), 259-270 (2013).
- [102] Tas R.P., Chazeau A., Cloin B.M.C., Lambers M.L.A., Hoogenraad C.C. and Kapitein L.C. Differentiation between oppositely oriented microtubules controls polarized neuronal. *Neuron*. 96(6), 1264-1271.e5 (2017).
- [103] Uchida S., Martel G., Pavlowsky A, et al. Learning-induced and stathmin-dependent changes in microtubule stability are critical for memory and disrupted in ageing. *Nat Commun*. 5, 4389 2014.
- [104] Scheff S.W., Price D.A., Schmitt F.A. and Mufson E.J. Hippocampal synaptic loss in early Alzheimer's disease and mild cognitive impairment. *Neurobiol Aging*. 27(10), 1372-1384 (2006).
- [105] Muratore C.R., Rice H.C., Srikanth P., et al. The familial Alzheimer's disease APPV717I mutation alters APP processing and Tau expression in iPSC-derived neurons. *Hum Mol Genet*. 23(13), 3523-3536 (2014).
- [106] Nadal A., Eritja, R., Esteve T. and Pla, M. "Parallel" and "Antiparallel Tail-Clamps" Increase the Efficiency of Triplex Formation with Structured DNA and RNA Targets. *ChemBioChem*. 6(6), 1034-1042 (2005).
- [107] Bennun A. The Regenerative Processes Involving the cAMP Unzipping of DNA. The Synthesis of Proteins Integrating Plasticity and Longevity. *Biochemistry Research Trends*. Book Published by Nova Biomedical, Copyright 2017 by Nova Science Publishers, Inc. <https://novapublishers.com/shop/the-regenerative-processes-involving-the-camp-unzipping-of-dna-the-synthesis-of-proteins-integrating-plasticity-and-longevity/>

- [108] Tai No K., Ha Chang B., Yeon Kim S., Shik Jhon M. and Scheraga, H.A.. Description of the potential energy surface of the water dimer with an artificial neural network. *Chemical Physics Letters*. 271(1-3), 152-156 (1997)
- [109] Tai No, K., Ha Chang, B., Yeon Kim, S., Shik Jhon, M., & Scheraga, H. A.. Description of the potential energy surface of the water dimer with an artificial neural network. *Chemical Physics Letters*, 271(1-3), 152–156 (1997).
- [110] Cantero M.R., Villa Etchegoyen C., Perez P.L., Scarinci N. and Cantiello H.F. Bundles of Brain Microtubules Generate Electrical Oscillations. *Sci Rep*. 8(1), 11899 (2018 Aug 9).
- [111] Bennun, A. Quantum State Transition from Liquid to Vapor Water by Physiological Entanglement. *viXra.org > Biochemistry > viXra:2106.0053* <https://vixra.org/abs/2106.0053> (2021-06-08).
- [112] Pokorný J., Pokorný J. and Vrba, J. Generation of Electromagnetic Field by Microtubules. *International Journal of Molecular Sciences*. 22(15), 8215 (2021).
- [113] Shu-Hsien Sheu et al. A serotonergic axon-cilium synapse drives nuclear signaling to alter chromatin accessibility. *Cell*. 185(18), 3390-3407.e18 (2022 Sep 1).
- [114] Peris L., Wagenbach M., Lafanechere L., et al. Motor-dependent microtubule disassembly driven by tubulin tyrosination. *J Cell Biol*. 185(7), 1159-1166 (2009).
- [115] Peris L, They M, Faure J, et al. Tubulin tyrosination is a major factor affecting the recruitment of CAP-Gly proteins at microtubule plus ends. *J Cell Biol*. 174(6), 839-849 (2006).
- [116] Nirschl J.J., Magiera M.M., Lazarus J.E., Janke C. and Holzbaur E.L.F.  $\alpha$ -tubulin tyrosination and CLIP-170 phosphorylation regulate the initiation of dynein-driven transport in neurons. *Cell Rep*. 14(11), 2637-2652 (2016).
- [117] Cai D., McEwen D.P., Martens J.R., Meyhofer E. and Verhey K.J. Single molecule imaging reveals differences in microtubule track selection between Kinesin motors. *PLoS Biol*. 7(10), e1000216 (2009).
- [118] Schwarz T.L. Mitochondrial trafficking in neurons. *Cold Spring Harb Perspect Biol*. 5, a011304 (2013).
- [119] Setou M., Seog D.H., Tanaka Y., et al. Glutamate-receptor-interacting protein GRIP1 directly steers kinesin to dendrites. *Nature*. 417(6884), 83-87 (2002).
- [120] Hoerndli F.J., Maxfield D.A., Brockie P.J., et al. Kinesin-1 regulates synaptic strength by mediating the delivery, removal, and redistribution of AMPA receptors. *Neuron*. 80(6), 1421-1437 (2013).
- [121] Chin J.Y., Knowles R.B., Schneider A., Drewes G., Mandelkow E.M. and Hyman B.T. Microtubule-affinity regulating kinase (MARK) is tightly associated with neurofibrillary tangles in Alzheimer brain: a fluorescence resonance energy transfer study. *J Neuropathol Exp Neurol*. 59(11), 966-71 (2000 Nov).
- [122] Pokorný, J., Pokorný, J. and Vrba, J. Generation of Electromagnetic Field by Microtubules. *International Journal of Molecular Sciences*. 22(15), 8215 (2021).
- [123] Li S., Wang C. and Nithiarasu P. Electromechanical vibration of microtubules and its application in biosensors. *J R Soc Interface*. 16(151), 20180826 (2019 Feb 28).
- [124] Bennun A. and Ledesma N. The Photon Structure in Interference Processes, Quantum Entanglement and Self-Organized Cosmos. *viXra.org > Relativity and Cosmology > viXra:2109.0214* (2021-09-30).
- [125] Bennun A. Emisión-Absorción de Energía Cuántica Relativista. *Casanchi* (29 noviembre, 2008).
- [126] Li Z., Sun H., Turek J., Jalal S., Childress M. and Nolte D.D. Doppler fluctuation spectroscopy of intracellular dynamics in living tissue. *J Opt Soc Am A Opt Image Sci Vis*. 36(4), 665-677 (2019 Apr 1).
- [127] Pockett S. The electromagnetic field theory of consciousness: a testable hypothesis about the characteristics of conscious as opposed to non-conscious fields. *Journal of Consciousness Studies*. 19 (11-12), 191-223 (2012).
- [128] Maday S., Twelvetrees A.E., Moughamian A.J. and Holzbaur E.L.F. Axonal Transport: Cargo-Specific Mechanisms of Motility and Regulation. *Neuron*. 84 (2), 292–309 (October 2014).
- [129] Brown A. Axonal transport of membranous and nonmembranous cargoes: a unified perspective. *The Journal of Cell Biology*. 160 (6), 817-21 (March 2003).

- [130] Trogden K.P., Lee J.S., Bracey K.M., et al. Microtubules regulate pancreatic  $\beta$  cell heterogeneity via spatiotemporal control of insulin secretion hot spots. *eLife*. 10, e59912 (2021).
- [131] Davidkova G. and Carroll R.C. Characterization of the Role of Microtubule-Associated Protein 1B in Metabotropic Glutamate Receptor-Mediated Endocytosis of AMPA Receptors in Hippocampus. *The Journal of Neuroscience*. 27(48), 13273-13278 (November 28, 2007).
- [132] Oakie A. and Wang R.  $\beta$ -Cell Receptor Tyrosine Kinases in Controlling Insulin Secretion and Exocytotic Machinery: c-Kit and Insulin Receptor. *Endocrinology*. 159(11), 3813-3821 (2018 Nov 1).
- [133] Bennun A. and Ledesma N. Advances in the efficiency of beta-scintillator batteries and its adapting to support electric vehicles. *Book Series: International Journal of Energy, Environment, and Economics*. Volume 23, Number 1 (pages:41 to 52). 2015. ISSN: 1054-853X. [https://www.researchgate.net/publication/334657807\\_Advances\\_in\\_the\\_efficiency\\_of\\_beta-scintillator\\_batteries\\_and\\_its\\_adapting\\_to\\_support\\_electric\\_vehicles\\_Book\\_series\\_International\\_Journal\\_of\\_Energy\\_Environment\\_and\\_Economics\\_Volume\\_23\\_Number\\_1\\_pages\\_](https://www.researchgate.net/publication/334657807_Advances_in_the_efficiency_of_beta-scintillator_batteries_and_its_adapting_to_support_electric_vehicles_Book_series_International_Journal_of_Energy_Environment_and_Economics_Volume_23_Number_1_pages_)
- [134] Bennun A. Innovative Use of Light-Weight Radioisotopes in Therapeutics and the Engineering of Light-Power Generators. *Open Journal of Biophysics*. 3, 1A, 86-90 (2013).
- [135] Bennun A. Book: Thermodynamics structuring of the universe. Editorial: Amazon (1 Febrero 2021) ISBN-13: 979-8706660116. [https://www.amazon.com/-/es/Alfred-Bennun/dp/B08WJZBZJV/ref=tmm\\_pap\\_swatch\\_0?\\_encoding=UTF8&qid=1627602555&sr=8-1](https://www.amazon.com/-/es/Alfred-Bennun/dp/B08WJZBZJV/ref=tmm_pap_swatch_0?_encoding=UTF8&qid=1627602555&sr=8-1)
- [136] Romera M., Talatchian P., Tsunegi S., Yakushiji K., Fukushima A., Kubota H., Yuasa S., Cros V., Bortolotti P., Ernoult M., Querlioz D. and Grollier J. Binding events through the mutual synchronization of spintronic nano-neurons. *Nat Commun*. 13(1), 883 (2022 Feb 15).
- [137] Penrose, R. and Hameroff, S. Consciousness in the universe: a review of the 'Orch OR' theory. *Phys Life Rev.*, 11(1), 39-78 (2014 Mar).
- [138] Hameroff, S. Consciousness, Neurobiology and Quantum Mechanics. In Tuszynski, Jack (ed.). *The Emerging Physics of Consciousness* (2006).
- [139] "Can Quantum Physics Explain Consciousness? One Scientist Thinks It Might". *Discover Magazine*. Archived from the original on 3 October 2020. Retrieved 7 October 2020.
- [140] Tegmark Max. The importance of quantum decoherence in brain processes. *Physical Review E*. 61 (4): 4194–4206 (2000). arXiv:quant-ph/9907009.
- [141] Bennun, Alfredo. Libro: Estructuración termodinámica del universo. Editorial: Amazon (16 Junio 2021) ISBN-13: 979-8521552344 [https://www.amazon.com/-/es/Alfredo-Bennun/dp/B098GY42CD/ref=tmm\\_pap\\_swatch\\_0?\\_encoding=UTF8&qid=1627603134&sr=8-1](https://www.amazon.com/-/es/Alfredo-Bennun/dp/B098GY42CD/ref=tmm_pap_swatch_0?_encoding=UTF8&qid=1627603134&sr=8-1)
- [142] Prigogine I. (1997) *Las leyes del caos*. Editorial: Crítica Barcelona. ISBN 978-84-8432-239-9.
- [143] Prigogine I. (1993). *Chaotic Dynamics and Transport in Fluids and Plasmas: Research Trends in Physics Series*. Nueva York: American Institute of Physics. ISBN 0883189232.
- [144] Bennun, A. The Thermodynamic Inwardly Open System by Locally Decreasing Entropy Originates Life. *viXra.org > Relativity and Cosmology* > viXra:2104.0155 <https://vixra.org/abs/2104.0155> (2021-04-25).
- [145] Bennun, A. The Model of the Universe as Thermodynamics Inwardly Open System Flattened by the Velocity of Light. *viXra.org > Relativity and Cosmology* > viXra:2011.0016 <https://vixra.org/abs/2011.0016> (2020-11-02).
- [146] Grollier J., Querlioz D., Camsari K.Y., Everschor-Sitte K., Fukami S. and Stiles M. D. Neuromorphic spintronics. *Nature Electronics*. 3, 360-370 (2020).
- [147] Schuler A.L., Ferrazzi G., Colenbier N., Arcara G., Piccione F., Ferreri F., Marinazzo D. and Pellegrino G. Auditory driven gamma synchrony is associated with cortical thickness in widespread cortical areas. *Neuroimage*. 255, 119175 (2022 Jul 15).
- [148] Romera M. Vowel recognition with four coupled spin-torque nano-oscillators. *Nature*, 563, 230-234 (November 2018).
- [149] Abhronil Sengupta, Priyadarshini Panda, Parami Wijesinghe, Yusing Kim, Kaushik Roy. Corrigendum: Magnetic Tunnel Junction Mimics

Stochastic Cortical Spiking Neurons. Sci Rep. 7:46894 (2017 Aug 29).

[150] Bennun, Alfred. Book: Thermodynamics structuring of the universe. Editorial: Amazon (1 Febrero 2021) ISBN-13: 979-8706660116.

[151] Bennun, A. Dynamics of the Hydrophilic to Hydrophobic Proteins and Enzymes Turnover in A. Bennun's Biochemical-Physics Neurotransmission Model for the Glycerol Assay of the Hydration Shell Dynamics on the Hydrophilic Structure of the Active Site of CF1-ATPase. Book Title: Advances in Chemistry Research (James C Taylor Editor) in Volume 47 Chapter 5, pages: 165-182. January 2019. <https://novapublishers.com/shop/advances-in-chemistry-research-volume-47/>